Accelerated Prediction of Atomically Precise Cluster Structures Using On-the-fly Machine Learning

Yunzhe Wang, Shanping Liu, Peter Lile, Sam Norwood, Alberto Hernandez, Sukriti Manna, and Tim Mueller*

Department of Materials Science and Engineering, Johns Hopkins University, Baltimore, MD 21218

*Corresponding Author Email: tmueller@jhu.edu

KEYWORDS: nanocluster, genetic algorithm, machine learning interatomic potential, active learning, transferrable potential, structure search

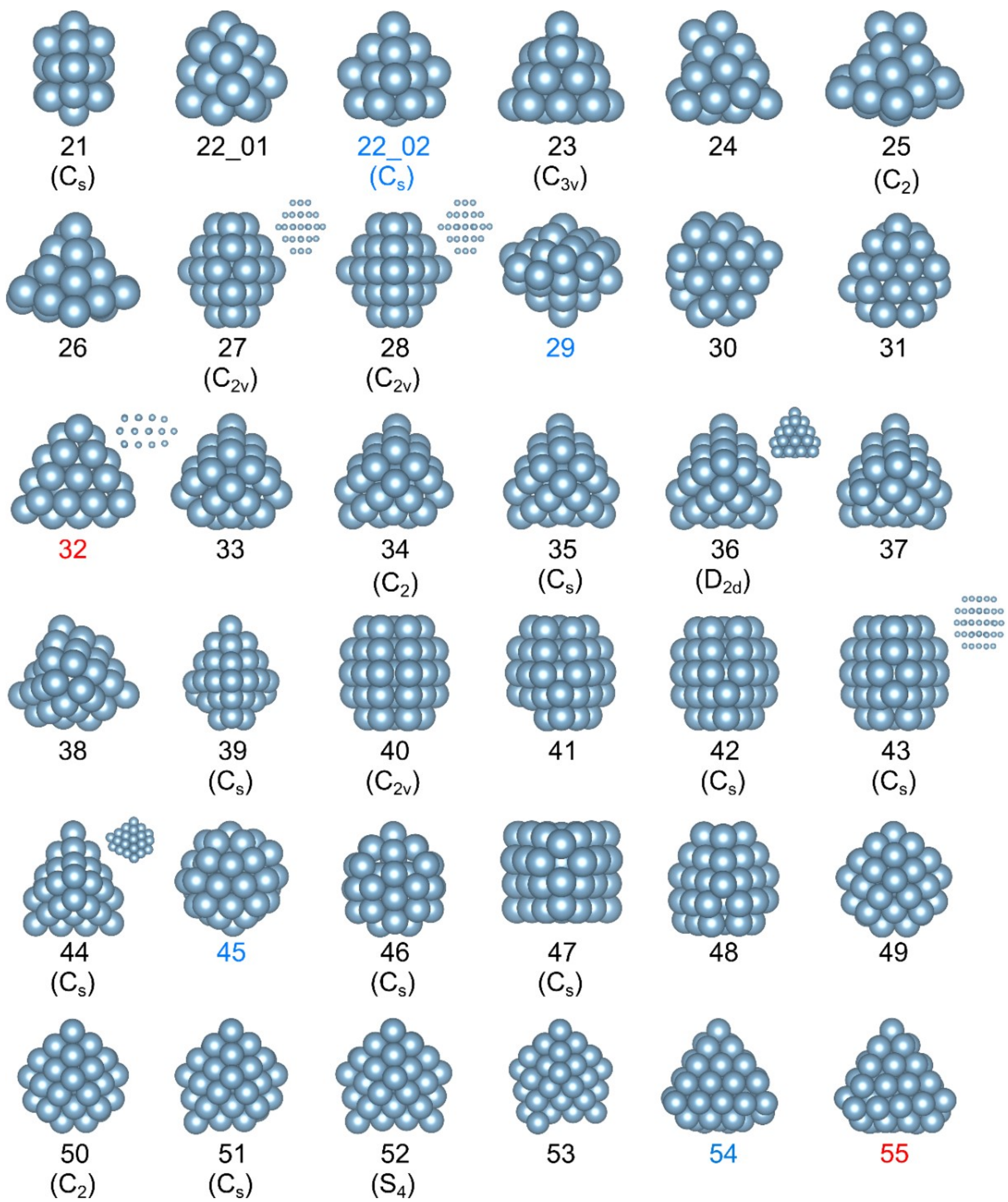

Accelerated Prediction of Atomically Precise Cluster Structures Using On-the-fly Machine Learning

Yunzhe Wang, Shanping Liu, Peter Lile, Sam Norwood, Alberto Hernandez, Sukriti Manna, and Tim Mueller*

Department of Materials Science and Engineering, Johns Hopkins University, Baltimore, MD 21218

*Corresponding Author Email: tmueller@jhu.edu

KEYWORDS: nanocluster, genetic algorithm, machine learning interatomic potential, active learning, transferrable potential, structure search

ABSTRACT: The chemical and structural properties of atomically precise nanoclusters are of great interest in numerous applications, but predicting the stable structures of clusters can be computationally expensive. In this work, we present a procedure for rapidly predicting low-energy structures of nanoclusters by combining a genetic algorithm with interatomic potentials actively learned on-the-fly. Applying this approach to aluminum clusters with 21 to 55 atoms, we have identified structures with lower energy than any reported in the literature for 25 out of the 35 sizes. Our benchmarks indicate that the active learning procedure accelerated the average search speed by more than an order of magnitude relative to genetic algorithm searches using only density functional calculations. This work demonstrates a feasible way to systematically discover stable structures for large nanoclusters and provides insights into the transferability of machine-learned interatomic potentials for nanoclusters.

INTRODUCTION

Nanoclusters have drawn much attention due to their special physical and chemical properties[1,2] which are distinct from molecules or bulk crystal materials. These properties make them useful in diverse research fields including catalysis,[3-6] chemical sensing,[7] fluorescence,[8,9] and medicine.[10] The unique properties of nanoclusters are largely the consequence of distinct size-dependent atomic structures, quantum finite size effects, and very large surface-to-volume ratios.[11,12] These properties are generally not smooth functions of cluster sizes and can fluctuate with the addition or removal of a single atom.

Computational screening is a promising way to identify nanoclusters with desirable properties, but to predict the properties of a nanocluster from first principles it is necessary to first identify the low-energy atomic structures of the cluster. Many optimization methods have been proposed to perform global structure searches for nanoclusters, including the basin hopping method,[13,14] unbiased random sampling[15], particle swarm optimization,[16,17] simulated annealing[18,19] and genetic algorithms (GA).[20-24] Each of these methods involves the evaluation of the energies of a large number of candidate structures, which makes it critically important to evaluate structure energies with a method that is both fast and sufficiently accurate to distinguish between competing structures. Density functional theory (DFT) provides a high level of accuracy, but its speed and scalability typically limit the search to nanoclusters of sizes up to only several dozen atoms.[25-28] Classical interatomic potentials, which typically have simple functional forms derived from fundamental physics, are several orders of magnitude faster than DFT and have been used to search for ground state structures with up to a few hundred atoms.[13,29,30] However, classical interatomic potentials often lack the accuracy required to resolve the energy differences between competing candidate structures, especially for the low-lying local minima on the potential energy surface (PES) that are often only tens of meV apart.[20,31]

In recent years, an alternative type of interatomic potential has emerged in the form of machine-learned interatomic potentials (MLIPs),[32-36] which are parameterized by fitting to a set of training data. Examples of MLIPs are neural network potentials,[37-39] Gaussian approximation potentials (GAP),[40-42] spectral neighbor analysis potentials (SNAP),[43,44] moment tensor potentials (MTP),[45-47] the Atomic Cluster Expansion (ACE),[48] and potentials found through symbolic regression.[49] Although they may be slower than traditional interatomic potentials by an order of magnitude or more, MLIPs are generally more accurate and are still orders of magnitude faster than *ab initio* calculations.[50]

Here we demonstrate how machine-learned interatomic potentials, in the form of moment tensor potentials, can be used to significantly accelerate a genetic algorithm search for low-energy cluster structures. Moment tensor potentials have been shown to have a good balance between accuracy and speed for bulk materials,[50] and we demonstrate that they also work well for small atomic clusters. One of the challenges in using machine-learned interatomic potentials to search for ground state structures is that because the ground state is unknown, it is difficult to ensure that the potential is constructed in a way that will yield accurate ground state energies. To address this challenge we use active learning, in which the potential is trained adaptively with new data generated during the search. The idea of refining an interatomic potential model during the structural search was introduced by Hartke using classical interatomic potentials and proved to be capable of discovering new low-energy silicon clusters.[51] Recently, similar strategies have also been successfully applied using MLIPs for global optimization of bulk crystalline materials[52-55] and nanoclusters.[56,57]

We demonstrate our approach by searching for low-energy structures for aluminum clusters of between 21 and 55 atoms. Using this approach, we have discovered new cluster structures for 25 out of the 35 sizes that are at least 1 meV/atom lower in DFT-calculated energy than the lowest-energy structures we have found in the literature.[28,29,58-60] New low-energy structures for an additional two sizes were discovered by DFT-only genetic algorithms used for benchmarking. Our approach, described in detail below, provides a template that can be used to significantly accelerate the computational design of atomic clusters, and paves the way for determining atomic structures of large nanoclusters.

RESULTS

Hyperparameter selection for Moment Tensor Potentials

Existing benchmarks of MTP on bulk crystalline structures[50,61] give generally good sets of parameters for training reliable MTP, but little information is available on good parameters for training clusters. To identify a good set of parameters for our calculations we used Al clusters with 24 atoms as a model system and tested various combinations of hyperparameters, including potential complexity (defined by the parameter lev_{max}),[47] the amount of training data, and the weight for force components (the "force weight") relative to the weight for energies. One quarter of the structures were randomly selected for validation, with the rest used to train the potential. Additional details about the construction of this dataset are provide in the Methods section and Section 2.1 of the Supplementary Information.

For a fixed training set, both energy and force errors decrease steadily as increasingly complex potentials are used (Figure 1b). However, such a gain is at the expense of an exponential growth in training costs (Figure 1c). Additional analysis of other combinations of hyperparameters (Figure S4 to Figure S7 of Supplementary Information) shows similar trends as in Figure 1. To balance accuracy and training costs we used and $lev_{max} = 14$ and a force weight that was 1/1000 that of the energy weight for all subsequent active learning genetic algorithm (GA_AL) runs. Using these parameters, we found that force and energy errors plateau after the training set exceeded about 1000 structures (Figure 1d).

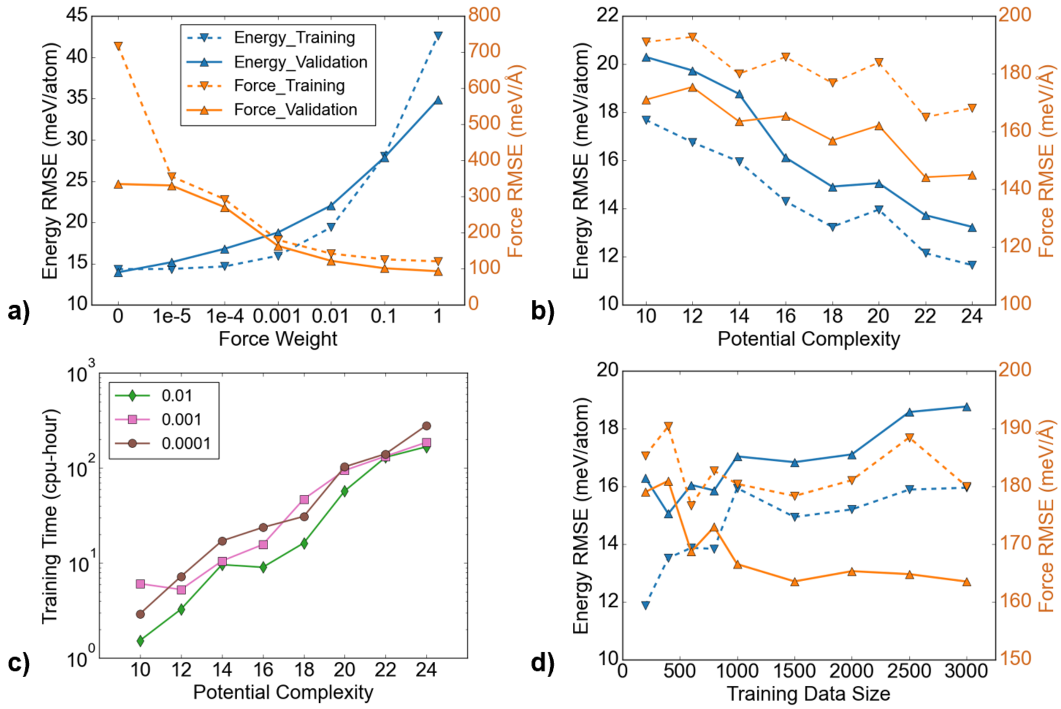

Figure 1. Benchmarks of hyperparameters for training MTP potentials. Training (dashed lines) and validation (solid lines) root-mean-squared errors for both energies and force components are plotted against **a)** force weights relative to the energy weight, **b)** potential complexity lev_{max}, and **d)** the number of structures in the training set. **a)**, **b)** and **d)** share the same legend as shown in **a**). Training costs of potentials with different relative force weights and complexities are shown in **c)**. Where not specified, the training data contained 3000 clusters, $lev_{max} = 14$, and the force weight was 1/1000th that of the energy weight.

Prediction of cluster structures for Al clusters with 21–40 atoms

We evaluated our approach by predicting structures of aluminum nanoclusters with 21 to 40 atoms (Figure 2). The performance of the GA_AL algorithm was evaluated by comparing it with a genetic algorithm that used only DFT to calculate energies (GA_DFT), where both algorithms were run for the same amount of computing time. For our initial evaluation, GA_AL was initialized with untrained potentials and a new potential was trained at each cluster size. Details of how we performed the comparison are provided in the Methods section.

For 8 cluster sizes (21, 23, 24, 26, 28, 33, 35 and 36), mostly among the smaller clusters, GA_AL and GA_DFT found essentially the same lowest-energy clusters, with similarity scores, a measure of geometrical differences, below 0.3 (see the Methods section). For 10 out of the 20 sizes (25, 27, 30 – 32, 34, 37 – 40), GA_AL found clusters that were lower in energy than those found by GA_DFT by at least 1 meV / atom, with an average energy difference of -5.06 meV/atom (or -169.64 meV/cluster). For clusters of 22 atoms, GA_AL identified a distinct cluster with a calculated energy within 0.1 meV / atom of the lowest-energy cluster identified by GA_DFT. The lowest-energy 33-atom cluster found by GA_AL is 1.47 meV/atom lower in energy than the one found by GA_DFT, but it is structurally similar based on both the similarity score and visual inspection (see Figure S14 of Supplementary Information). Therefore it is not counted as a new lowest-energy cluster. There was only one cluster size (29 atoms), for which GA_DFT found a distinct cluster with lower energy than that found by GA_AL. For this size the cluster found by GA_DFT was lower in energy by 3.61 meV/atom (104.69 meV/cluster). On average, the energies of structures found by GA_AL are lower by 2.43 meV/atom (82.27 meV/cluster).

To quantify how much more quickly the GA_AL approach finds low-energy structures, we define the "acceleration ratio" as the ratio of time it took GA_DFT to find its lowest-energy structure divided by the time it took GA_AL to find a structure with at least as low of the energy. In the case of size 29, GA_AL failed to discover better or equivalent configurations, so the ratio is set to 0. The average acceleration ratio across all 20 sizes is 2.29 (Figure 2b). GA_DFT often did not find a cluster with energy as low as that found by GA_AL (Figure 2b), suggesting that if the acceleration ratio were based on the time required to find the lowest-energy structure it would be larger. Additional data illustrating the acceleration of GA_AL relative to GA_DFT are provided in Figure S11 and Figure S12 of the Supplementary Information.

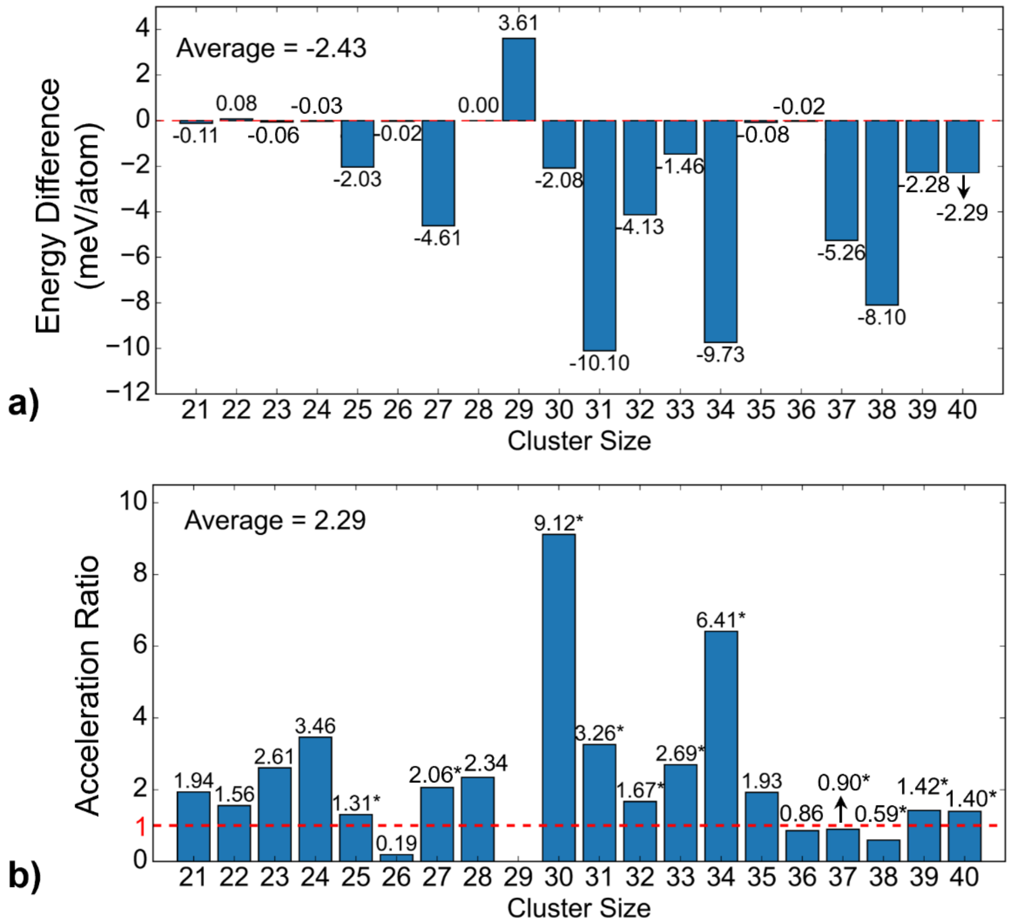

Figure 2. Performance benchmarks between GA_AL initialized with an untrained potential and GA_DFT. **a)** DFT-calculated energy differences between the lowest-energy structures found in GA_AL and GA_DFT. Negative values indicate GA_AL discovered structures with lower energies. **b)** Acceleration ratios of GA_AL relative to GA_DFT. The sizes for which GA_AL discovered better structures are marked with *, suggesting that they could be larger if GA_DFT were allowed to run for longer time.

Size-transferable interatomic potentials for nanoclusters

The results presented in the previous section were obtained by training a new potential at every cluster size, as there is a risk that a potential trained on one cluster size might not work well for clusters of another size due to the fact that the properties of atomic clusters can change discontinuously with the number of atoms in the cluster. However using a potential trained at one size to find structures of a different size could significantly speed up the structure search by reducing the total amount of training data that must be generated. In particular, using potentials trained with smaller clusters to predict the structures of larger clusters can have significant performance advantages, as the cost of generating training data using DFT typically scales as approximately the cube of the number of valence electrons in the cluster.[62]

We examined how accurately potentials trained on clusters of a range of small sizes are able to predict the energies of clusters with larger sizes. Training data was separated into a group of 3000 clusters with an even number of atoms (22, 26, 30, 34, and 38) and another group of 3000 clusters with an odd number of atoms (21, 25, 29, 33, and 37), as DFT calculations indicate that even-sized clusters and odd-sized clusters have distinct ground state magnetic moments (see Section 4 of the Supplementary Information). A third training set was created by combining the even and odd sets. The validation sets were composed of about 3000 clusters for each cluster size between 50–55 atoms. Details of the construction of the training and validation sets can be found in the Methods section.

All three mixed-size potentials predicted energies of the large clusters with validation errors (~10 meV/atom) comparable to training errors (Figure 3a and Figure 3b). The errors in the predicted forces (~165 meV/Å) were slightly worse than the fitting errors. These errors are similar to the training and validation errors achieved when all of the training and validation data consisted of clusters of 24 atoms (Figure 1). Mixing training data with different magnetic moments did not have a significant adverse effect on model predictions (Figure 3). The potential trained on clusters with an odd number of atoms has slightly smaller prediction errors for both force and energy than potential trained on clusters with an even number of atoms regardless of whether the validation set contains even-sized or odd-sized clusters. The potential trained with both even and odd clusters has larger energy training errors than both of the even and odd potentials, but energy validation errors between the validation errors for even and odd potentials. For forces, the potential trained with both even and odd clusters has the lowest training and validation errors in all cases.

For comparison, we evaluated the ability of potentials trained on clusters of a single size. For each size, the training data consisted of 3000 dissimilar clusters, with exception of clusters with 21 atoms (the smallest size) for which our training set only had 2136 clusters after removing structurally similar clusters (see Methods section). For potentials trained on clusters of a single size, training and validation errors were similar for forces, and potentials trained on a single size may predict forces with significantly lower errors than the potentials trained on a mixed set of sizes. However validation errors for energies are notably worse than the training errors, especially for potentials trained on small clusters (Figure 3a and Figure 3b). The accuracy strongly depends on the size of the clusters in the training set, with larger sizes having the lowest errors. This suggests that quantum finite-size effects may be particularly pronounced for clusters with fewer than about 30 atoms, limiting the extent to which potential models trained at these sizes can be transferred to larger sizes. The training algorithm may also have a difficult time determining how the undercoordination of surface atoms in a cluster affects its energy when all clusters in the training set have approximately the same surface area. In contrast, training sets with a mixture of cluster sizes provide more information on how the energy is affected by the cluster surface area, which may improve the prediction accuracy for clusters of varying size.

Because of the particular importance of identifying the structures of low-energy clusters, we evaluated the potentials on the lowest-energy structures we found or collected from the literature with 50 to 55 atoms. The diversity of the training sets with mixed cluster sizes proved beneficial for identifying low-energy clusters, as the MTP extrapolation grade (see Methods section) for the lowest-energy clusters in the validation set is less than one, suggesting interpolation, with respect to the training sets of odd-sized and even-sized clusters. On the other hand, the low-energy structures had an extrapolation grade above 1, suggesting extrapolation, with respect to the training sets of single-sized clusters. Accordingly, the mixed-size potentials had much lower energy errors than the single-size ones (see Figure S14 of the Supplementary Information).

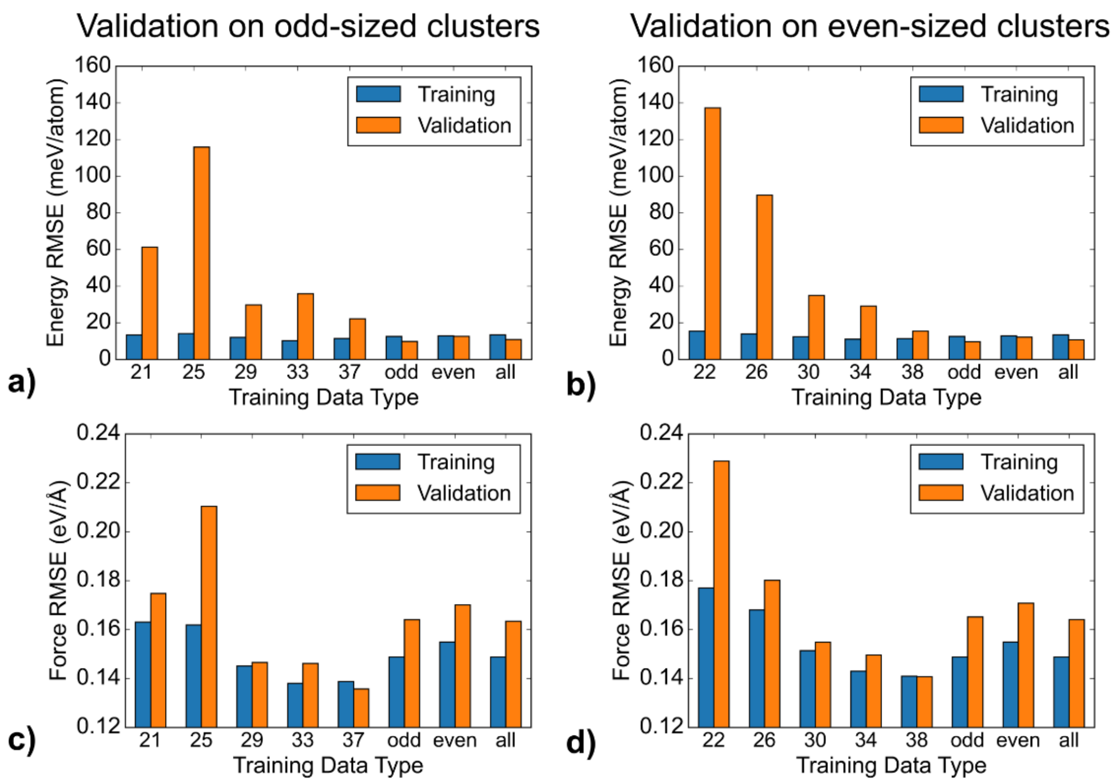

Figure 3. Training and validation root-mean-square errors in energy and force components for different potentials. The validation data consisted of clusters with 50-55 atoms. Plots in the left column show a) energy and c) force errors for potentials validated on odd-sized clusters, while the right column displays b) energy and d) force errors for potentials validated on even-sized structures. Potentials are labeled by the type of training data used to generate them. Numeric labels represent single-size potentials whose training sets contain exclusively clusters of the labelled sizes. The labels “odd”, “even” and “all” represent potentials whose training sets are made up by clusters with odd, even, and mixture of odd and even number of atoms respectively.

Prediction of structures for Al clusters with 41–55 atoms

To identify low-energy structures with 41-55 atoms, we used the mixed-size potentials trained on clusters with an odd or even number of atoms to initialize GA_AL searches for clusters with an odd or even number of atoms respectively. Initializing the GA_AL algorithm with a pre-trained potential demonstrated significant performance advantages, with an average acceleration ratio of 12.1 compared to GA_DFT. For sizes 45 and 54, the acceleration ratio was set to 0 since they failed to discover better or equivalent configurations as GA_DFT.

The sizable increase of acceleration ratios for GA_AL with pre-trained potentials can be credited to a significant reduction in the number of times DFT is called for learning on the fly in the early stages of the search. For GA_AL runs initialized with an untrained potential, clusters in the early stages of the runs tend to have high energies (Figure 4a), so training steps in the early stages are sampling a relatively high-energy region of configuration space. For GA_AL runs initialized with well-trained potentials, computational resources are more efficiently spent exploring the low-energy configurations.

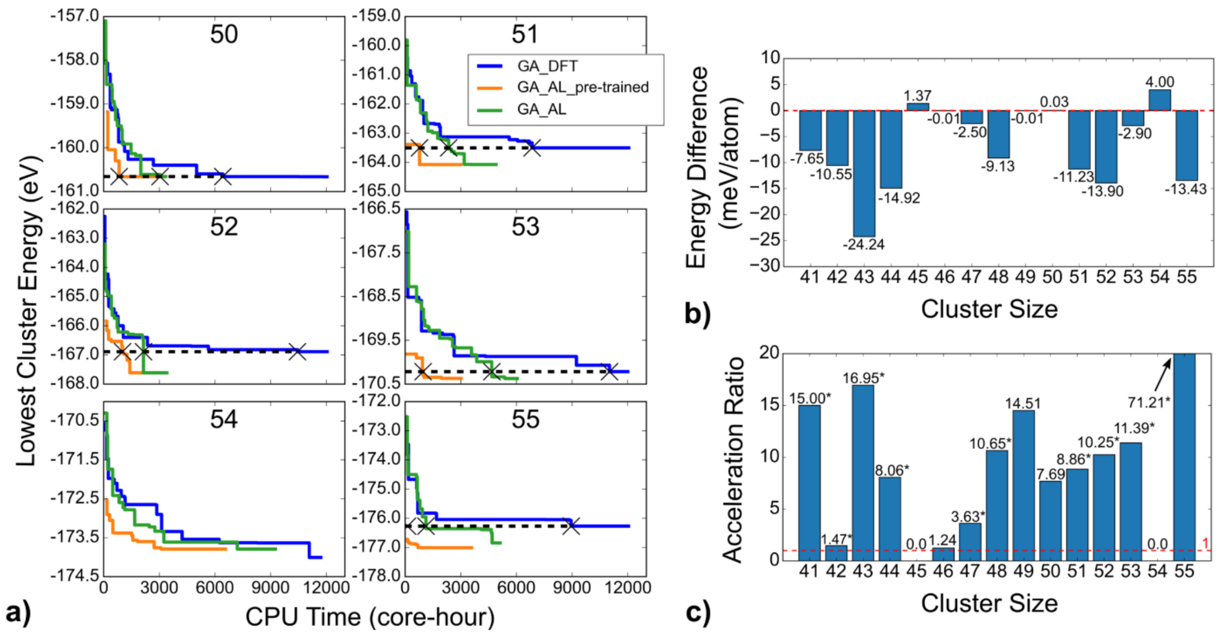

Figure 4. Performance benchmark of GA_AL against GA_DFT on clusters with 41 to 55 atoms. a) Energy evolution plots for GA_AL initialized with untrained potentials (green), GA_AL initialized with mixed-size potentials (orange) and GA_DFT (blue), for clusters with 50 to 55 atoms. The energy levels used to calculate acceleration ratios are marked by dashed lines. The CPU times used to compute acceleration ratios are marked by crosses. **b)** Energy differences between the lowest energies of GA_AL and GA_DFT at the end of simulations. **c)** Acceleration ratios of GA_AL relative to GA_DFT. The sizes for which GA_AL successfully discovered configurations with lower energy than the lowest of GA_DFT are marked by *.

Literature comparison

We examine the quality of the ground state configurations discovered using GA_AL for clusters of 21-55 atoms by comparing them with lowest-energy structures that have been previously reported for aluminum clusters. Here we only consider studies for which we were able to find the atomic coordinates of the discovered structures.[28,29,58-60] All structures collected from the literature were reoptimized by DFT using the same settings as those used in GA_AL. For 25 of the 35 sizes, GA_AL found structures at least 1 meV / atom lower in energy than the lowest-energy structure in the literature, and for another 7 sizes it identified the same lowest-energy structure as was available in the literature. For clusters of 22 atoms, GA_DFT found a structure that is structurally distinct from the lowest-energy structure reported in literature[28] but has only slightly lower energy (by 0.15 meV / atom). The GA_DFT algorithm discovered structures lower in energy than those discovered by GA_AL and the literature for 2 sizes. For clusters of 45 atoms, GA_DFT rediscovered the best-known structure from the literature but GA_AL did not. Detailed results are provided in Figure 5 and Table S4. A complete panel of lowest-energy clusters with 21 to 55 atoms is included in Figure S15 of the Supplementary Information and coordinates of these clusters are listed in a second Supplementary Information file.

Structures found using GA_AL have lower energies than the lowest-energy literature structures by an average of 16.81 meV/atom, with a maximum of 51.81 meV/atom at size 36 (1.87 eV/cluster). For the five sizes for which GA_AL did not discover the best structures (Figure 5a), the energies are no more than 4.0 meV/atom above those of the structures with the lowest known energies. The preferred morphologies of the lowest-energy clusters of aluminum alter between layered close-packed structures with FCC stacking order and tetrahedrons. The cluster with 36 atoms is particularly stable relative to its neighboring sizes (see Section 7.2 of the Supplementary Information), suggesting that it may be particularly likely to be synthesizable. Experimentally, positively-charged Al clusters with around 36 atoms have been observed to have relatively high melting temperatures.[63,64]

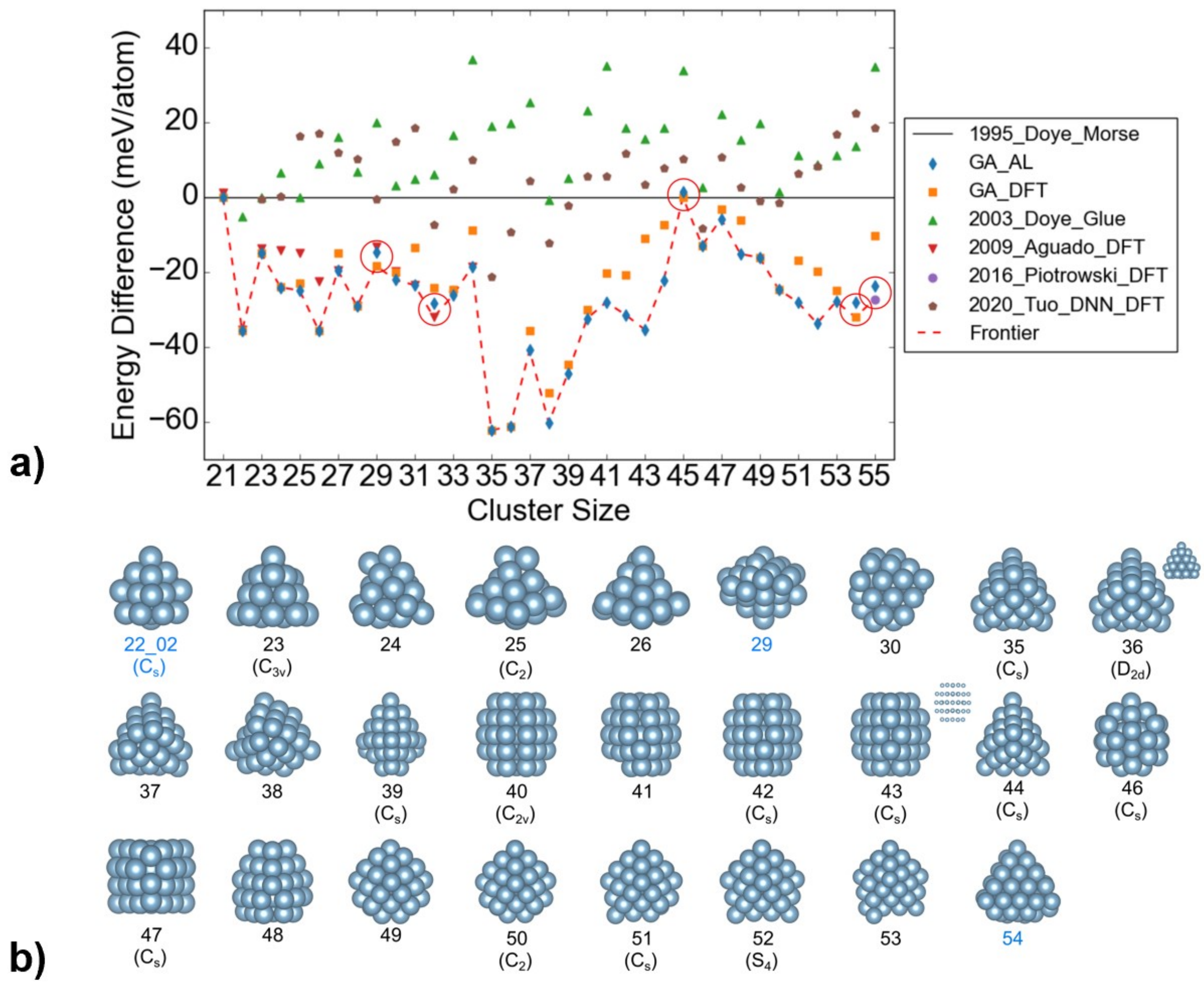

Figure 5. Comparison between lowest-energy clusters reported in the literature and those discovered by GA_AL and GA_DFT. a) Energy differences of lowest-energy clusters from various methods relative to the energies of clusters reported by Doye and coworkers.[58] The lowest-energy frontier is connected by a red dashed line, and the sizes for which GA_AL did not discover the best configurations are circled. "Morse", "Glue" and "DNN" in the legend represents the Morse potential, a glue potential and a deep neural network potential. **b)** New lowest-energy clusters discovered by GA_AL and GA_DFT. The labels of clusters identified by GA_DFT and not GA_AL are blue and corresponding symmetries are denoted in parentheses. Alternative views of representative layered close-packed structure (43) and tetrahedral clusters (36) are included above and to the right of the clusters.

DISCUSSION

Although the GA_AL approach presented here has clear advantages, including an order of magnitude acceleration compared to GA_DFT, there are potential areas for improvement. One is the relatively high energy prediction errors of MTP for nanoclusters compared with bulk systems.

Benchmarks by Zuo and coworkers[50] showed that MTP has energy errors generally less than 5 meV/atom and sometimes even lower than 1meV/atom for bulk elemental systems. However, for nanoclusters, as exhibited in Figure 3, validation energy errors are at the order of 10 meV/atom for small clusters with 24 atoms. They can be lowered by using smaller force weights, but the improvement comes at the expense of driving up force errors, which increases the possibility of creating artificial local minima. The relatively large energy errors increase the chance that the energy of the lowest-energy cluster is overestimated and never enters the pool. To mitigate this risk we used a relatively large pool size (25 clusters) to expand the energy window of pool clusters and raise the chance of the lowest-energy cluster being captured in the pool. A large pool has also been shown to increase the success rate of identifying the lowest-energy isomer due to the structural diversity of the pool,[21] although at the expense of slowing convergence speed.[20,21]

We found that the energy window of pool clusters became narrower as the structure search continued, implying a high density of metastable states with energies close to the global minimum, especially for large clusters. This is not unexpected since the dimension of configuration space dramatically increases as system size grows. The relatively narrow energy window increases the chance of the pool missing the lowest-energy isomer, as the window size may be comparable to the error in MTP energy predictions. A possible workaround is to run GA_AL and then use the discovered low-energy clusters to seed a GA_DFT search. This would consume additional computational resources but decrease the uncertainty in the proposed lowest-energy structures.

Another area for improvement is the relationship between the extrapolation grades (used to identify structures that trigger retraining) and prediction errors. A high extrapolation grade normally implies an energy evaluation with high uncertainty, but a low grade does not necessarily guarantee an accurate prediction (see Figure S17 of Supplementary Information). In practice, we addressed this challenge by starting DFT re-optimization and retraining whenever the majority of clusters in the pool had MTP-calculated energies but not DFT-calculated energies. An alternative approach would be to implement similarity-based measurements of uncertainty, which might more accurately identify structures for which the prediction errors are likely to be large.

Although we have demonstrated that potentials trained on small clusters can be used to predict the structures of clusters about twice as large, it is not clear how well these potentials will work on significantly larger particles. If transferability can be retained up to larger clusters, the methods we have presented could be used to efficiently create a comprehensive datasets of cluster structures for small particles with structures that cannot be simply described as that of a truncated crystal.

METHODS

Similarity measurement

We quantify geometric similarity between two cluster structures of same size by a similarity score calculated using an approach based on the spectral decomposition of extended distance matrices.[65] The score is non-negative and a smaller value implies higher similarity. Identical clusters have a score of 0, and visually distinguishable clusters typically have a score above about 0.3. The similarity measure is used to prevent geometrically similar clusters from being simultaneously included in the pool, which can improve the efficiency of GA,[21] and to select diverse training data for the moment tensor potentials.[55]

Genetic algorithm

A genetic algorithm is a global optimization method inspired by the principles of natural selection.[66] We developed our own code based off the pool-based Birmingham Parallel Genetic Algorithm[23] with some variations. A pool of low-energy clusters of fixed size is maintained during the search. Initial clusters are generated by randomly distributing atoms in space. Once the pool is filled, genetic operations, namely, crossover and mutation, are applied to parent clusters selected from the pool to generate child clusters. Child clusters that are dissimilar to all pool clusters and have a lower energy than the pool cluster with the highest energy will replace the highest-energy pool cluster. Additional details of the genetic algorithm can be found in Section 1 of the Supplementary Information.

Genetic algorithm with actively learned interatomic potentials

To accelerate the genetic algorithm search for new stable nanoclusters, we use machine-learned interatomic potentials (to improve speed) trained on-the-fly using active learning (to maintain accuracy). We refer to this combination of genetic algorithms and active learning as "GA_AL". The active-learning query strategy uses the generalized D-Optimality criterion implemented in the MLIP package,[46,47] which assigns unlabeled data an "extrapolation grade" based on a measure of the extent to which the unlabeled data is outside of the space spanned by the training data. An extrapolation grade above 1 implies extrapolation relative to the current training set and large errors should be expected, while a value below 1 indicates interpolation.[47]

The GA_AL runs batch retraining cycles and maintains a waitlist of structures to be included in the next cycle (Figure 6). Two extrapolation grade thresholds are used when determining whether a newly-generated cluster should be added to the waitlist. The first threshold, γ_{break}, is used to screen clusters before relaxation using MTP. The trained potential may struggle to relax clusters with extrapolation grades above this threshold, so they are automatically added to the waitlist. Structures with extrapolation grades below γ_{break} are relaxed. If the extrapolation grade of the relaxed structure is greater than the second threshold, γ_{select}, then it too is added to the waitlist. In this work γ_{break} was set to 10 for GA_AL initialized with untrained potential, as the default value recommend by MTP code.[47] A looser value of 1000 was used for the pre-trained potential, as it is not as important to add training data to a potential that has already been trained. As-generated clusters with extrapolation grades about 1000 typically cannot be evaluated accurately by MTP potentials, but we found they could still be relaxed by MTP to reasonable configurations. Starting DFT relaxations from configurations pre-relaxed using MTP was used to reduce computational costs. The parameter γ_{select} was set to 1.01 for all searches. When the waitlist reaches a user-defined value (here set to 5), the genetic algorithm is paused and a retraining cycle begins. All new clusters in the pool as well as clusters on the waitlist are relaxed using DFT and added to the training set. Before retraining the potential, a similarity screen is applied to select the most geometrically diverse set of configurations from all relaxation steps (discussed below), which maximizes structural diversity and reduces training cost.

Because of the uncertainty in MTP-predicted energies, there is a risk that the pool over time becomes polluted with structures with erroneously low MTP-predicted energies. To mitigate this risk, a retraining cycle is also started whenever a majority of the clusters in the pool (>50%) have energies that were calculated using MTP and not DFT. GA_AL is considered to be converged when no cluster with an energy lower than the lowest-energy pool cluster has been found for 4000 new clusters.

When initializing GA_AL with pre-trained potentials, it is beneficial to switch off retraining at the beginning of the search. In this approach, extrapolating clusters are discarded and new ones are regenerated until they are interpolating, allowing the GA to more fully explore the potential energy surface of the pre-trained potential. We did this for the first 5000 clusters in GA_AL runs initialized with mixed-size potentials when generating clusters with 41 to 55 atoms. Additional discussion and justification for this approach are provided in Section 1.4 of the Supplementary Information.

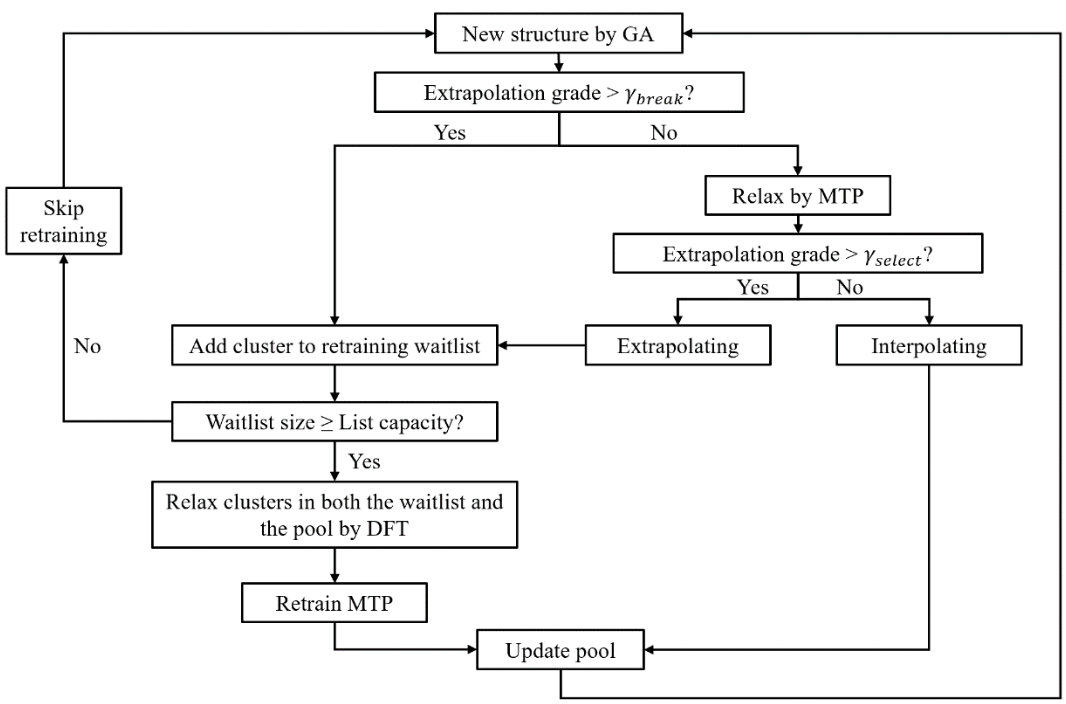

Figure 6. Schematic workflow of genetic algorithm with on-the-fly active learning (GA_AL). A double-threshold scheme is employed in which a looser threshold, γ_{break}, and a tighter threshold, γ_{select}, are used to determine extrapolation of as-generated structures and MTP-relaxed structures, respectively. Retraining starts when the waitlist exceeds a user-defined capacity, which was set to 5 in this work.

Moment tensor potentials

We used the MLIP package[47] to train moment tensor potentials. The hyperparameters for training include potential complexity, energy weight, force weight and stress weight. Potential complexity is characterized by the maximum level of moments, lev_{max}, of basis functions.[45,47] The energy weight was always set to 1, so the force weight can be seen as the weight of force components relative to the weight of the energy. The stress weight was set to 0 since it is irrelevant in the case of clusters due to the lack of lattice. We generated potentials with lev_{max}=14 and a force weight of 1/1000 relative to the energy weight, to balance between accuracy and training cost, as shown in the Results section and Section 2.2 of Supplementary Information. The inner and outer cutoff radii defining the local atomic neighborhood were set to the default values of 2 Å and 5 Å, and eight radial basis functions were used.[47] A maximum number of 5000 training iterations were allowed for potential fitting. This limit was never reached, as the maximum number of training iterations in any GA_AL run was 1399.

Training data selection for pre-trained potentials

To select the training data for the pre-trained mixed-size potentials, we used a diversity-based strategy and an energy-based strategy to select structurally diverse structures from DFT relaxations and to improve accuracy in the low-lying regions of the potential energy surface. All DFT calculations were collected from GA_DFT and GA_AL runs on clusters with 21–40 atoms. For each of the constituent cluster sizes, relaxation trajectories were only kept if the corresponding local ground states have similarity scores larger than 0.3 with the local ground states of all other trajectories already included in the training set. Within each trajectory, only dissimilar ionic steps were selected as well. We accomplished this by including the fully relaxed structure and iterating backwards through the relaxation until encountering a structure with a similarity score, relative to the most recently-added structure, that was at least 0.3. That structure was then added to the training set, and we repeated this procedure until all relaxation steps were exhausted. This diversity-based strategy was applied throughout this work, in data preparation processes for both training and validation sets.

Following the similarity screening, we performed an energy-based selection strategy. First, all structures that passed through the diversity screening were grouped into sets based on the number of atoms in the cluster. 50% of the training data selected from each set consisted of the structures with lowest energy, 10% consisted of the structures with the highest energy, and the remaining 40% were randomly from the remaining ionic steps.

A total of 3000 structures were selected for each of the training sets. For potentials trained with clusters of multiple sizes (the ones labelled by “odd”, “even” and “all” in Figure 3), equal numbers of structures were chosen for each constituent sizes. For potentials trained with clusters of a single size, all 3000 structures were chosen from clusters of that size. The training set for the potential trained with clusters of 21 atoms only contains 2136 structures after the diversity filtering of DFT calculations, and were all included in the training set.

Validation data selection for pre-trained potentials

We collected validation data for mixed-size potentials from GA_DFT runs on clusters with 50–55 atoms. The diversity-based strategy discussed above was used to select a structurally diverse set of structures. The validation sets contain around 3000 structures for each size (details are provided in Section 3.1 of the Supplementary Information).

Training data selection for on-the-fly retraining in GA_AL

We also use similarity filtering, as described above, to select structures for retraining on-the-fly. Similarity filtering is used to select distinct clusters from each relaxation trajectory during active learning. We used a tight similarity threshold of 0.3 on small to medium clusters (21–40) and a looser threshold of 0.15 on large clusters (41–55). The looser threshold is meant to increase the fraction of available data used for retraining for large clusters, as generating this data is computationally more expensive. We do not check similarity between new training data and all existing data on-the-fly, as this is computationally costly.

Comparison of GA_AL against GA_DFT

Both GA_AL and GA_DFT were run using the same set of genetic algorithm parameters (see Section 1.3 of the Supplementary Information) on all 24 cores of Intel E5-2680 V3 processors. The GA_AL runs were performed until 4000 consecutive new clusters had been generated without identifying a new lowest-energy cluster. GA_DFT runs were performed for at least the same amount of time as GA_AL runs for fair comparison. For large clusters with 50–55 atoms, GA_DFT searches were executed for a much longer time of 21 days, to reach comparable energy levels as GA_AL runs (see also Section 1.2 of the Supplementary Information). The reported time spent for GA_AL includes the time spent in the genetic algorithm search, time required to generate training data using DFT, and time spent training the interatomic potential. For GA_AL runs initialized with pre-trained potentials, the time spent pre-training the potential was also included. The only difference between the GA_AL and GA_DFT algorithms was that GA_AL used moment tensor potentials with active learning, whereas GA_DFT used only DFT for relaxation. Low-energy structures identified in GA_AL were re-optimized using DFT at the retraining stage and only DFT-evaluated energies were reported at the end, to ensure an *ab initio* level of accuracy.

To determine whether a new low-energy structure had been found, we considered both the DFT-calculated energy and similarity scores. A cluster that is lower in energy by at least 1 meV/atom and at the same time has a similarity score, compared to the existing lowest-energy structure, that is greater than 0.3 is identified as a new lowest-energy cluster. Clusters that have a total energy within 1 meV/atom to the existing lowest-energy cluster but are structurally dissimilar are considered as energetically similar clusters and are not counted as new lowest-energy clusters. Borderline cases were inspected manually. More details of how we determined whether the algorithm had found a new lowest-energy structure can be found in Section 6 of the Supplementary Information.

DFT calculations

All DFT calculations were carried out using the Vienna ab-initio simulation package (VASP)[62,67-69] with the Perdew-Burke-Ernzerhof (PBE) exchange-correlation functional.[70-72] The projector augmented wave (PAW) dataset shipped with VASP with the title "PAW_PBE Al 04Jan2001" was used.[73,74] Reciprocal space was sampled by a single *k*-point at the Γ point and the kinetic energy cutoff for the plane-wave basis was set to 240 eV. The electronic self-consistency loop was considered to reach convergence when subsequent steps had an energy difference below 10^{-5} eV and the convergence criterion for ionic relaxation was set to a force difference below 0.01 eV/Å. Our dataset[75] shows that ground state Al nanoclusters with even sizes above 18 and odd sizes above 7 have net spins of 0 μ_B and 1 μ_B, respectively (see Section 4 of Supplementary Information). Therefore, all *ab initio* calculations fix the magnetic moment to 0 μ_B for even-sized clusters and to 1 μ_B for odd-sized clusters using the parameter NUPDOWN in VASP.

DATA AVAILABILITY

Structure files for the lowest-energy clusters with 21 to 55 atoms are listed in a separate Supplementary Information file in the XYZ format.

CODE AVAILABILITY

Our implementation of the GA_AL procedure is open-sourced under the Apache License 2.0 at https://gitlab.com/muellergroup/cluster-ga. The code also supports genetic algorithm searches using only DFT or interatomic potentials through interfaces with VASP and LAMMPS. Input templates and documentation of input parameters can be found in the repository.

ACKONWLEDGEMENT

We thank Prof. Alexander V. Shapeev for providing helpful guidance in using the MLIP package. The work was supported by the Office of Naval Research under the grant No. ONR MURI N00014-15-1-2681. Calculations were performed using computational resources from the Maryland Advanced Research Computing Cluster (MARCC), the Stampede2 supercomputer at the Texas Advanced Computer Center (TACC) and the Gordon supercomputer in Department of Defense High Performance Computing Modernization Program. TACC resources were provided through the XSEDE program with NSF award DMR-140068. Images of the atomic structures of clusters were generated using VESTA.[76]

AUTHOR CONTRIBUTIONS

T.M. conceptualized and managed the project. Y.W., S.L., P.L., S.N., A.H. and T.M. developed the software. Y.W., S.L. and T.M. wrote the manuscript. Y.W. performed the benchmarks on MTP. Y.W., S.L., and S.M. carried out GA searches and analyzed data. S.L., Y.W. and S.M. collected structures from literatures. All the authors proposed, discussed, or developed ideas that improved the performance of the GA_AL procedure and the quality of the data.

References

1 Kang, X., Li, Y., Zhu, M. & Jin, R. Atomically precise alloy nanoclusters: syntheses, structures, and properties. *Chemical Society Reviews* **49**, 6443-6514, doi:10.1039/C9CS00633H (2020).

2 Jena, P. & Castleman, A. W. Clusters: A bridge across the disciplines of physics and chemistry. *Proceedings of the National Academy of Sciences* **103**, 10560, doi:10.1073/pnas.0601782103 (2006).

3 Gawande, M. B. *et al.* Cu and Cu-Based Nanoparticles: Synthesis and Applications in Catalysis. *Chemical Reviews* **116**, 3722-3811, doi:10.1021/acs.chemrev.5b00482 (2016).

4 Liu, L. & Corma, A. Metal Catalysts for Heterogeneous Catalysis: From Single Atoms to Nanoclusters and Nanoparticles. *Chemical Reviews* **118**, 4981-5079, doi:10.1021/acs.chemrev.7b00776 (2018).

5 Jin, R., Zeng, C., Zhou, M. & Chen, Y. Atomically Precise Colloidal Metal Nanoclusters and Nanoparticles: Fundamentals and Opportunities. *Chemical Reviews* **116**, 10346-10413, doi:10.1021/acs.chemrev.5b00703 (2016).

6 Li, G. & Jin, R. Atomically Precise Gold Nanoclusters as New Model Catalysts. *Accounts of Chemical Research* **46**, 1749-1758, doi:10.1021/ar300213z (2013).

7 Saha, K., Agasti, S. S., Kim, C., Li, X. & Rotello, V. M. Gold Nanoparticles in Chemical and Biological Sensing. *Chemical Reviews* **112**, 2739-2779, doi:10.1021/cr2001178 (2012).

8 Kang, X. & Zhu, M. Tailoring the photoluminescence of atomically precise nanoclusters. *Chemical Society Reviews* **48**, 2422-2457, doi:10.1039/C8CS00800K (2019).

9 Jin, R. Atomically precise metal nanoclusters: stable sizes and optical properties. *Nanoscale* **7**, 1549-1565, doi:10.1039/C4NR05794E (2015).

10 White, R. J., Luque, R., Budarin, V. L., Clark, J. H. & Macquarrie, D. J. Supported metal nanoparticles on porous materials. Methods and applications. *Chemical Society Reviews* **38**, 481-494, doi:10.1039/B802654H (2009).

11 Martin, T. P. Shells of atoms. *Physics Reports* **273**, 199-241, doi:https://doi.org/10.1016/0370-1573(95)00083-6 (1996).

12 Ferrando, R., Jellinek, J. & Johnston, R. L. Nanoalloys: From Theory to Applications of Alloy Clusters and Nanoparticles. *Chemical Reviews* **108**, 845-910, doi:10.1021/cr040090g (2008).

13 Wales, D. J. & Doye, J. P. K. Global Optimization by Basin-Hopping and the Lowest Energy Structures of Lennard-Jones Clusters Containing up to 110 Atoms. *The Journal of Physical Chemistry A* **101**, 5111-5116, doi:10.1021/jp970984n (1997).

14 Wales, D. J. & Scheraga, H. A. Global Optimization of Clusters, Crystals, and Biomolecules. *Science* **285**, 1368, doi:10.1126/science.285.5432.1368 (1999).

15 Pickard, C. J. & Needs, R. J. Ab initio random structure searching. *J Phys-Condens Mat* **23** (2011).

16 Call, S. T., Zubarev, D. Y. & Boldyrev, A. I. Global minimum structure searches via particle swarm optimization. *Journal of Computational Chemistry* **28**, 1177-1186, doi:https://doi.org/10.1002/jcc.20621 (2007).

17 Wang, Y., Lv, J., Zhu, L. & Ma, Y. Crystal structure prediction via particle-swarm optimization. *Physical Review B* **82**, 094116, doi:10.1103/PhysRevB.82.094116 (2010).

18 Weigend, F. & Ahlrichs, R. Quantum chemical treatments of metal clusters. *Philosophical Transactions of the Royal Society a-Mathematical Physical and Engineering Sciences* **368**, 1245-1263, doi:10.1098/rsta.2009.0268 (2010).

19 Ahlrichs, R. & D. Elliott, S. Clusters of aluminium, a density functional study. *Phys Chem Chem Phys* **1**, 13-21, doi:10.1039/A807713D (1999).
20 Johnston, R. L. Evolving better nanoparticles: Genetic algorithms for optimising cluster geometries. *Dalton Transactions*, 4193-4207, doi:10.1039/B305686D (2003).
21 Vilhelmsen, L. B. & Hammer, B. A genetic algorithm for first principles global structure optimization of supported nano structures. *J Chem Phys* **141** (2014).
22 Tipton, W. W. & Hennig, R. G. A grand canonical genetic algorithm for the prediction of multi-component phase diagrams and testing of empirical potentials. *Journal of Physics: Condensed Matter* **25**, 495401, doi:10.1088/0953-8984/25/49/495401 (2013).
23 Shayeghi, A., Götz, D., Davis, J. B. A., Schäfer, R. & Johnston, R. L. Pool-BCGA: a parallelised generation-free genetic algorithm for the ab initio global optimisation of nanoalloy clusters. *Phys Chem Chem Phys* **17**, 2104-2112, doi:10.1039/C4CP04323E (2015).
24 Deaven, D. M. & Ho, K. M. Molecular-Geometry Optimization with a Genetic Algorithm. *Phys Rev Lett* **75**, 288-291 (1995).
25 Vargas, J. A., Buendía, F. & Beltrán, M. R. New Au_N (N = 27–30) Lowest Energy Clusters Obtained by Means of an Improved DFT–Genetic Algorithm Methodology. *The Journal of Physical Chemistry C* **121**, 10982-10991, doi:10.1021/acs.jpcc.6b12848 (2017).
26 Davis, J. B. A., Shayeghi, A., Horswell, S. L. & Johnston, R. L. The Birmingham parallel genetic algorithm and its application to the direct DFT global optimisation of Ir_N (N = 10–20) clusters. *Nanoscale* **7**, 14032-14038, doi:10.1039/C5NR03774C (2015).
27 Drebov, N. & Ahlrichs, R. Structures of Al_n, its anions and cations up to n=34: A theoretical investigation. *The Journal of Chemical Physics* **132**, 164703, doi:10.1063/1.3403692 (2010).
28 Aguado, A. & López, J. M. Structures and stabilities of Al_n^+, Al_n, and Al_n^- (n=13–34) clusters. *The Journal of Chemical Physics* **130**, 064704, doi:10.1063/1.3075834 (2009).
29 Doye, J. P. K. A model metal potential exhibiting polytetrahedral clusters. *The Journal of Chemical Physics* **119**, 1136-1147, doi:10.1063/1.1574797 (2003).
30 Xiang, Y., Jiang, H., Cai, W. & Shao, X. An Efficient Method Based on Lattice Construction and the Genetic Algorithm for Optimization of Large Lennard-Jones Clusters. *The Journal of Physical Chemistry A* **108**, 3586-3592, doi:10.1021/jp037780t (2004).
31 Galvão, B. R. L. & Viegas, L. P. What Electronic Structure Method Can Be Used in the Global Optimization of Nanoclusters? *The Journal of Physical Chemistry A* **123**, 10454-10462, doi:10.1021/acs.jpca.9b09309 (2019).
32 Behler, J. Perspective: Machine learning potentials for atomistic simulations. *The Journal of Chemical Physics* **145**, 170901, doi:10.1063/1.4966192 (2016).
33 Mueller, T., Hernandez, A. & Wang, C. Machine learning for interatomic potential models. *The Journal of Chemical Physics* **152**, 050902, doi:10.1063/1.5126336 (2020).
34 Schmidt, J., Marques, M. R. G., Botti, S. & Marques, M. A. L. Recent advances and applications of machine learning in solid-state materials science. *Npj Comput Mater* **5**, 83, doi:10.1038/s41524-019-0221-0 (2019).
35 Deringer, V. L., Caro, M. A. & Csányi, G. Machine Learning Interatomic Potentials as Emerging Tools for Materials Science. *Advanced Materials* **31**, 1902765, doi:10.1002/adma.201902765 (2019).

36 Ramprasad, R., Batra, R., Pilania, G., Mannodi-Kanakkithodi, A. & Kim, C. Machine learning in materials informatics: recent applications and prospects. *Npj Comput Mater* **3**, 54, doi:10.1038/s41524-017-0056-5 (2017).
37 Quaranta, V., Behler, J. & Hellström, M. Structure and Dynamics of the Liquid–Water/Zinc-Oxide Interface from Machine Learning Potential Simulations. *The Journal of Physical Chemistry C* **123**, 1293-1304, doi:10.1021/acs.jpcc.8b10781 (2019).
38 Houchins, G. & Viswanathan, V. An accurate machine-learning calculator for optimization of Li-ion battery cathodes. **153**, 054124, doi:10.1063/5.0015872 (2020).
39 Chiriki, S. & Bulusu, S. S. Modeling of DFT quality neural network potential for sodium clusters: Application to melting of sodium clusters (Na20 to Na40). *Chemical Physics Letters* **652**, 130-135, doi:https://doi.org/10.1016/j.cplett.2016.04.013 (2016).
40 Bartók, A. P., Payne, M. C., Kondor, R. & Csányi, G. Gaussian Approximation Potentials: The Accuracy of Quantum Mechanics, without the Electrons. *Phys Rev Lett* **104**, 136403, doi:10.1103/PhysRevLett.104.136403 (2010).
41 Bartók, A. P., Kondor, R. & Csányi, G. On representing chemical environments. *Physical Review B* **87**, 184115, doi:10.1103/PhysRevB.87.184115 (2013).
42 Szlachta, W. J., Bartók, A. P. & Csányi, G. Accuracy and transferability of Gaussian approximation potential models for tungsten. *Physical Review B* **90**, 104108, doi:10.1103/PhysRevB.90.104108 (2014).
43 Thompson, A. P., Swiler, L. P., Trott, C. R., Foiles, S. M. & Tucker, G. J. Spectral neighbor analysis method for automated generation of quantum-accurate interatomic potentials. *J Comput Phys* **285**, 316-330, doi:https://doi.org/10.1016/j.jcp.2014.12.018 (2015).
44 Wood, M. A. & Thompson, A. P. Extending the accuracy of the SNAP interatomic potential form. *The Journal of Chemical Physics* **148**, 241721, doi:10.1063/1.5017641 (2018).
45 Shapeev, A. V. Moment Tensor Potentials: A Class of Systematically Improvable Interatomic Potentials. *Multiscale Model Sim* **14**, 1153-1173 (2016).
46 Podryabinkin, E. V. & Shapeev, A. V. Active learning of linearly parametrized interatomic potentials. *Comp Mater Sci* **140**, 171-180, doi:10.1016/j.commatsci.2017.08.031 (2017).
47 Novikov, I. S., Gubaev, K., Podryabinkin, E. V. & Shapeev, A. V. The MLIP package: moment tensor potentials with MPI and active learning. *Machine Learning: Science and Technology* **2**, 025002, doi:10.1088/2632-2153/abc9fe (2021).
48 Drautz, R. Atomic cluster expansion for accurate and transferable interatomic potentials. *Physical Review B* **99**, 014104, doi:10.1103/PhysRevB.99.014104 (2019).
49 Hernandez, A., Balasubramanian, A., Yuan, F., Mason, S. A. M. & Mueller, T. Fast, accurate, and transferable many-body interatomic potentials by symbolic regression. *Npj Comput Mater* **5**, 112, doi:10.1038/s41524-019-0249-1 (2019).
50 Zuo, Y. X. *et al.* Performance and Cost Assessment of Machine Learning Interatomic Potentials. *J Phys Chem A* **124**, 731-745, doi:10.1021/acs.jpca.9b08723 (2020).
51 Hartke, B. Global geometry optimization of clusters guided by N-dependent model potentials. *Chemical Physics Letters* **258**, 144-148, doi:https://doi.org/10.1016/0009-2614(96)00629-X (1996).
52 Deringer, V. L., Proserpio, D. M., Csányi, G. & Pickard, C. J. Data-driven learning and prediction of inorganic crystal structures. *Faraday Discussions* **211**, 45-59, doi:10.1039/C8FD00034D (2018).

53 Podryabinkin, E. V., Tikhonov, E. V., Shapeev, A. V. & Oganov, A. R. Accelerating crystal structure prediction by machine-learning interatomic potentials with active learning. *Physical Review B* **99**, 064114, doi:10.1103/PhysRevB.99.064114 (2019).
54 Gubaev, K., Podryabinkin, E. V., Hart, G. L. W. & Shapeev, A. V. Accelerating high-throughput searches for new alloys with active learning of interatomic potentials. *Comp Mater Sci* **156**, 148-156 (2019).
55 Bernstein, N., Csányi, G. & Deringer, V. L. De novo exploration and self-guided learning of potential-energy surfaces. *Npj Comput Mater* **5**, 99, doi:10.1038/s41524-019-0236-6 (2019).
56 Kolsbjerg, E. L., Peterson, A. A. & Hammer, B. Neural-network-enhanced evolutionary algorithm applied to supported metal nanoparticles. *Physical Review B* **97**, 195424, doi:10.1103/PhysRevB.97.195424 (2018).
57 Tong, Q., Xue, L., Lv, J., Wang, Y. & Ma, Y. Accelerating CALYPSO structure prediction by data-driven learning of a potential energy surface. *Faraday Discussions* **211**, 31-43, doi:10.1039/C8FD00055G (2018).
58 Doye, J. P. K., Wales, D. J. & Berry, R. S. The effect of the range of the potential on the structures of clusters. *The Journal of Chemical Physics* **103**, 4234-4249, doi:10.1063/1.470729 (1995).
59 Piotrowski, M. J. *et al.* Theoretical Study of the Structural, Energetic, and Electronic Properties of 55-Atom Metal Nanoclusters: A DFT Investigation within van der Waals Corrections, Spin–Orbit Coupling, and PBE+U of 42 Metal Systems. *The Journal of Physical Chemistry C* **120**, 28844-28856, doi:10.1021/acs.jpcc.6b10404 (2016).
60 Tuo, P., Ye, X. B. & Pan, B. C. A machine learning based deep potential for seeking the low-lying candidates of Al clusters. *The Journal of Chemical Physics* **152**, 114105, doi:10.1063/5.0001491 (2020).
61 Nyshadham, C. *et al.* Machine-learned multi-system surrogate models for materials prediction. *Npj Comput Mater* **5**, 51, doi:10.1038/s41524-019-0189-9 (2019).
62 Kresse, G. & Furthmuller, J. Efficient iterative schemes for ab initio total-energy calculations using a plane-wave basis set. *Physical Review B* **54**, 11169-11186 (1996).
63 Neal, C. M., Starace, A. K. & Jarrold, M. F. Melting transitions in aluminum clusters: The role of partially melted intermediates. *Physical Review B* **76**, 054113, doi:10.1103/PhysRevB.76.054113 (2007).
64 Aguado, A. & Jarrold, M. F. Melting and Freezing of Metal Clusters. *Annual Review of Physical Chemistry* **62**, 151-172, doi:10.1146/annurev-physchem-032210-103454 (2011).
65 Li, X.-T., Yang, X.-B. & Zhao, Y.-J. Geometrical eigen-subspace framework based molecular conformation representation for efficient structure recognition and comparison. *The Journal of Chemical Physics* **146**, 154108, doi:10.1063/1.4981212 (2017).
66 Holland, J. H. *Adaptation in natural and artificial systems*. (University of Michigan Press, 1975).
67 Kresse, G. & Hafner, J. Ab initio molecular dynamics for liquid metals. *Physical Review B* **47**, 558-561, doi:10.1103/PhysRevB.47.558 (1993).
68 Kresse, G. & Hafner, J. Ab initio molecular-dynamics simulation of the liquid-metal--amorphous-semiconductor transition in germanium. *Physical Review B* **49**, 14251-14269, doi:10.1103/PhysRevB.49.14251 (1994).
69 Kresse, G. & Furthmuller, J. Efficiency of ab-initio total energy calculations for metals and semiconductors using a plane-wave basis set. *Comp Mater Sci* **6**, 15-50 (1996).

70 Perdew, J. P., Burke, K. & Wang, Y. Generalized gradient approximation for the exchange-correlation hole of a many-electron system. *Physical Review B* **54**, 16533-16539, doi:10.1103/PhysRevB.54.16533 (1996).
71 Perdew, J. P., Burke, K. & Ernzerhof, M. Generalized Gradient Approximation Made Simple. *Phys Rev Lett* **77**, 3865-3868, doi:10.1103/PhysRevLett.77.3865 (1996).
72 Perdew, J. P. & Yue, W. Accurate and simple density functional for the electronic exchange energy: Generalized gradient approximation. *Physical Review B* **33**, 8800-8802, doi:10.1103/PhysRevB.33.8800 (1986).
73 Blöchl, P. E. Projector augmented-wave method. *Physical Review B* **50**, 17953-17979, doi:10.1103/PhysRevB.50.17953 (1994).
74 Kresse, G. & Joubert, D. From ultrasoft pseudopotentials to the projector augmented-wave method. *Physical Review B* **59**, 1758-1775, doi:10.1103/PhysRevB.59.1758 (1999).
75 Manna, S. *et al.* A Database to Enable the Design and Discovery of Atomically Precise Nanoclusters. (Manuscript in preparation).
76 Momma, K. & Izumi, F. VESTA 3 for three-dimensional visualization of crystal, volumetric and morphology data. *Journal of Applied Crystallography* **44**, 1272-1276, doi:10.1107/s0021889811038970 (2011).

Supplementary Information

for

"Accelerated Prediction of Atomically Precise Cluster Structures Using On-the-fly Machine Learning"

Yunzhe Wang, Shanping Liu, Peter Lile, Sam Norwood, Alberto Hernandez, Sukriti Manna, and Tim Mueller*

Department of Materials Science and Engineering, Johns Hopkins University, Baltimore, MD 21218

*Corresponding Author Email: tmueller@jhu.edu

1 Genetic Algorithm

A genetic algorithm (GA) is a global optimization method inspired by the principle of natural selection.[1] Genetic algorithms have been successfully applied to discover ground state configurations for a diverse set of systems including elemental metal clusters,[2-5] binary and ternary alloys,[6-8] crystals,[9,10] oxides,[11] perovskites,[12] and metal organic frameworks (MOFs).[13] The efficiency of genetic algorithms comes from the fact that they can identify low-energy local atomic motifs and re-use them when generating candidate structures.[3] This section provides additional details about the genetic algorithm (GA) implementation used in this work.

1.1 Workflow of GA_DFT

Our core implementation of the genetic algorithm, which we refer to as GA_DFT, uses only density functional theory (DFT) to evaluate energies. Our approach is based off the pool-based Birmingham Parallel Genetic Algorithm (BPGA)[5] with some variations. In a pool-based GA, a fixed-size pool is maintained and comprises the lowest energy clusters among all structures that have been evaluated. This ensures that after each update the pool is at least as good as the old one. In this section we describe the general workflow of our code, with the specific parameters used in this work reported in later sections.

The GA has two phases: an initial phase when the pool starts off unfilled, and the genetic phase when the pool is full and child structure are generated by genetic operations. During the initial phase, structures can be generated by either a random distribution of atoms or by a seeding operation. We used the former method of random distribution of atoms in this work. With the former method, a cluster is generated by randomly distributing atoms in a cubic box with a side length of $2r\sqrt[3]{N}$ where r is the atomic radius of corresponding element and N is the number of atoms. This approach ensures cluster volumes grow proportionately with the system size yet are not too sparsely populated.

In the **seeding** operation, new structures are generated from seed structures which are typically known low-energy structures with different numbers of atoms. Atoms are either randomly added or subtracted from the seed structure until it reaches the target size. If a seed cluster consists of a different element, the atomic coordinates and cell size are scaled proportionately to the ratio of atomic radii. Although it is available in the open-source code, this operation was not used in this work.

Once the pool has been filled, the genetic algorithm begins to generate clusters using one of the three genetic operations: seeding (as described above), mutation, and crossover.

In a **mutation** operation, a parent cluster is randomly selected from the pool and a randomly chosen subset of atoms is either globally displaced or rotated around the center of mass to create a child configuration.

In a **crossover** operation, a roulette wheel scheme is used to pick pairs of parents from the pool, and the probability of a cluster being chosen is proportional to its selectability, which is designed to reward low-energy clusters and panelize those that have been picked many times.[3,4] The selectability of i^{th} cluster is defined as

$$S_i = f_i \times v_i \,, \tag{1}$$

where f_i represents the fitness of the i^{th} cluster and v_i is a penalty term that depends on parenting frequency. The fitness is defined using a hyperbolic function of a normalized total energy,

$$f_i = \tfrac{1}{2}\left[1 - \tanh\left(2\rho_i - 1\right)\right], \tag{2}$$

where the normalized energy ρ_i is given by

$$\rho_i = \frac{E_i - E_{min}}{E_{max} - E_{min}} \,, \tag{3}$$

where E_{min} and E_{max} are the lowest and highest energies of the clusters in the pool.[3] The lower total energy one cluster has relative to the others, the higher probability it has to be selected as parent. The penalty term is formulated to avoid overusing of the same cluster and is calculated as

$$v_i = \frac{1}{1 + \sqrt{n_i}} \,, \tag{4}$$

where n_i stands for the number of times the i^{th} cluster has been picked as one of the parents in crossover during the entire GA run. It has been shown that the use of both the fitness function and the frequency penalty to determine selectability can accelerate the convergence speed and increase the success rate of GA.[3,4] Once a pair of parents is chosen, a child cluster is created by the cut-and-splice operation devised by Deaven and Ho.[14] In addition to the common practice in which a child cluster inherits equal share of total atoms from each parent (even), varying percentages are allowed. The inheritance ratio can be proportional to fitness of clusters (weighted) or be randomly decided (random).

Newly generated configurations from all methods are checked for occurrences of atom overlap. Two atoms are considered as overlapping if their pairwise distances are smaller than 80% of the sum of atomic radii. If overlap exists, the corresponding cluster is regenerated by the same type of operation until it clears the examination.

Following successful cluster generation, the clusters are put in simulation boxes with lengths that allow at least 10 Å between adjacent periodic images, and the atomic coordinates are relaxed using either density functional theory (DFT) or interatomic potentials. Currently, our code supports VASP[15-17] and LAMMPS,[18] but any other energy-evaluation methods can be applied. Once child clusters are relaxed, they are compared with pool clusters. Child clusters which have lower energies than pool clusters and are structurally unique (defined here as having a similarity score above 0.3) are added to the pool, and the highest energy pool clusters are removed to maintain a constant pool size. If a new cluster has a similarity score of less than 0.3 with one or more pool clusters and lower energy than all of those pool structures, it will replace either the most similar pool cluster if the smallest score is less than 0.1 or the similar pool cluster with the highest energy if all scores are larger than 0.1. The similarity examination maintains the structural diversity of the pool, which improves the convergence speed and the success rate.[3] Following the update of pool, new parents are picked to reproduce next round of child clusters. This cycle continues until the genetic algorithm reaches a convergence criterion or the total number of clusters exceeds a maximum value. A schematic workflow summarizing this workflow is shown in Figure S1.

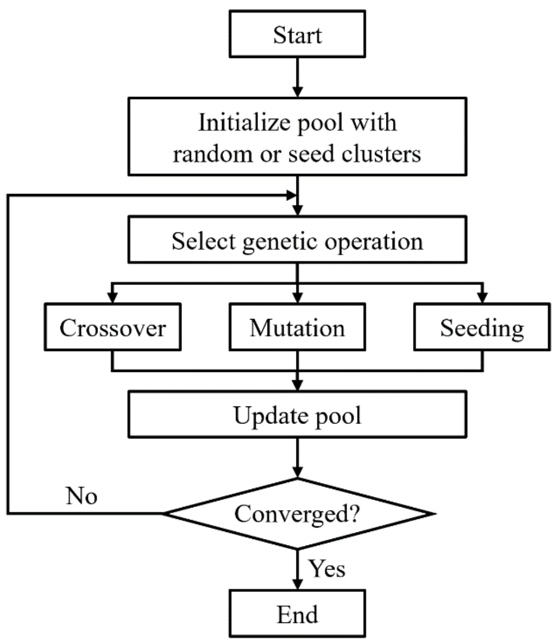

Figure S1. Schematic workflow for the primitive genetic algorithm without active learning acceleration.

1.2 Convergence criteria and total running time

We consider the GA to be converged when the pool becomes stagnant, which is defined here as occurring after the GA continuously generates 4000 or more clusters without discovering a cluster with lower energy than the current lowest value. For the calculations presented in the main text, GA_ALs were initially run for 3 days (1728 CPU-hours) for sizes 21 to 40 and for 6 days (3456 CPU-hours) for sizes 41 to 55, followed with a check for stagnation. For the sizes in which the convergence criterion was not met, the GAs were resumed until convergence. GA_DFT, on the other hand, is computationally expensive and evaluating 4000 clusters or more can be prohibitively expensive for the sizes investigated in this work. To ensure a fair comparison with GA_ALs, GA_DFT calculations were run for at least the same number of CPU-hours as the corresponding GA_AL calculations. For clusters with 50 to 55 atoms, GA_DFT calculations were run for 21 days, much longer than GA_DFT calculations on small to medium-sized clusters, to reach similar energy levels as GA_AL calculations and to make comparisons meaningful. Table S1 summarizes computational time for all GA runs in this work. The computing center (MARCC) we used has a wall-time limit of 3 days for each individual job, so calculations were mostly performed for a multiple of 3 days. Some calculations that were very close to convergence (e.g., for sizes 39, 40, 47, 55) were continued for only one or two days, which was sufficient to reach convergence.

Table S1. Computation time in days for all GA calculations in the main text.

Cluster Size	GA_AL with pre-trained potentials	GA_AL without pre-trained potentials	GA_DFT	Cluster Size	GA_AL with pre-trained potentials	GA_AL without pre-trained potentials	GA_DFT
21	--	3	3	39	--	5	5
22	--	3	3	40	--	4	4
23	--	3	3	41	6	--	6
24	--	3	3	42	6	--	6
25	--	3	3	43	6	--	6
26	--	3	3	44	6	--	6
27	--	3	3	45	6	--	6
28	--	3	3	46	6	--	6
29	--	3	3	47	7	--	7
30	--	3	3	48	6	--	6
31	--	3	3	49	6	--	6
32	--	3	3	50	6	6	21
33	--	3	3	51	6	9	21
34	--	3	3	52	6	6	21
35	--	3	3	53	6	11	21
36	--	3	3	54	12	17	21
37	--	3	3	55	7	9	21
38	--	3	3				

1.3 GA input parameters

Parameters controlling the GA workflow can affect the convergence speed.[3,4] Figure S2 presents energy evolution plots of GA runs with varying ratios of mutated atoms in mutation operations and different inheritance ratios in crossover operations. The benchmarks were performed on clusters of sizes 54 and 55 with the mixed-size potentials labelled as “even” and “odd” in the main text. Since we are primarily concerned about the efficiency of GA operations instead of prediction accuracy, energies were only evaluated by MTP and the primitive GA workflow (Figure S1) was used (GA_MTP). All runs were stopped once the total number of clusters exceeded 5000. For both sizes, crossover is more efficient than both types of mutation operations in terms of the rate of convergence to low-energy structures. Among the two types of mutation operations, rotation is better than random moves. Within crossover benchmarks, the random method for calculating inheritance ratios of parents outperformed the even method, while it was close to the weighted method. As for mutation, the lowest energy for both sizes and both types of mutation operations was achieved when 10% of the atoms were moved, although this approach did not have the fastest convergence speed (Figure S1a and Figure S1f). These findings suggest that adjustments to a small number of atoms are more efficient in minimizing the energy, while operations involve large number of atoms often stagnate at elevated energy levels. This can be explained from the fact that often only a small fragment of atoms is out of place compared with the lowest-energy structure in the late stages of a GA optimization. Relocating only a few atoms is more likely to put dislocated atoms into the right positions than simultaneously displacing a large chunk of atoms from a structure which is already close to the lowest-energy isomer.

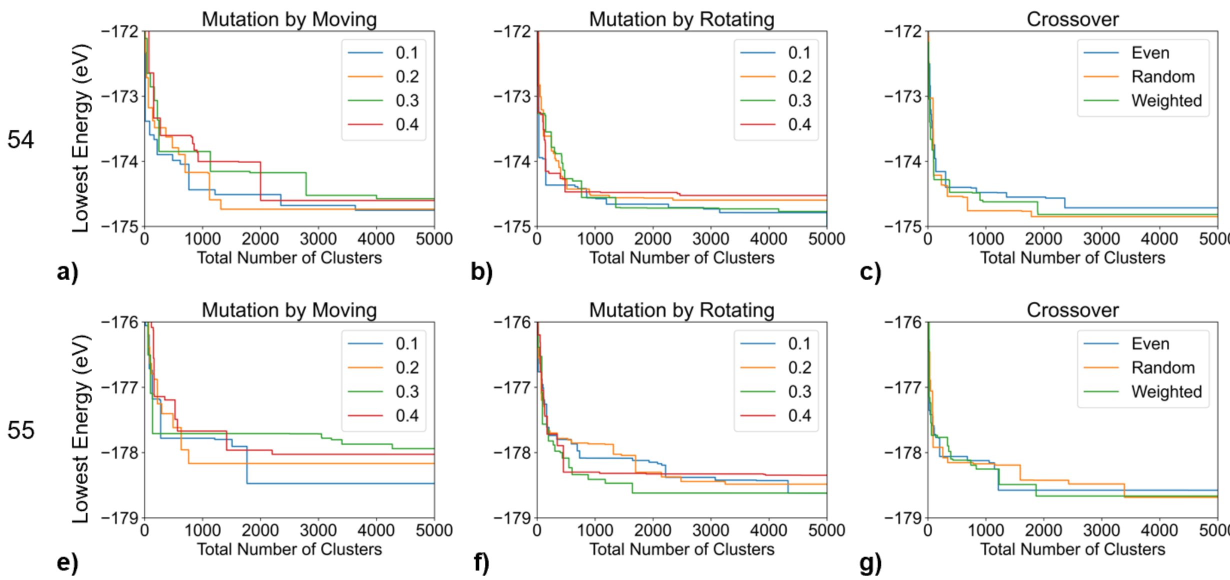

Figure S2. Energy evolution plots of GA_MTP for different GA operations and controlling parameters. a) and **e)** mutation by randomly displacing atoms with varying ratios of mutated atoms. **b)** and **f)** mutation by randomly rotating atoms around center of mass with different ratios of mutated atoms. **c)** and **g)** crossover with various calculation methods for ratios of inherited atoms from parents. The plots on first row uses the "even" potential discussed in main text on size 54, while those on the second row uses the "odd" potential on size 55.

For all GA runs in the main text, both move and rotation were used in mutation, and in each mutation operation a maximum 10 % of atoms were allowed to be displaced. For crossover, both random and weighted methods were used with an equal probability. Moreover, since crossover is more efficient than mutation, the frequency of applying mutation in cluster generation was suppressed by capping the fraction of pool clusters created by mutation at 0.2.[5] In other words, if

20% or more pool clusters are produced by mutation, the subsequent GA operations will always be crossover until the percentage drops below 20%. The pool size was kept at 25, as it offers a good balance between convergence speed and success rate of identifying the lowest-energy cluster.[3,4]

1.4 GA_AL input parameters

When initializing GA_AL with pre-trained potentials, it is beneficial to switch off retraining at the beginning of the search, to let GA fully explore the potential energy surfaces of pre-trained potentials. We call the parameter controlling the number of clusters that can be generated before retraining is turned on "preprocessing". During the preprocessing period, extrapolating structures are discarded, and new clusters are generated until all MTP-relaxed configurations are interpolating. This ensures the GA search stays in interpolating region of the pre-trained potential in configuration space. As Figure S3 shows, the lowest energies in the first retraining were achieved when preprocessing was between about 5000 and 7500 clusters. Exceeding this range, artificial local minima start to populate the pool and drive up the lowest energy. To accelerate GA_AL and minimize time spent in the preprocessing stage, we used a preprocessing value of 5000 in all GA_AL runs in this work initialized with pre-trained potentials.

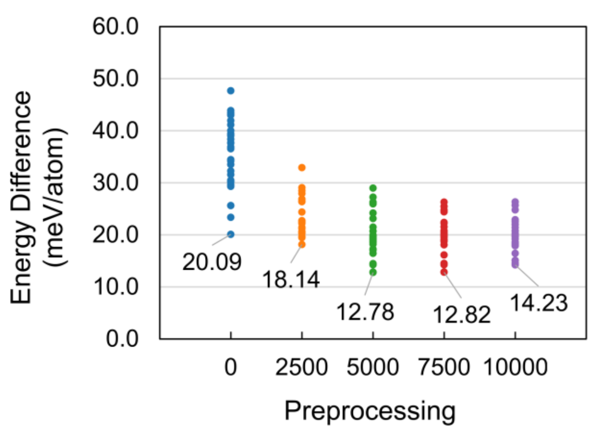

Figure S3. DFT energy distribution of pool clusters in the first retraining after preprocessing number of clusters has been generated in GA_AL. Tests were performed on clusters with 55 atoms and GA_AL runs were initialized with the mixed-size potential trained on odd number of clusters ("odd" potential in Figure 3 of the main text). Energies are reported relative to the energy of the lowest-energy cluster with 55 atoms.[19]

2 Hyperparameter selection for MTP

2.1 Data selection and training

To identify a good set of hyperparameters for training MTP potentials, we used Al clusters with 24 atoms as a model system and tested various combinations of hyperparameters, including potential complexity (defined by the level of moments, lev_{max}, of a MTP potential),[20] the amount of training data, and relative weights for force components and energies. We first performed GA_DFT searches on Al clusters with 24 atoms and then used the same diversity-based strategy as used in the preparation of mixed-size potentials (see Methods section of the main text) to select dissimilar configurations from the GA_DFT runs. We then randomly separated all DFT calculations into training and validation groups by keeping the ratio of the total number of dissimilar ionic steps in the training group to that of the validation group at approximately 3:1. To ensure structural dissimilarity of clusters in the training dataset from those in the validation set, we assign all ionic steps belonging to each relaxation trajectory to either the training or validation groups. This increases the likelihood that the validation results reliably reflect the accuracy of MTP potentials in areas of the configuration space that are not well-represented by the training data.

To assess the effect of training set size on potential accuracy, we used the same energy-based strategy as used for the preparation of mixed-size potentials (see Methods of the main text) to collect training datasets from the training group. We evaluated training sets containing 200, 400, 600, 800, 1000, 1500, 2000, 2500, and 3000 structures. For the validation dataset, we selected the 1000 lowest-energy ionic steps from the DFT calculations in the validation group, as the accuracy on low-lying areas of potential energy surfaces matters the most in ground state structure search.

The maximum number of iterations in Broyden-Fletcher-Goldfarb-Shanno algorithm[21-24] for training the potentials was set to 5000, which is 5 times larger than the default value of 1000.[20] Only trainings using small relative force weights less than 0.001 for potentials with levels of moments of 20, 22 and 24 stopped because of reaching this limit. We expect none of these trainings will affect the conclusions we draw from the set of benchmarks. None of the trainings in Figure 1 of the main text were terminated due to hitting the limit.

2.2 Analysis of various combinations of parameters

The main text presents the benchmarks that are most relevant to the hyperparameters that we used in GA_AL runs. Here, we give a more comprehensive analysis of all parameter combinations that we tested. They all show similar trends as the ones shown in the main text. A force weight that is 1/1000 of the energy weight offers the best balance between prediction accuracies on force components and energies (Figure S4). Both force and energy root-mean-square errors (RMSEs) decrease as potential complexity rises (Figure S5). However, the training cost increases dramatically with both training data size and potential complexity (Figure S6). A somewhat surprising finding is that larger force weights took less time to train than smaller ones. A possible explanation is that the potential energy surface for atomic clusters is very rough, making it difficult to reproduce energies with a high accuracy, whereas there was less variation in the forces for nearly-relaxed structures. The potentials with lev_{max} of 10 and 12 see a steady increase of energy validation RMSEs as the training set grows. Potentials with lev_{max} larger than 14 have relatively flat force and energy RMSEs after the training set size exceeds 2000, but there can be significant variation with respect to training set size for training sets with fewer than 1000 structures (Figure S7).

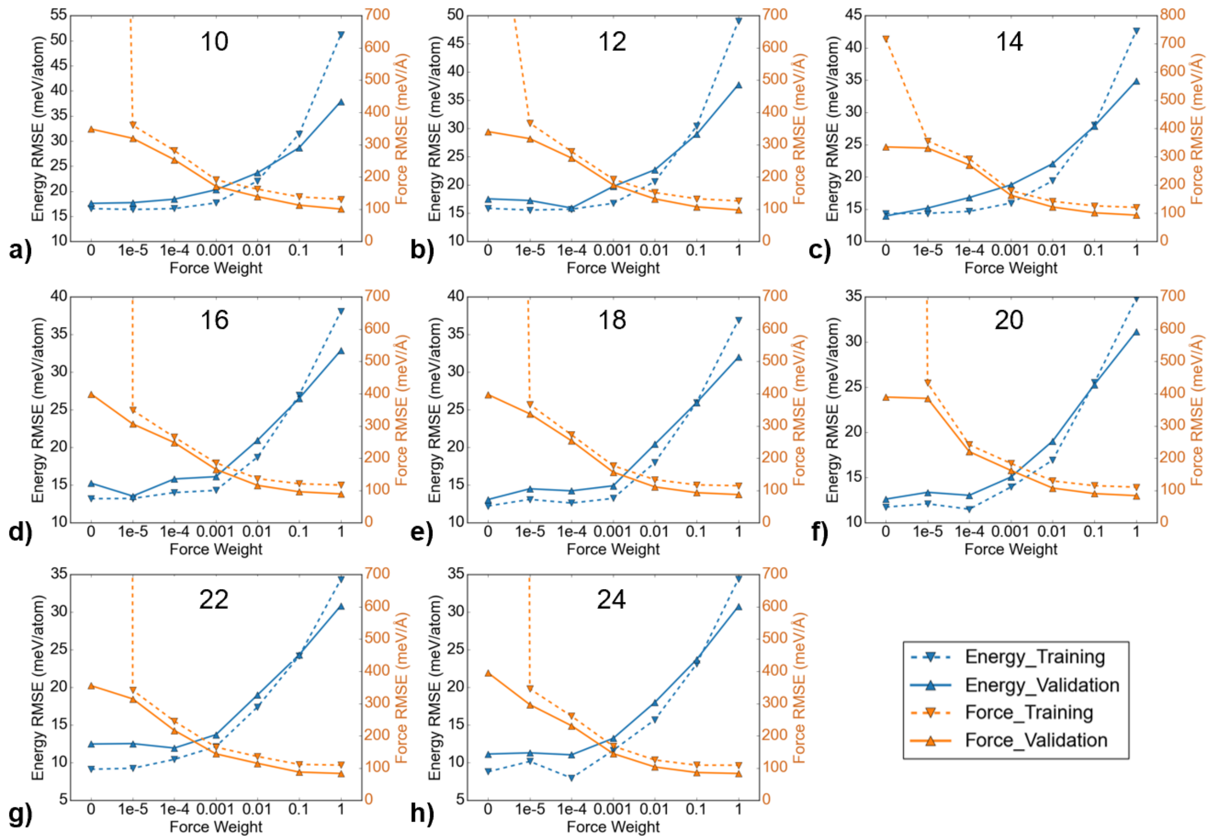

Figure S4. Training and validation errors against relative force weights to energy across different potential complexities. Training and validation RMSEs are marked by dashed and solid lines, respectively. In all benchmarks, the energy weight was set to 1 and a training set of 3000 structures was used.

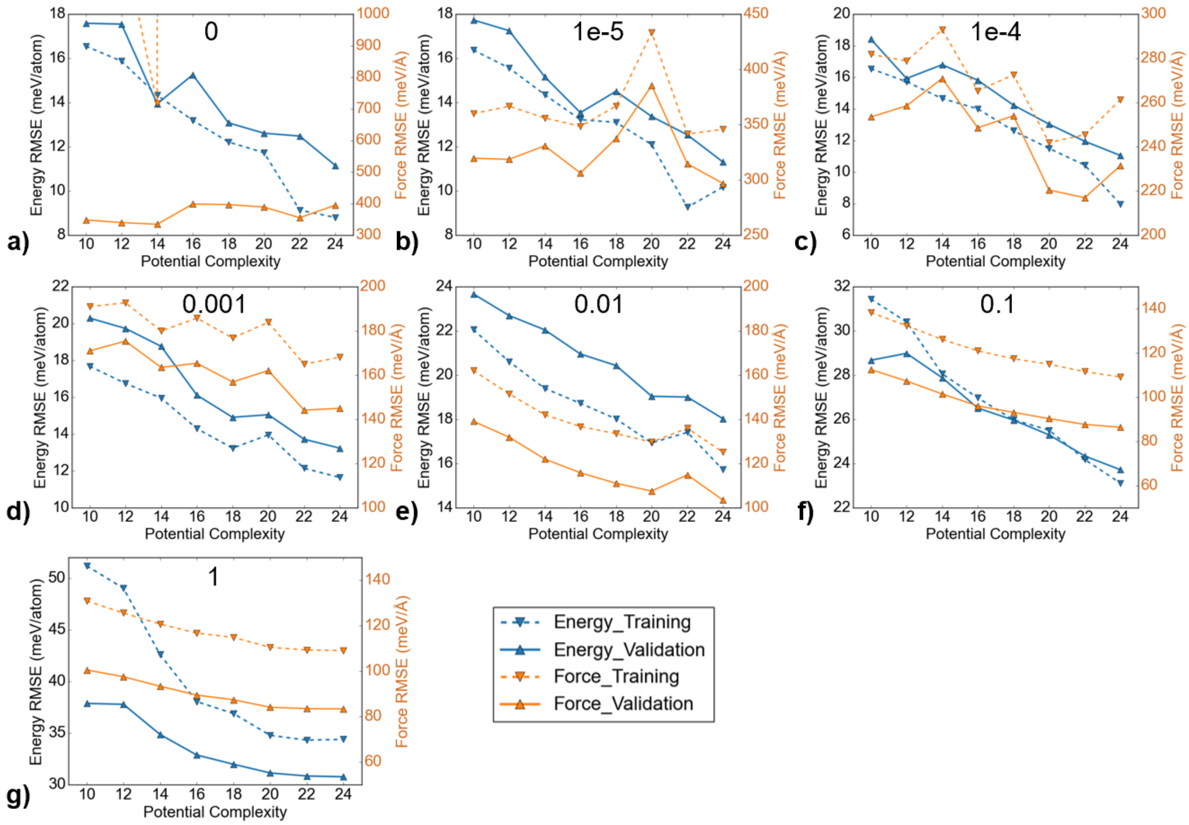

Figure S5. Training and validation errors against increasing potential complexities across varying force weights relative to energies. For all benchmarks, the energy weight was kept at 1 and a training set of 3000 structures was used.

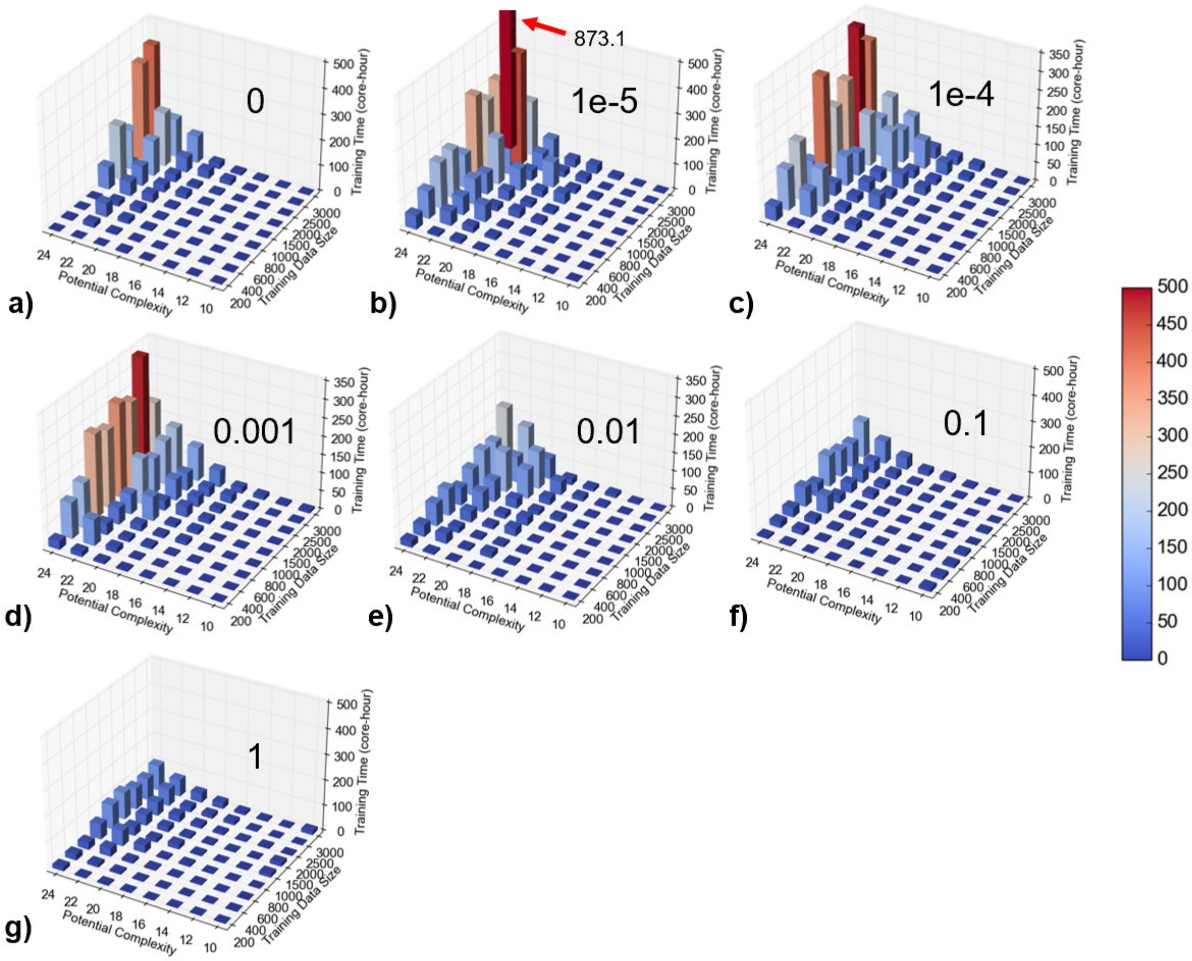

Figure S6. Training time plots in unit of core-hour against potential complexity and training set size for increasing force weights relative to energy.

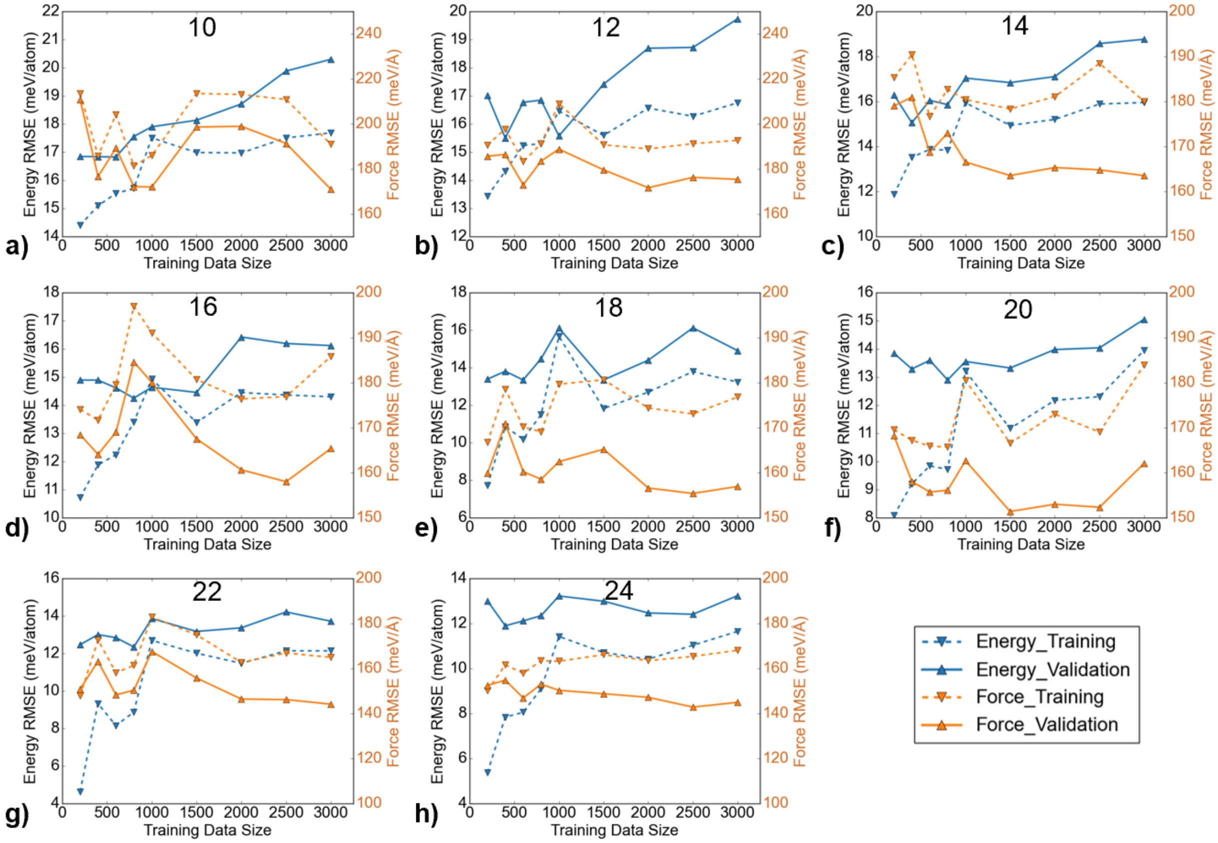

Figure S7. Training and validation errors against size of training set across different potential complexity. In all benchmarks, relative weight of force components to energies was kept at 1/1000.

3 Validation of pre-trained potentials

3.1 Validation dataset for pre-trained potentials

The validation data are collected from GA_DFT runs on clusters with 50-55 atoms. The same diversity-based method as the one used in preparation of the training data of the pre-trained potentials (see Methods section of the main text) was used to select a structurally diverse set of structures. Table S2 lists the total number of validation structures for each cluster size.

Table S2. Total number of structures in validations sets of clusters with 50 to 55 atoms.

Cluster Size	Number of Validation Structures
50	3840
51	2946
52	3653
53	2581
54	3578
55	2604

3.2 Energy parity plots for pre-trained potentials

Figure S8 shows parity plots of MTP predicted energies against DFT calculated energies for the same set of validations presented in Figure 3 of the main text. The single-size potentials trained solely on small clusters of 21, 22, 25 and 26 atoms consistently underestimated low-lying structures of large sizes by a relatively large error, while the underestimation was smaller for potentials trained on clusters of 29 to 38 atoms. The mixed-size potentials exhibit a better fit for all validation sets, indicating enhanced transferability compared with single-size potentials.

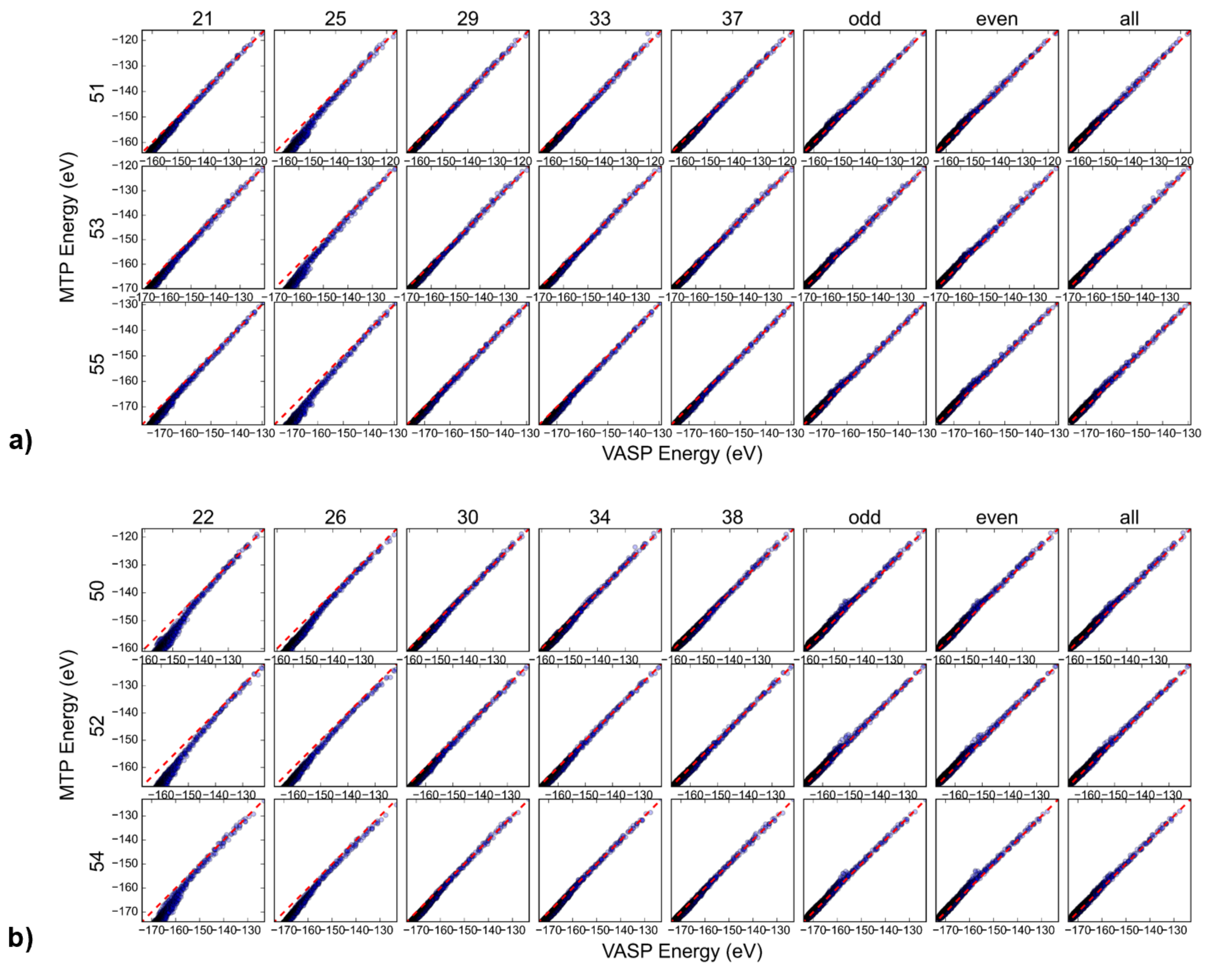

Figure S8. Energy scatter plots for validation of single-size and mixed-size potentials on large clusters with 50-55 atoms. Plots are grouped by parity of number of atoms into **a)** an odd group, and **b)** an even group.

3.3 Validation of mixed-size potentials on lowest-energy clusters with 50 to 55 atoms

Since we are primarily concerned with potential accuracies on low-energy structures, the single-size and mixed-size potentials were also validated on the lowest-energy clusters of sizes with 50-55 atoms, which were collected from GA_AL and GA_DFT runs of this work, and from the literature.[19] The lowest-energy clusters were grouped into a set of even-sized clusters and a set of odd-sized clusters.

Figure S9 displays the average energy errors of MTP predictions, and the average extrapolation grades of the lowest-energy clusters in different potentials. The errors follow a similar trend as the energy validation RMSEs in Figure 3a and Figure 3b of the main text. Prediction errors are larger for single-size potentials trained with clusters with small number of atoms, and these errors decrease gradually as the size of the clusters in the training set increases. Mixed-size potentials have consistently lower errors than any single-size potentials. Potentials trained with clusters of both even and odd number of atoms, hence different magnetic moments, do not greatly deteriorate accuracy. Surprisingly, the odd potential gave a better prediction than the even potential for the lowest-energy clusters with even number of atoms, which is also the case for the even potential on lowest-energy clusters with odd number of atoms. This suggests the gap between potential energy surfaces with different magnetic moments is not larger than the uncertainty of the moment tensor potentials. Mixing training structures of different magnetic moments results in an average effect: errors for the potential trained on clusters with both even and odd number of atoms are between the errors of the potentials trained on clusters with only even or odd numbers of atoms.

The trend in extrapolation grades provides additional evidence showing that mixing training data across a range of number of atoms can systematically enhance transferability to clusters of sizes that were not in the training set. For all six of the lowest-energy clusters, extrapolation grades of single-size potentials get smaller as the number of atoms in the training structures grows. Nearly all of them are extrapolating (i.e., the extrapolation grade is above 1), with the exception of the potential trained on clusters with 37 atoms, which has an extrapolation grade of 0.95. However, for the even and odd potentials, these lowest-energy clusters are interpolating, and energy predictions are in good agreement of DFT calculations, with errors well within potential uncertainties as shown in Figure 3 of the main text. Since the goal of the structure search is to discover unknown low energy configurations, high prediction accuracy on low-lying regions of potential energy surface is vital. Thus, validations on the lowest-energy clusters demonstrate that our strategy of constructing mixed-size potentials transferrable to clusters with number of atoms not present in the training data can be very helpful in improving the efficiency and success rate of the genetic algorithm.

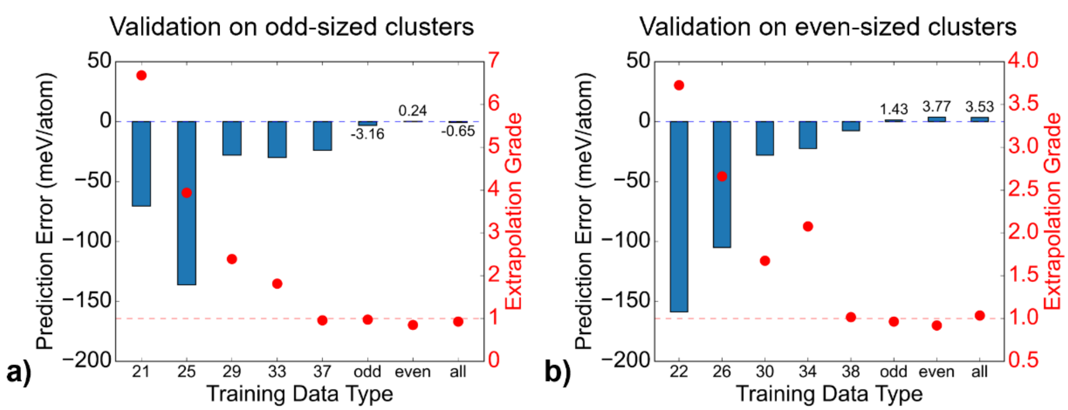

Figure S9. Validations of different potentials on the lowest-energy clusters with a) 50, 52, 54 atoms, and b) 51, 53, 55 atoms. Labels on x-axis share the same meaning as those in Figure 3 of the main text. The primary y-axis on the left and blue bars indicate average energy prediction errors for the lowest-energy clusters. The secondary y-axis on the right and the red dots represent the average extrapolation grades of the lowest-energy clusters in corresponding potentials.

4 Magnetic moments of low-energy clusters

We assembled in another work a database comprising low-energy clusters of 55 elements in the first five periods of the periodic table.[25] For aluminum clusters, the even-sized structures having the lowest energies are always non-magnetic when they have more than 16 atoms, while the low-lying odd-sized structures always have a net magnetic moment within 0.002 μ_B of 1 μ_B. Figure S10 displays the magnetic moments of the lowest-energy clusters in the database at the time we submitted this manuscript.

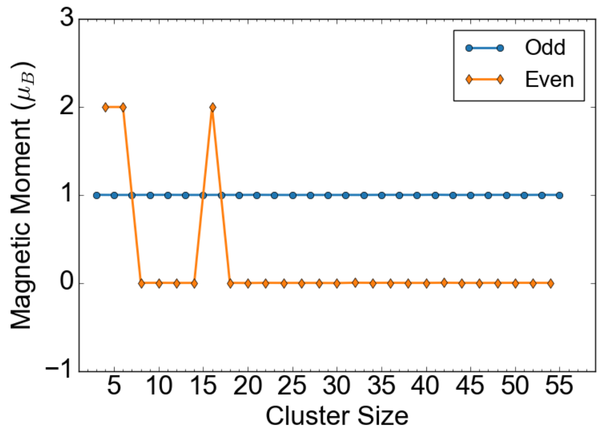

Figure S10. Magnetic moments of the lowest-energy aluminum clusters in the database with 3 to 55 atoms.

5 Performance analysis of GA_AL and GA_DFT

5.1 Energy evolution plots for GA_AL and GA_DFT on clusters with 21 to 49 atoms

Figure S11 and Figure S12 present the energies of the lowest-energy clusters as GA_AL and GA_DFT proceeded, for clusters with 21 to 49 atoms. Acceleration ratios are computed by dividing the earliest time that GA_AL discovers clusters with equal or lower energy than the energy of the lowest-energy cluster found by GA_DFT over the earliest time that GA_DFT finds that lowest energy cluster. These energy values are marked by black dashed lines in the energy evolution plots. The time points at which the step lines cross the dashed lines indicate the times used in acceleration ratio measurement and are marked by black crosses. In cases where GA_AL did not discover equivalent or better clusters (size 29 and 45), the acceleration ratios are 0, and the dashed lines and crosses are not drawn.

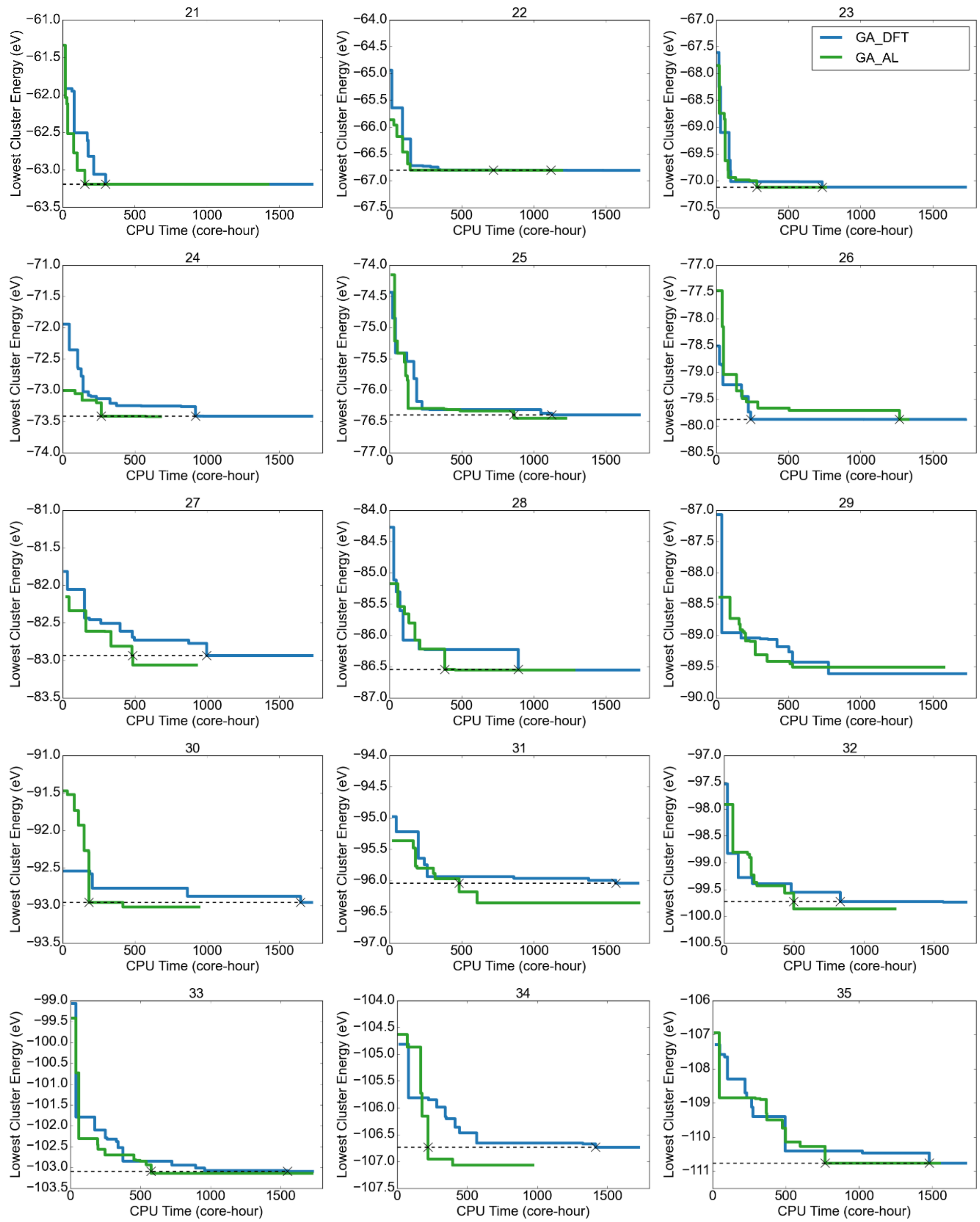

Figure S11. Energy evolution plots of GA runs for clusters with 21–35 atoms. The blue, and green step lines represent GA_DFT and GA_AL initialized with untrained potentials. The black dashed lines mark the energy levels that are used in determining acceleration ratios. The black crosses mark the earliest time at which each method reached the corresponding energy levels. These times are used in computing the acceleration ratios. For size 29 in which GA_AL did not find clusters with energies as low as the lowest-energy cluster in GA_DFT, the ratio is set to 0 and no crosses were marked.

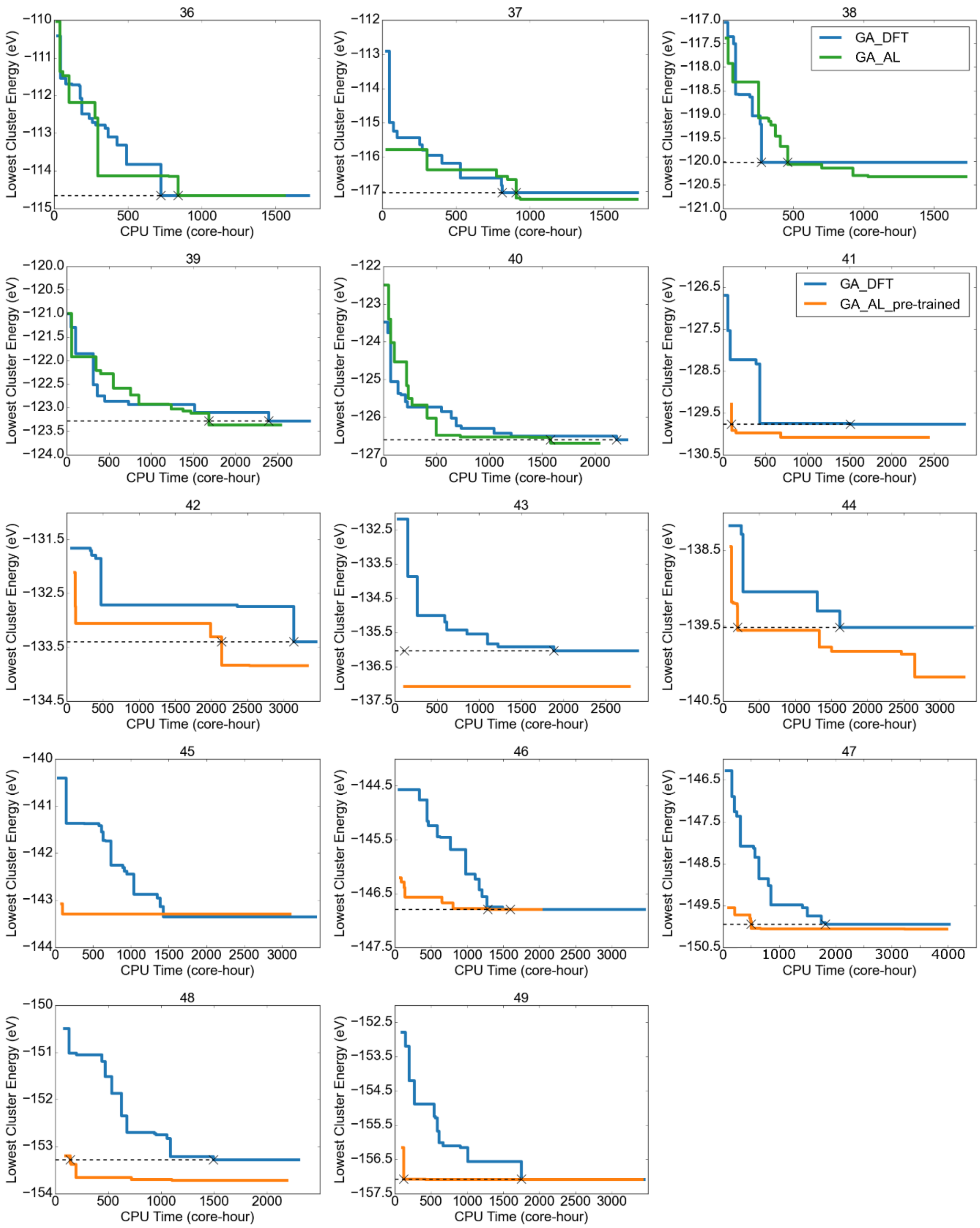

Figure S12. Energy evolution plots of GA runs for clusters with 36 to 49 atoms. The blue lines represent GA_DFT, green lines represent GA_AL initialized with untrained potentials, and orange lines represent GA_AL initialized with pre-trained transferable potentials. The black dashed lines mark the energy levels that are used in determining acceleration ratios. The black crosses mark the earliest time at which each method reached the corresponding energy levels. These times are used in computing the acceleration ratios. For size 45 in which GA_AL did not find clusters with energies as low as the lowest-energy cluster in GA_DFT, the ratio is set to 0 and no crosses were marked.

5.2 Performance comparison of GA_AL with and without pre-trained potentials

We performed both GA_AL initialized with pre-trained potentials and GA_AL initialized with untrained potentials on clusters of 50 to 55 atoms. The latter approach took longer time than the former to find the same lowest-energy clusters (see Figure 4a of the main text). Figure S13 shows the acceleration ratios and differences of lowest energies compared to GA_DFT for both approaches. Averaged over cluster sizes of 50 to 55, GA_AL initialized with untrained potentials had an acceleration ratio of 3.37, compared with the much larger ratio of 18.23 for GA_AL initialized with the mixed-size potentials.

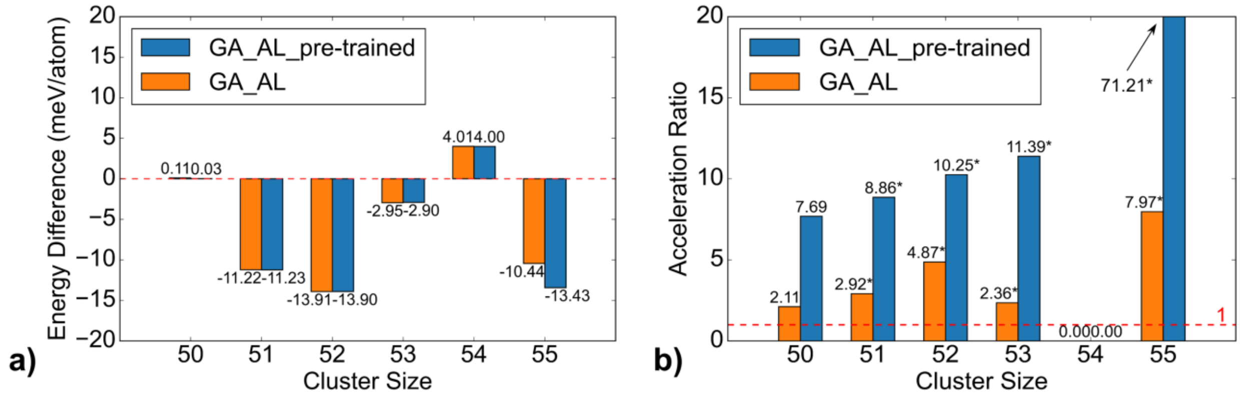

Figure S13. Comparison of performances between GA_AL initialized with pre-trained mixed-size potentials and with untrained potentials on clusters with 50 to 55 atoms. Acceleration ratios and energy differences of lowest-energy clusters are calculated in the same way as Figure 2b and Figure 4c of the main text.

6 Identification of new lowest-energy clusters

In the main text, low-energy clusters were collected from three sources: GA_AL runs, GA_DFT runs and literature. To determine whether we have identified a new lowest-energy structure for a cluster size and to compare performance between the GA_AL and GA_DFT algorithms, the lowest-energy clusters found from different sources are compared both in total energies and similarity. A cluster is said to be a new lower-energy cluster than another if it is lower in total energy by at least 1meV/atom and the similarity score between the two clusters is larger than 0.3. If a cluster has an energy difference smaller than 1meV/atom but is structurally dissimilar to another cluster, we count it as an "energetically similar" cluster. For the borderline cases where a cluster is lower in energy by more than 1 meV/atom, but the similarity score between the two clusters is slightly less than 0.3, we manually checked the structures to determine whether they are equivalent or not. These scenarios are summarized in Table S3.

Table S3. Summary of comparison results between clusters by total energy and structural similarity.

		Similarity Comparison	
		Similarity Score > 0.3	Similarity Score ≤ 0.3
Energy Comparison	$\Delta E > 1$ meV/atom	New, lower-energy	Visually check
	$\Delta E \leq 1$ meV/atom	Energetically similar	Equivalent

The same comparison methods are used in deciding whether a GA search (GA_DFT or GA_AL) has identified a new lowest-energy cluster compared with those reported in the literature[19,26-28] and in comparing between clusters found by the GA_AL and GA_DFT algorithms. Cluster sizes for which there is a cluster that is energetically similar to the current lowest-energy cluster are considered to have multiple lowest-energy isomers.

Table S4 listed the total energies and the similarity scores for lowest-energy clusters identified in GA_AL and GA_DFT runs of this work, and the ones reported in literature. The total energies are reported relative to the energies of the clusters found in GA_AL runs.

Three cluster sizes, 22, 33 and 46, requires additional examination. GA_DFT identified an isomer for clusters with 22 atoms that is energetically similar to the lowest-energy cluster reported in literature[27] and found by GA_AL. For size 33, although the two low-energy clusters from GA_DFT and GA_AL have an energy difference larger than 1 meV/atom, the similarity score and visual inspection (Figure S14) show that they are equivalent. For size 46, the lowest-energy cluster reported in literature has a similarity score with the ones found in GA_AL and GA_DFT that is less than 0.3, but the energy difference and visual inspection show the structures are not equivalent. Therefore, the genetic algorithm is considered to have identified new lowest-energy clusters for sizes 22 and 46, but only confirmed the literature-reported cluster for size 33.

GA_AL identified new lowest-energy clusters for 23 sizes out of the total 35 sizes studied in this work. GA_AL runs and GA_DFT runs together identified 25 new lowest-energy clusters (26 if counting the energetically similar cluster for size 22) and confirmed the literature-reported lowest-energy clusters for 8 sizes. Overall, the GA runs of this work only missed the lowest-energy literature structures for clusters with 32 and 55 atoms. It is likely that these clusters could have been found more quickly if as seeing operation was used, given the similarity between the lowest-energy clusters of these two sizes to the clusters with close number of atoms (see Figure S15).

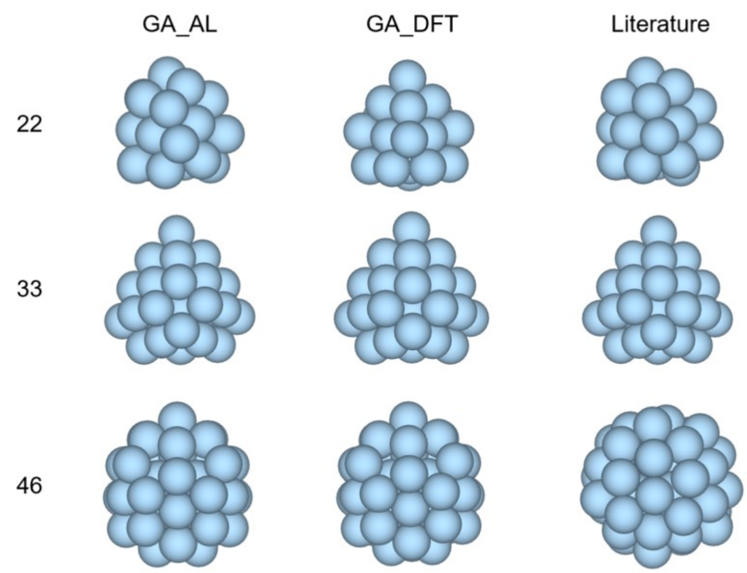

Figure S14. Lowest-energy clusters from GA_AL, GA_DFT and the literature[27,28] for clusters with 22, 33, and 46 atoms.

Table S4. Total energy differences and similarity scores between lowest-energy clusters found in GA_AL and GA_DFT runs of this work, and the ones reported in literature. "Lit." is the abbreviation for "Literature". Energy differences are reported in meV/atom relative to the total energies of lowest-energy clusters from GA_AL (include GA_AL initialized with untrained potentials or pre-trained potentials). Similarity scores are calculated using the same method reported in Methods section of the main text. The origins of the final lowest-energy clusters are listed in the last column. Three cluster sizes that display large energy differences but small similarity scores or small energy differences but large similarity scores are marked with asterisks and are discussed in detail in Section 6.

size	ΔE relative to GA_AL (meV/atom)			Similarity Score			Origin of lowest-energy cluster
	GA_AL	GA_DFT	Lit.	GA_AL-GA_DFT	GA_AL-Lit.	GA_DFT-Lit.	
21	0.00	0.11	0.14	0.010	0.008	0.015	GA_AL / GA_DFT / Lit.
22*	0.00	-0.08	0.15	0.556	0.013	0.554	GA_AL / GA_DFT / Lit.
23	0.00	0.06	1.31	0.009	0.766	0.767	GA_AL / GA_DFT
24	0.00	0.03	9.98	0.009	1.611	1.614	GA_AL / GA_DFT
25	0.00	2.03	10.11	0.560	1.672	1.460	GA_AL
26	0.00	0.02	13.10	0.009	1.411	1.411	GA_AL / GA_DFT
27	0.00	4.61	0.02	1.191	0.010	1.193	GA_AL / Lit.
28	0.00	0.00	0.04	0.018	0.019	0.006	GA_AL / GA_DFT / Lit.
29	0.00	-3.62	1.63	1.118	1.083	1.373	GA_DFT
30	0.00	2.08	2.21	0.820	0.754	1.070	GA_AL
31	0.00	10.10	-0.07	0.663	0.011	0.662	GA_AL / Lit.
32	0.00	4.13	-3.78	0.694	1.111	0.992	Lit.
33*	0.00	1.46	0.06	0.240	0.008	0.241	GA_AL / GA_DFT / Lit.
34	0.00	9.73	0.03	0.600	0.010	0.603	GA_AL / Lit.
35	0.00	0.08	40.99	0.008	0.953	0.953	GA_AL / GA_DFT
36	0.00	0.02	51.81	0.008	1.090	1.089	GA_AL / GA_DFT
37	0.00	5.26	40.87	0.611	1.525	1.337	GA_AL
38	0.00	8.10	48.28	0.661	1.445	1.355	GA_AL
39	0.00	2.28	44.85	0.879	1.296	1.229	GA_AL
40	0.00	2.29	32.45	1.022	1.011	1.213	GA_AL
41	0.00	7.65	28.09	0.941	1.159	0.993	GA_AL
42	0.00	10.55	31.44	0.609	0.986	1.086	GA_AL
43	0.00	24.24	35.38	1.138	1.100	1.047	GA_AL
44	0.00	14.92	22.25	0.901	1.257	1.293	GA_AL
45	0.00	-1.37	-1.38	1.600	1.602	0.027	GA_DFT / Lit.
46*	0.00	0.02	4.65	0.017	0.269	0.272	GA_AL / GA_DFT
47	0.00	2.50	5.80	1.423	1.465	0.350	GA_AL
48	0.00	9.13	15.21	1.025	1.052	0.453	GA_AL
49	0.00	0.01	15.21	0.026	0.603	0.602	GA_AL / GA_DFT
50	0.00	-0.03	23.21	0.010	0.815	0.816	GA_AL / GA_DFT
51	0.00	11.23	28.12	0.909	1.117	1.100	GA_AL
52	0.00	13.91	33.77	1.118	1.462	1.238	GA_AL
53	0.00	2.95	27.97	1.021	1.254	0.991	GA_AL
54	0.00	-4.00	28.11	1.009	1.117	1.383	GA_DFT
55	0.00	13.43	-3.71	0.853	1.084	1.307	Lit.

7 Analysis of lowest-energy clusters with 21 to 55 atoms

7.1 Visualization of lowest-energy clusters

Visualizations of the lowest-energy aluminum clusters with 21–55 atoms were generated using VESTA[29] and assembled into a panel in Figure S15. Symmetries were determined using Materials Studio[30] with a spatial tolerance of 0.1 Å. The lowest-energy cluster with 21 atoms has a dumbbell shape, which packs a 13-atom icosahedron at one end and a 14-atom variant resembling an icosahedron on the other end. From size 22 to 28, the lowest-energy clusters gradually transform from irregular shapes to layered close-packed structures, with 27 and 28 having ordered layers in triangles stacked in the FCC stacking order. Lowest-energy configurations then start to alter the stacking order, with the cluster of 32 atoms forming a structure with closed-packed triangular layers stacking in HCP order. Starting from size 33, the lowest-energy isomers begin to favor tetrahedral shapes, and the 36-atom cluster has the most ordered shape and highest order of symmetry (D_{2d}) among all lowest-energy clusters. After 36, the preference of lowest-energy morphology changes back to layered close-packed structure. Lowest-energy clusters with 37, 38 and 39 atoms form transitional shapes between tetrahedron and layered configuration. Lowest-energy clusters with 40 to 43 atoms regain the FCC stacking order with close-packed layers, some of which have trapezoidal shapes instead of triangular. The 44-atom lowest-energy isomer loses the layered morphology but mostly retrains close-packed outer surfaces. Lowest-energy clusters of 45 and 46 have spherical shapes, while the cluster with 47 atoms have a layered structure with HCP stacking order. From size 49 to 53, lowest-energy clusters are neither layered nor tetrahedral, but still favor close-packed outer surfaces. Finally, the 54-atom and 55-atom lowest-energy structure transform back to tetrahedral configurations with close-packed surfaces. The preferred morphologies adopted by lowest-energy aluminum clusters periodically transform between layered close-packed structures and tetrahedrons with close-packed outer surfaces. This observation reflects the facts that Al in its bulk phase has an FCC crystal structure, and (111) surfaces possess the lowest free surface energies among low-index surfaces.[31] The prevalence of preferred morphologies for lowest-energy isomers across a wide range of sizes also suggests that the seeding operation, which generates new clusters from seed structures of other sizes, can potentially accelerate ground state search by a large extent, when low-energy structures of neighboring sizes are available.

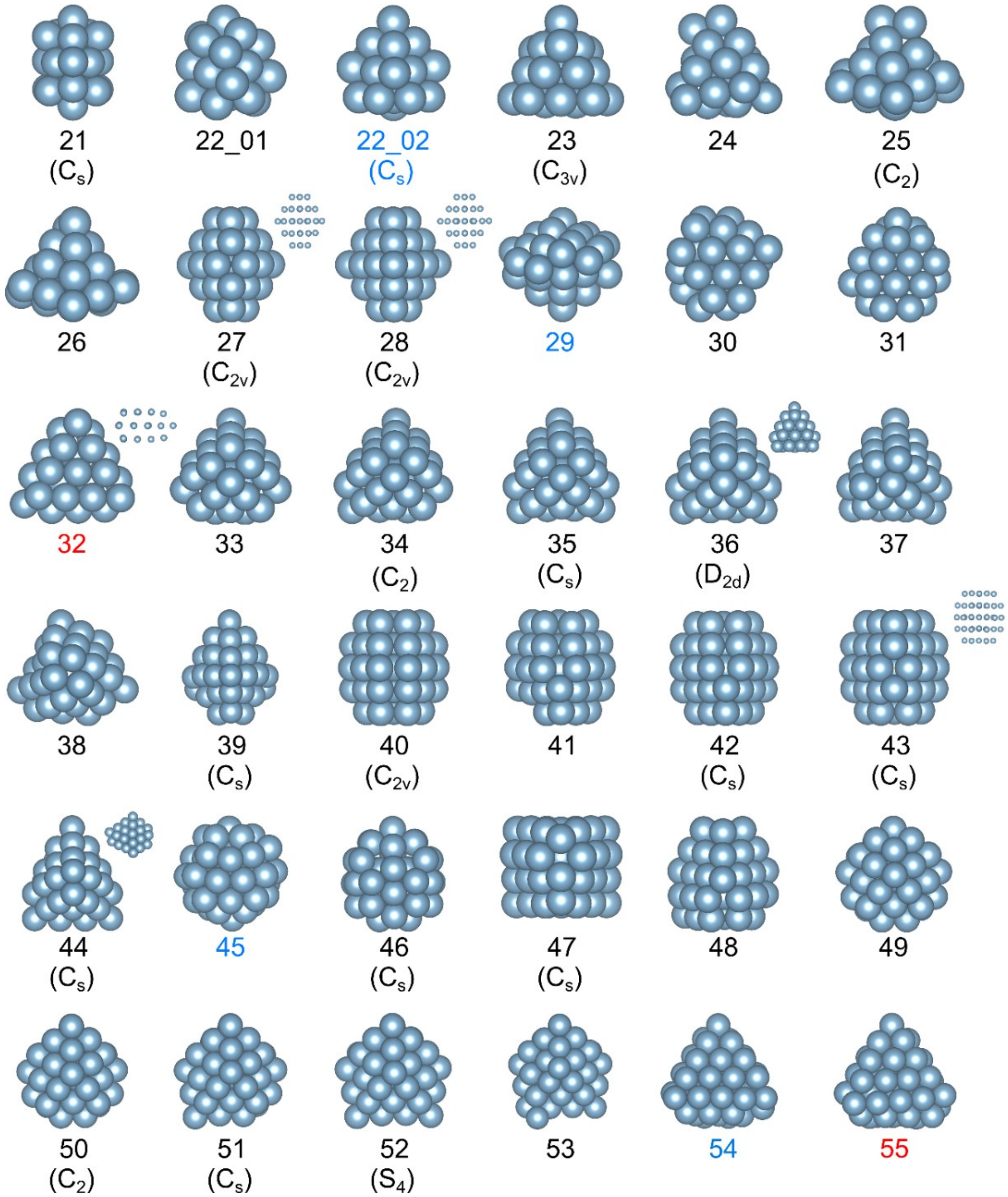

Figure S15. Lowest-energy clusters assembled from GA_AL, GA_DFT and the literature. Labels of the lowest-lowest energy clusters discovered by GA_AL and GA_DFT are colored in black and blue, while the ones reported in the literature[19,27] are labelled in red. Proposed symmetries are included below corresponding clusters. Informative alternative views are put at the top right corner.

7.2 Stability Analysis

To measure relative stabilities, cohesive energies, binding energies, and the second energy differences were calculated and plotted in Figure S16. The cohesive energy is defined as the energy required to break the cluster into isolated neutral atoms at 0K and is computed by

$$E_c(n) = \left[n \times E_1 - E_n\right]/n, \quad (5)$$

where $E_c(n)$, E_1, and E_n represent the cohesive energy per atom for an n-atom cluster, the total energy of an isolated aluminum atom, and the total energy of a cluster with n atoms respectively. The binding energy measures the energy necessary to break one atom from the cluster and is calculated as

$$E_b(n) = E_{n-1} + E_1 - E_n, \tag{6}$$

where $E_b(n)$ represents the binding energy and the other symbols carry the same meaning as those in equation (5). The second energy difference describes the stability of the lowest-energy cluster of one size relative to the adjacent sizes and is calculated as

$$\Delta_2 E(n) = E_{n+1} + E_{n-1} - 2E_n, \tag{7}$$

of which a positive value implies higher stability.

Cohesive energies steadily increase as clusters grow, and values of all sizes are still well below the bulk value of 3.39 eV/atom,[32] suggesting clusters in this size are significantly less stable than the bulk crystal. The binding energies and the second energy differences display an odd-even oscillation, which can be attributed to the existence of one unpaired electron in odd-sized clusters. The lowest-energy cluster with 36 atoms exhibits peaks in both the second energy differences and cohesive energies, meaning it is more stable than lowest-energy clusters of neighboring sizes. This suggests it could exist in relatively high abundance in gas-phase experiments and agrees with the experimental observation of surprisingly high melting temperatures of Al cation clusters with around 36 atoms.[33,34]

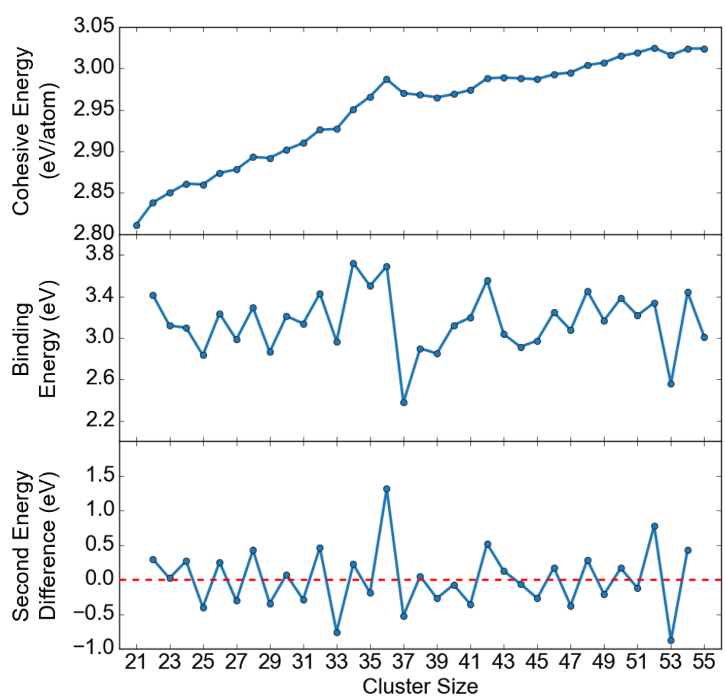

Figure S16. Cohesive energy, binding energy and second energy difference for clusters with 21 to 55 atoms.

8 Relationship between extrapolation grade and energy prediction error

Although high extrapolation grades generally indicate a large predication error, lower extrapolation grades below the extrapolation threshold (1.0) do not necessarily guarantee smaller prediction errors. Figure S17 shows the extrapolation grades of DFT-relaxed clusters at each retraining step for GA_AL runs on clusters with 21, 38 and 55 atoms. We focus on the local ground states of DFT relaxations because we are primarily interested in low-energy structures for the purpose of the structure search. Extrapolation grades decrease as more retraining steps were performed. However, the prediction errors of those having extrapolation grades smaller than 1.0 scatter randomly with a tendency of over-estimating the total energy (i.e., MTP predicted an energy higher than corresponding DFT energy).

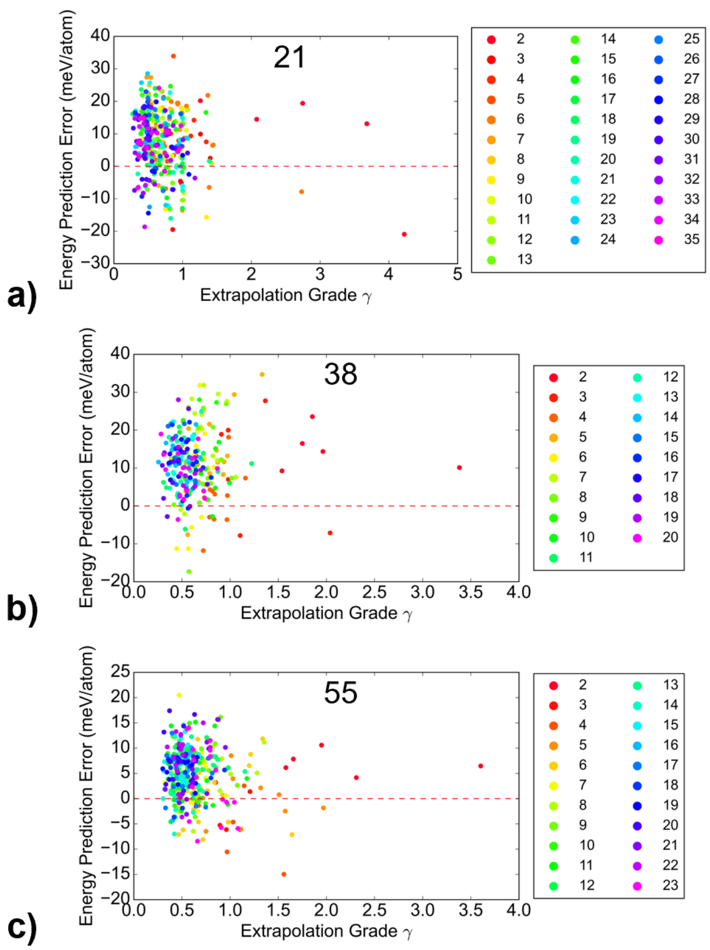

Figure S17. Energy prediction errors against extrapolation grades for ground states of DFT calculations at retraining steps of GA_AL for clusters with a) 21, b) 38 and c) 55 atoms. The legends represent the retraining step of a GA_AL run.

References

1 Holland, J. H. *Adaptation in natural and artificial systems*. (University of Michigan Press, 1975).

2 Ho, K.-M. *et al.* Structures of medium-sized silicon clusters. *Nature* **392**, 582-585, doi:10.1038/33369 (1998).

3 Johnston, R. L. Evolving better nanoparticles: Genetic algorithms for optimising cluster geometries. *Dalton Transactions*, 4193-4207, doi:10.1039/B305686D (2003).

4 Vilhelmsen, L. B. & Hammer, B. A genetic algorithm for first principles global structure optimization of supported nano structures. *J Chem Phys* **141** (2014).

5 Shayeghi, A., Götz, D., Davis, J. B. A., Schäfer, R. & Johnston, R. L. Pool-BCGA: a parallelised generation-free genetic algorithm for the ab initio global optimisation of nanoalloy clusters. *Phys Chem Chem Phys* **17**, 2104-2112, doi:10.1039/C4CP04323E (2015).

6 Aslan, M., Davis, J. B. A. & Johnston, R. L. Global optimization of small bimetallic Pd–Co binary nanoalloy clusters: a genetic algorithm approach at the DFT level. *Physical Chemistry Chemical Physics* **18**, 6676-6682, doi:10.1039/C6CP00342G (2016).

7 Sun, J., Xie, X., Cao, B. & Duan, H. A density-functional theory study of Au_{13}, Pt_{13}, $Au_{12}Pt$ and $Pt_{12}Au$ clusters. *Computational and Theoretical Chemistry* **1107**, 127-135 (2017).

8 Buendía, F., Vargas, J. A., Johnston, R. L. & Beltrán, M. R. Study of the stability of small AuRh clusters found by a Genetic Algorithm methodology. *Computational and Theoretical Chemistry* **1119**, 51-58, doi:https://doi.org/10.1016/j.comptc.2017.09.008 (2017).

9 Tipton, W. W., Bealing, C. R., Mathew, K. & Hennig, R. G. Structures, phase stabilities, and electrical potentials of Li-Si battery anode materials. *Physical Review B* **87**, 184114, doi:10.1103/PhysRevB.87.184114 (2013).

10 Tipton, W. W. & Hennig, R. G. A grand canonical genetic algorithm for the prediction of multi-component phase diagrams and testing of empirical potentials. *Journal of Physics: Condensed Matter* **25**, 495401, doi:10.1088/0953-8984/25/49/495401 (2013).

11 Dong, R., Chen, X., Wang, X. & Lu, W. Structural transition of hexagonal tube to rocksalt for $(MgO)_{3n}$, $2 \leqslant n \leqslant 10$. *The Journal of Chemical Physics* **129**, 044705, doi:10.1063/1.2956508 (2008).

12 Choi, I.-G. *et al.* Energetically-favorable distribution of oxygen vacancies and metal atoms in perovskite $BaCe_xZr_{0.85-x}Y_{0.15}O_{2.925}$ solid solutions using a genetic algorithm and lattice statics. *Comp Mater Sci* **170**, 109184, doi:https://doi.org/10.1016/j.commatsci.2019.109184 (2019).

13 Collins, S. P., Daff, T. D., Piotrkowski, S. S. & Woo, T. K. Materials design by evolutionary optimization of functional groups in metal-organic frameworks. *Science Advances* **2**, e1600954, doi:10.1126/sciadv.1600954 (2016).

14 Deaven, D. M. & Ho, K. M. Molecular-Geometry Optimization with a Genetic Algorithm. *Phys Rev Lett* **75**, 288-291 (1995).

15 Kresse, G. & Furthmuller, J. Efficiency of ab-initio total energy calculations for metals and semiconductors using a plane-wave basis set. *Comp Mater Sci* **6**, 15-50 (1996).

16 Kresse, G. & Furthmuller, J. Efficient iterative schemes for ab initio total-energy calculations using a plane-wave basis set. *Physical Review B* **54**, 11169-11186 (1996).

17 Kresse, G. & Hafner, J. Abinitio Molecular-Dynamics for Liquid-Metals. *Physical Review B* **47**, 558-561 (1993).

18 Plimpton, S. Fast Parallel Algorithms for Short-Range Molecular Dynamics. *J Comput Phys* **117**, 1-19, doi:https://doi.org/10.1006/jcph.1995.1039 (1995).
19 Piotrowski, M. J. *et al.* Theoretical Study of the Structural, Energetic, and Electronic Properties of 55-Atom Metal Nanoclusters: A DFT Investigation within van der Waals Corrections, Spin–Orbit Coupling, and PBE+U of 42 Metal Systems. *The Journal of Physical Chemistry C* **120**, 28844-28856, doi:10.1021/acs.jpcc.6b10404 (2016).
20 Novikov, I. S., Gubaev, K., Podryabinkin, E. V. & Shapeev, A. V. The MLIP package: moment tensor potentials with MPI and active learning. *Machine Learning: Science and Technology* **2**, 025002, doi:10.1088/2632-2153/abc9fe (2021).
21 Broyden, C. G. The Convergence of a Class of Double-rank Minimization Algorithms 1. General Considerations. *IMA Journal of Applied Mathematics* **6**, 76-90, doi:10.1093/imamat/6.1.76 (1970).
22 Fletcher, R. A new approach to variable metric algorithms. *The Computer Journal* **13**, 317-322, doi:10.1093/comjnl/13.3.317 (1970).
23 Goldfarb, D. A family of variable-metric methods derived by variational means. *Mathematics of computation* **24**, 23-26 (1970).
24 Shanno, D. F. Conditioning of quasi-Newton methods for function minimization. *Mathematics of computation* **24**, 647-656 (1970).
25 Manna, S. *et al.* A Database to Enable the Design and Discovery of Atomically Precise Nanoclusters. (Manuscript in preparation).
26 Doye, J. P. K. A model metal potential exhibiting polytetrahedral clusters. *The Journal of Chemical Physics* **119**, 1136-1147, doi:10.1063/1.1574797 (2003).
27 Aguado, A. & López, J. M. Structures and stabilities of Al_n^+, Al_n, and Al_n^- (n=13–34) clusters. *The Journal of Chemical Physics* **130**, 064704, doi:10.1063/1.3075834 (2009).
28 Tuo, P., Ye, X. B. & Pan, B. C. A machine learning based deep potential for seeking the low-lying candidates of Al clusters. *The Journal of Chemical Physics* **152**, 114105, doi:10.1063/5.0001491 (2020).
29 Momma, K. & Izumi, F. VESTA 3 for three-dimensional visualization of crystal, volumetric and morphology data. *Journal of Applied Crystallography* **44**, 1272-1276, doi:10.1107/s0021889811038970 (2011).
30 BIOVIA, Dassault Systèmes, Materials Studio (San Diego: Dassault Systèmes).
31 Patra, A., Bates, J. E., Sun, J. & Perdew, J. P. Properties of real metallic surfaces: Effects of density functional semilocality and van der Waals nonlocality. *Proceedings of the National Academy of Sciences* **114**, E9188, doi:10.1073/pnas.1713320114 (2017).
32 Kittel, C. *Introduction to solid state physics*. (Wiley, 2005).
33 Neal, C. M., Starace, A. K. & Jarrold, M. F. Melting transitions in aluminum clusters: The role of partially melted intermediates. *Physical Review B* **76**, 054113, doi:10.1103/PhysRevB.76.054113 (2007).
34 Aguado, A. & Jarrold, M. F. Melting and Freezing of Metal Clusters. *Annual Review of Physical Chemistry* **62**, 151-172, doi:10.1146/annurev-physchem-032210-103454 (2011).

Supplementary File: Atomic Coordinates for Clusters

for

"Accelerated Prediction of Atomically Precise Cluster Structures Using On-the-fly Machine Learning"

Table of Contents

1 Format description

The following sections list the atomic coordinates of the lowest-energy structures discovered in this work and reported in literature for aluminum nanoclusters with 21 to 55 atoms. For clusters with 22 atoms, a cluster which has total energies close to the lowest-energy structure (difference below 0.1 meV/atom) but is structurally dissimilar is also listed.

Clusters are provided in the XYZ format with the center of mass positioned at the origin. The first line provides the number of atoms of the cluster, with a trailing blank comment line. The following lines list the element name and atomic coordinates in the Cartesian coordinate system.

2 Atomic coordinates for clusters

2.1 Al_21

21

Al	-0.596503690031571	0.159271003097976	-3.637482070185255
Al	2.286585294345931	0.830951886913486	-2.958567160431452
Al	1.033664713140647	-1.711617999236393	-2.828193465536144
Al	-0.042429815500894	2.514381907574577	-2.676371340719141
Al	-1.994125385900171	-0.685373895053791	-1.472730847744709
Al	0.612813037104070	0.428119171309620	-1.022610715335517
Al	1.833938631530993	3.051752633436998	-0.952245932007926
Al	3.291204481516125	0.981503395903907	-0.306840864540883
Al	2.789670119756137	-1.552478690758089	-0.867246860234246
Al	-1.664565852575888	2.027852564097188	-0.560851053283410
Al	0.009875492165804	-2.207470007291898	-0.318426825750153
Al	-3.604814527091738	0.276220671025232	0.598594008319584
Al	-2.522434942937107	-2.342980190580137	0.716628552719046
Al	-0.985441439688779	-0.079146205215778	0.984734309665225
Al	0.542902588090966	2.164276391641030	1.265649863144239
Al	1.644517023945994	-0.349686734470989	1.467023095161313
Al	2.126418896541706	-3.156685964118831	1.350095917319861
Al	-2.058244515402470	2.002878305992782	2.268744418261399
Al	-0.197081901030137	-2.178984135548673	2.442399216653241
Al	-2.523049637430812	-0.694121355932231	3.032404506840242
Al	0.017101429451174	0.521337247214026	3.475293247684695

2.2 Al_22

22

Al	0.849728635095090	0.305009796490726	-3.641055973590975
Al	-0.454824354095036	2.443823170741856	-2.806899464901289
Al	0.200621843188900	-2.141129322536001	-2.552127948594587
Al	2.782544148441950	-0.774659877732478	-2.197050280925546
Al	-2.394278740440318	-2.130111060577140	-1.676982107194558
Al	-0.854519914911067	0.085643404371087	-1.434072955075608
Al	-2.644206095113693	2.085007797081076	-1.389093002230260
Al	1.625569506058016	1.598954010301494	-1.345107336727165
Al	-3.752206017392702	-0.164218898227926	-0.568191139334245
Al	-0.689465884416474	-3.752523983064122	-0.344462829080266
Al	1.259316911884746	-1.841946607729521	-0.183061918330887
Al	-0.411116837144375	2.845396321557978	-0.042262882594020
Al	3.220950536848502	0.151081614879093	0.366981695883849
Al	-1.627935327892790	-1.409536831307928	0.753515558904583
Al	0.461794221361892	0.421670607211276	0.952522431393229
Al	2.077040383287498	2.576923997608393	1.110497092794137
Al	-2.366524639077721	1.077835212236092	1.359454454187127
Al	0.093044330099149	-2.968377169100195	2.070980544702035
Al	-0.467048104567413	2.399369999028631	2.677518521706466
Al	2.144295536701726	-1.318854489262010	2.370380580588957
Al	-0.747427286109438	-0.477667969318798	3.149598326185417
Al	1.694647148193528	0.988310277348424	3.368918632233607

2.3 Al_22 alternative

22

Al	-0.273801078607146	-1.340367421326714	-3.539314417717854
Al	0.631529234117727	1.279665740298393	-3.239023148413977
Al	-2.444039637864109	-1.927089695781956	-2.177553151957000
Al	1.828964825895078	-0.828965378053382	-2.064753233220965
Al	-1.297437102997620	0.356793147320385	-1.596541602866242
Al	2.543496086157049	1.773103591436458	-1.359611348464474
Al	-0.143376031862703	2.799614407693678	-1.124717451371499
Al	-3.680389476081229	-0.199129038131561	-0.414782086796510
Al	-0.180165326010709	-2.204536632151846	-0.636085018634361
Al	2.487504027315685	-2.792688091329786	-0.529716013261412
Al	-2.333658271352760	1.995225721572432	0.329205761692021
Al	0.691084087782505	0.415975152092672	0.177439435331653
Al	3.365751811688295	-0.344826198924196	0.239165595951697
Al	-2.690379192424030	-2.644302807473455	0.389749848834397
Al	-0.784357279261744	4.114047510257121	1.071995641485788
Al	1.602456637337488	2.883314037886288	0.954819139639666
Al	2.154889262873093	0.695381808328641	2.507738222190516
Al	1.454132773891089	-1.857863952216194	1.639150680508083
Al	-1.572787833253606	-0.449174592458125	1.286605771852454
Al	-0.847037290909182	-2.953433510123781	2.237982687877929
Al	-0.476532277352966	1.827788708617755	2.351101666908820
Al	-0.035847949080184	-0.598532507532829	3.497143020431277

2.4 Al_23

23

Al	-1.056193001906759	1.777458535036345	-4.036878242070214
Al	-1.662845417163185	-0.872606028202219	-3.488247009877295
Al	0.653104718818746	0.286429079172084	-2.656690502518004
Al	0.089152507202098	-2.255358054416752	-1.927324851136791
Al	0.156320098678565	2.904917665603040	-1.876940119742804
Al	-1.932600585443816	1.091473573747804	-1.626174040440808
Al	2.464785313255726	1.716796485701495	-1.298765167302959
Al	2.318705617130146	-0.951961493967749	-1.129356311861211
Al	-2.395356756729070	-1.481344920235703	-0.936044132261309
Al	-0.589089941602092	-2.806354368148527	0.714849590896245
Al	1.856699371701371	-3.483994907661041	-0.259740100527672
Al	0.191299236238606	0.430005959652693	0.145207098402887
Al	-1.433579596687037	2.930858856737441	0.255628372498501
Al	3.275887497917266	0.592648304426140	0.971365198075032
Al	1.279634692163729	2.904809352806383	0.939964029986895
Al	-2.562934555885653	0.568457707329271	0.817290499861969
Al	1.615349035816470	-1.534377231181534	1.625564926792130
Al	-2.992212418616184	-1.973084496731546	1.674942847302498
Al	4.027255095758347	-1.997848032972129	0.613465689831806
Al	-0.684719772516469	-0.817934721112872	2.544071910146068
Al	-2.985833973130648	0.187957288239364	3.410903288896693
Al	1.395881851760645	0.849361539831863	2.835401906179976
Al	-1.028709016760793	1.933689906346157	2.687505118868362

2.5 Al_24

24

Al	-0.433675090612311	-3.258981745336208	-3.378502173492810
Al	0.975993444053721	-1.141796800024916	-2.714739942358611
Al	-0.406944439062864	1.112899725983780	-2.548662634934395
Al	-1.795507514705186	-1.229779723794793	-2.355963455822907
Al	1.990309770384018	-3.674831856940134	-2.175416678832782
Al	1.154584705385499	3.257141858896498	-1.762800392526183
Al	2.270405035823764	0.766150852993876	-1.672058591354554
Al	-2.746882840456522	0.781275028755681	-1.059218370740322
Al	-1.261365489727298	3.011745934298293	-0.717479950215399
Al	-0.298114585330627	-2.991831670807974	-0.768205229815478
Al	3.381195691765104	2.953934334762456	-0.400716225806839
Al	2.085592426481522	-1.670240935735511	-0.210946215893742
Al	-0.083385372808253	0.028157967689429	-0.059502118294979
Al	-2.254062459338492	-1.600119730350939	0.305774694150244
Al	-3.659666402918445	2.940422847274382	0.541119587657548
Al	0.968435432854637	2.632472455922597	0.860314543922312
Al	2.899900445572504	0.717613116960974	0.964069819991568
Al	-3.662661194791258	0.445080110257445	1.469965630185792
Al	-1.382412018774617	1.909540911259665	1.747158357600874
Al	0.113949285254231	-2.363662275207487	1.655713522091370
Al	-1.577724554743486	-0.582082277879082	2.789060302438751
Al	0.781898802339503	0.773829264452365	2.691423146855286
Al	0.460320630913570	-1.474161478643536	4.240447385427561
Al	2.479816292441303	-1.342775914786874	2.559164989767694

2.6 Al_25

25

Al	1.628563383619499	-2.624387910024781	-2.111071705976232
Al	-0.821696822560490	-1.446565006798433	-2.336395021395763
Al	1.492074868923996	0.074386302774872	-2.453532584112666
Al	3.826591781869309	-1.227357935876961	-2.637803243939576
Al	-0.832161932449985	1.092825957232115	-2.748175570065385
Al	-2.690695100695137	0.105368653977994	-0.921306739788555
Al	-3.043567168900930	2.497247908695186	-2.203179095981397
Al	3.840650452350468	1.032439502737924	-1.237340847512977
Al	1.219726208090211	2.366301839941899	-0.949605723206790
Al	-0.472394767765564	-4.116944395630505	-1.606064581936121
Al	-0.619433214951366	3.720962222388939	-2.460165055431859
Al	-1.421225692215415	2.715891969257697	-0.116056125714143
Al	-2.028719624739835	-2.523330114241594	-0.207692972251067
Al	2.705179925893926	-1.111959412037868	-0.087554927040285
Al	-0.012458736166073	-0.016658414538014	-0.014930779166127
Al	0.669178464717639	-2.732531845864647	0.504292626839518
Al	2.792092707439046	1.317997849142156	1.140935307668466
Al	-3.643879173553937	-1.364357759733855	1.489394563634551
Al	0.338576296641282	2.229903243699887	1.697248483423444
Al	-2.124608813550182	0.989880163624363	1.630294576112416
Al	1.482257833396979	-0.894685770593627	2.239271296685054
Al	-1.066137956879192	-1.659377157889812	2.186988800428161
Al	2.089700542531453	1.374332744449115	3.674168122345407
Al	-0.405227625559105	0.546057464111200	3.700958047238545
Al	-2.902385835486625	-0.345440098803257	3.827323149143382

2.7 Al_26

26

Al	3.782683677001378	-0.418392815828973	-2.858410831689532
Al	-0.486763736986296	-1.521568889561746	-2.132062776534922
Al	-3.061260669639445	-2.233174507576222	-2.778958895199447
Al	1.278781780032805	0.386113413412104	-2.724295337231490
Al	-3.242467759016775	0.379278399713737	-3.266240833033504
Al	-0.942711248110358	1.422049810851082	-2.086586893481969
Al	3.319608308251988	2.247295420261866	-2.552728267623671
Al	2.130190478968743	-1.950748659655162	-1.403189018998420
Al	-3.389396423456468	2.198437020405265	-1.274109547490195
Al	3.126251146198289	0.463867834189687	-0.470417668738532
Al	-2.685925525552402	-0.422228871048732	-0.760175795720453
Al	1.223725954615784	2.458445439292221	-0.710893364332282
Al	-2.213486995810824	-3.159129960584931	-0.466013162577058
Al	0.193643523973424	-0.039498752344796	0.064307418526331
Al	-1.320413924249091	3.496414485451142	-0.310319825099564
Al	0.361861763515163	-2.884885236303719	0.253447002852095
Al	2.321575244991342	-1.324110547363793	1.289829694318291
Al	-2.139019341650411	1.338761436057421	1.123230054181722
Al	2.048569723587674	1.382816798016947	1.698110458513286
Al	-1.868982742292058	-1.244912965060674	1.580288612473559
Al	-1.529732042616033	-3.930359961363529	1.990232815865880
Al	-0.077177051550805	3.097212082846887	1.921012754288045
Al	0.321795830027478	-2.207514015756094	2.896444179387792
Al	-0.402108715198768	0.492871207204681	2.911142031819303
Al	1.968936137725521	-0.310944794414389	3.977115038993714
Al	1.281822607240141	2.283906629159727	4.089242156530998

2.8 Al_27

27

Al	-0.729972903416934	0.051191731730603	-3.652518869609882
Al	-1.833601492497438	-3.963868559194810	-1.552264963279044
Al	0.787429330195128	2.140411459437814	-3.924882817576236
Al	-0.030504062560370	-2.028324198600061	-2.002115867469147
Al	-2.476518902489318	-1.937387226980463	-3.322412346090994
Al	1.681421598559602	-0.012004254169101	-2.353872188603862
Al	-0.755645024854486	2.153156256313910	-1.768960625648887
Al	2.027147246239759	2.624991267270104	-1.695692719389744
Al	-2.263607004118568	-0.071087674714011	-1.378576862882770
Al	-3.886850889775681	-2.197415245355524	-0.991950423476760
Al	0.482761122505865	-4.040072456756921	-0.157754474510627
Al	0.099545610586196	-0.141363561940334	0.045166100906236
Al	2.252224045382750	-2.008229998623601	-0.532430764401912
Al	2.786889915606045	0.600497183894170	-0.004183387493443
Al	-1.573981316842049	-2.313423569485248	0.549085497730886
Al	-2.117787957227561	1.903061143883610	0.479457118969760
Al	0.521640748601779	2.529963038826029	0.597133853963797
Al	3.116606806898345	3.284654801795167	0.647416622644364
Al	-3.554612629425213	-0.468323062521366	1.011500568715098
Al	0.785393625130418	-2.278326830322540	1.892975137038432
Al	-1.279138156041713	-0.556623444035065	2.535226852789702
Al	3.347333410204250	-1.365698376039774	1.874424837265808
Al	1.241728062335412	0.317301387771710	2.546253771123414
Al	3.753614172717208	1.253111236453163	2.413741856753340
Al	-3.288426491786304	1.391662622628694	2.802959446646666
Al	-0.798148947708869	2.106080821911476	2.966368038424658
Al	1.705060083781749	3.026065506822356	2.975906607461102

2.9 Al_28

28

Al	1.968660359780511	0.395161660166940	-2.396916656190634
Al	-2.954572153901250	-1.495581647192072	-3.221871477312488
Al	-0.433525647363364	-0.531407799583340	-2.844129639158764
Al	-2.713899064996837	0.992726404146676	-2.437915021807872
Al	-0.181782086499354	1.981203974506052	-1.899460570026360
Al	1.265451687816853	-2.019817778686984	-1.372503130719915
Al	-1.266876843967653	-3.008971608051977	-1.908254708331541
Al	4.295850936139832	1.337906003198112	-1.612791141799505
Al	-2.436230265589599	3.521076524194370	-1.611430743411053
Al	2.239105088180612	2.961600074288233	-1.085470351873552
Al	0.061769325135892	4.494514562508583	-0.914310833041249
Al	-2.655857772501116	-1.033494023786936	-0.553407953205239
Al	0.471388104615940	-4.515931117105588	-0.549865843842074
Al	3.684809854346396	-1.039907804075224	-0.554962939708741
Al	-0.010726291876393	-0.008674902489338	-0.034959245393072
Al	-2.276345578509611	1.512157671502719	0.247466692055621
Al	2.553002524879203	1.019753125895440	0.747248003852553
Al	0.393434299945612	2.564562711339734	0.961506579026395
Al	-0.828773783030927	-2.497617579770858	0.778149121464663
Al	-1.859556067763900	4.061099479752142	1.049109123844209
Al	2.951105221028033	-3.507111460348034	0.143742143410890
Al	1.836660614205726	-1.437173530523022	1.491368833355313
Al	-2.268855888248574	-0.553474424936402	1.991534085598262
Al	1.027728302510035	-3.945126503166433	2.108175259147171
Al	0.599299210747565	0.577177654361337	2.730167798101720
Al	-1.612164969173708	2.109390586091989	2.851397541328126
Al	-0.158291194239187	-1.922231758967897	3.384485443322319
Al	-1.690807921670738	-0.011808493268211	4.513899631314819

2.10 Al_29

29

Al	-2.128378260979966	-0.440914962218839	-3.786902108828111
Al	0.011462219120478	1.306890759017893	-3.457402527940071
Al	2.195255852912073	2.825977567879489	-3.004038395670577
Al	-1.647739474319252	-3.147029679954036	-2.889292076345215
Al	-4.422768355422162	0.301244684831222	-2.408559885355727
Al	0.148466000302117	-1.257135309050163	-2.460794410761399
Al	0.840550503591222	-4.005305806100899	-2.096471344518847
Al	2.185636303886357	0.420825432261076	-1.935132951653242
Al	-2.083860347824498	1.405591862735605	-1.698408207483228
Al	-2.715151934304025	-1.365676190247702	-1.199219589380829
Al	0.162921585375157	2.652613694759740	-1.109298450632182
Al	2.191281728597335	-1.927489628931908	-0.806307577389628
Al	2.856726453102976	2.710983552238535	-0.402383279143240
Al	-0.791219733002364	-2.840138338693492	-0.250628328853510
Al	-0.132762927851731	0.001772033336593	-0.055546454529715
Al	-3.854185832073336	0.597185873293027	0.254000936655494
Al	1.473044474694188	-4.115567230094621	0.522557710794771
Al	2.593294872389547	0.166704114507509	0.728433562437376
Al	-1.684051544105290	2.198013923652795	0.822593438906102
Al	0.856778192414717	2.333137173666717	1.428302806103323
Al	-2.117759275879060	-1.320910653889927	1.473678771386941
Al	3.238134869448590	-2.454519124645142	1.807538029786185
Al	0.559601763084926	-1.905146123693266	1.850073110829110
Al	3.441634108578743	2.251463545971056	2.220090717695797
Al	-3.125735659541575	0.892392378387145	2.835257451565498
Al	-0.439320481032574	0.269792670819207	2.827002079519024
Al	2.284500748329343	-0.344544834953746	3.318784503934596
Al	1.313371797066505	2.034531554864287	4.019636655539315
Al	-1.209727646558421	2.755257060251825	3.452435813331979

2.11 Al_30

30

Al	0.881568511723474	0.070655135789744	-3.878262665466415
Al	-0.664233206619651	2.582378216448971	-3.089607168828661
Al	-1.726085868102536	0.456632912649159	-4.224197547773762
Al	2.063630029699462	2.339981503311222	-2.865073706024676
Al	-3.449238064584084	-0.955008445458171	-2.770984526881142
Al	0.715014681373487	-2.241953991938430	-2.514019543321493
Al	-1.954630327002677	-2.922965910002024	-1.844797005641716
Al	-3.006333038042778	1.432297120808242	-1.808450213615561
Al	-0.860679098370364	-0.205586380834726	-1.600726806255257
Al	1.882236165291692	-0.002109583912432	-1.423159295472177
Al	0.059573934647661	-4.477739716359872	-1.065300335939657
Al	-1.975214858761119	3.728708876114695	-0.932527496238777
Al	0.348544692002207	2.298444715689380	-0.604685658902058
Al	3.088351345345545	2.206710157208528	-0.425509402143000
Al	1.795026720366222	-2.326061081623907	-0.056677888457273
Al	-3.116218433053360	-0.909465578988204	-0.116092545201562
Al	-0.910471254147824	-2.438195660522726	0.570204382018700
Al	-1.923030545791171	1.391772928860657	0.612507081286854
Al	0.360598506954162	-0.008113381291775	0.956715791458738
Al	3.150513553010123	-0.206266353997650	1.028421235931710
Al	0.729143610783305	-4.313286513564929	1.592451821555532
Al	-0.941875077700219	3.796197731116282	1.492319242764871
Al	1.524413818407353	2.908134957459119	1.796897225639610
Al	4.032759059921796	2.142867448813222	2.153662912362179
Al	-2.034609296088661	-0.806146029958185	2.378184310263860
Al	1.585495581309026	-1.902456971998199	2.535947828651981
Al	-0.720958047171461	1.487157283788720	3.038449318041092
Al	1.990500101290333	0.671749155328778	3.304389070030894
Al	-0.865565554634687	-3.070524807697399	3.338867307415706
Al	-0.058227642055279	-0.727807735238073	4.421054278741432

2.12 Al_31

31

Al	0.708787611284013	-1.230551523064696	-2.469245962379290
Al	2.575595354226735	0.433053351486643	-3.334671682065337
Al	0.254238203805901	1.439720984785383	-2.409884436070056
Al	-1.329142538480056	-2.937068578361913	-1.946102388845816
Al	2.533099984600616	2.805164816255616	-1.882789494483561
Al	-1.689204600512022	-0.234828698819417	-1.697259789173422
Al	4.672519509228687	0.760307917828008	-1.655134385539768
Al	-2.081434162899650	2.455744799755889	-1.530112106692224
Al	0.052574940094798	4.029845046852921	-1.496816686415030
Al	-3.902262802818930	-1.758724493743015	-1.547480564658239
Al	3.345504506611737	-1.667535994834702	-1.484826363262331
Al	-4.230072236160512	0.862878333559438	-1.228197515993820
Al	1.276272458473375	-3.371776568945472	-0.901927855959258
Al	1.920344921660744	0.403298517792779	-0.506558450891474
Al	-0.707888100708479	-4.669648407359550	0.260364098284301
Al	-0.529565641339952	-1.656478078946630	0.311318583247488
Al	3.780541265815447	2.248843958757385	0.493972932886445
Al	-0.793904520054939	1.087751031378575	0.531745804831779
Al	-2.895153198157868	-3.219867206282081	0.502320325233757
Al	1.228006827729304	2.955612954780394	0.695298790046010
Al	-3.042397432170222	-0.515007610329318	0.771247714159035
Al	-1.354810298784599	3.855541346576864	0.903815606759490
Al	4.271365927596479	-0.371104381487978	0.880002858067568
Al	-3.481408401754265	2.175589383570328	1.139671099200285
Al	2.093472484437257	-1.748896068368079	1.395746888006864
Al	2.102374040236345	0.916061459010731	2.164125897222496
Al	0.188679231733689	-3.306915209771034	2.415610233139345
Al	-0.024557290004356	-0.564981837756369	2.699573837429719
Al	-2.243383093815300	-2.073424514091212	2.855896696121919
Al	-0.235745890555968	2.213264630917990	2.928966171992744
Al	-2.462447059318009	0.684130638852494	3.141330145800362

2.13 Al_32

32

Al	-0.091651783915736	-3.488049905533137	2.080477719728476
Al	-0.266510392201306	-0.399717553765274	4.144445545897872
Al	-1.877113473541417	-1.996393878753715	-4.574300448644244
Al	-2.178337953248363	0.355515233285114	-2.966586571131538
Al	2.199902756664265	2.762636292246338	-1.236587248606588
Al	-0.275460593007566	4.200840085463836	1.659386422288318
Al	0.208321330028213	-3.035139311044789	-3.088786581403158
Al	2.368057685505292	-1.897895755303637	-4.344576076656026
Al	-0.203181961333707	4.182728799204483	-1.221454231001324
Al	-2.470693205831557	0.309339515492848	2.523109954577887
Al	2.197006682175518	-2.185002187249372	1.043235584654418
Al	-2.399743404915659	-2.401369907424343	0.755701490436779
Al	2.064387349840056	0.302988955206734	2.730605735928131
Al	0.192606983211656	-0.234179147713515	-4.237385809466016
Al	0.071556008280700	2.034921283434564	-2.846779434069552
Al	2.101983373314260	2.686197555039582	1.561964600305874
Al	-2.255384218940092	-2.175923786107688	-1.868024094644724
Al	2.384334912712429	-2.021863219562281	-1.585733999502546
Al	-2.449571914859204	2.659784234710573	1.240984190738317
Al	0.025559093804755	-3.294864320295940	-0.504900177485460
Al	-0.237411962197962	1.967966630953981	3.043590166178552
Al	2.385184987531686	0.468281476851869	-2.708053451547300
Al	-2.318589877831055	2.610516551334575	-1.492544044104644
Al	-2.315859353631772	0.168134021288532	-0.208861382680045
Al	2.202922839283959	0.345960065600883	0.017886943177253
Al	-0.114796998452910	1.754721079937203	0.129855089698482
Al	0.027651739781433	-0.593060548668300	-1.470562282558872
Al	-0.165391789055729	-0.765156905362067	1.374498464595041
Al	1.818471430318890	-2.177843621086925	3.634524193549007
Al	-2.244788236096563	-2.191673078965222	3.343068113093068
Al	-0.297824209136740	-3.117557355597104	4.787904223580187
Al	1.914364155744252	5.165158702382218	0.283897395074348

2.14 Al_33

33

Al	0.650617869267137	-0.252916929973676	-4.240450873506258
Al	-0.503980320029875	-2.667965498359179	-3.776107139505211
Al	-0.880627735606124	1.740014396608689	-3.262634579216585
Al	2.682080014665997	-0.896998546966751	-2.561528216962873
Al	-2.258448759384247	-0.857392800215715	-2.900885039160990
Al	1.557252641905301	1.514619018849791	-2.109244871634606
Al	1.432675754907310	-3.242096638865539	-1.996751197050518
Al	-2.510780789975382	3.429270046828128	-2.008712955646382
Al	0.146677220130405	-0.885311978647454	-1.543457646359300
Al	-1.436026794305230	-3.183805202057383	-1.316166925146238
Al	-3.820688662849577	1.055625774756663	-1.910403277527191
Al	0.017050231747145	3.498107679568834	-1.127845260657473
Al	3.637110622334049	0.767898159193777	-0.577798151138072
Al	2.421844993582495	3.221565576426201	-0.016151787703857
Al	-1.390290622713624	1.062922977579509	-0.615264312424788
Al	2.415389156231830	-1.577591600061815	0.044007408919585
Al	-3.117774263160652	-1.288028804803579	-0.363944368672358
Al	0.818904876395138	-3.728875974343579	0.547768730221916
Al	1.114168773871500	0.860327339049492	0.653673084567346
Al	-2.256182366657323	3.299131832384074	0.657502611711042
Al	-2.246283400045062	-3.543979971428013	1.166638954902140
Al	-0.546155494469399	-1.366574541690029	1.089602805951936
Al	4.764966798947498	2.374475585045991	1.253384746794977
Al	-3.765761457767328	1.041067692788474	0.795462416855665
Al	2.513733294677431	2.634651347472573	2.683735404673561
Al	-3.007717487857729	-1.225634831506701	2.329453496673363
Al	-1.496701637982474	1.041725762937613	2.216062044091220
Al	0.128514423229447	3.187730631156370	1.790093041555529
Al	3.386466539676645	0.091510748802319	2.111453269650431
Al	1.756588296049950	-1.939961839596496	2.640383742616658
Al	-0.261899401608501	-3.656554593563964	2.971787411921857
Al	0.892396694392090	0.717539045303500	3.438178448557107
Al	-0.837119007598830	-1.224493862672119	3.938158982648362

2.15 Al_34

34

Al	-0.208909008009144	0.618185771775696	-3.644036212665020
Al	2.398911892151920	1.106880562712949	-3.867445022702866
Al	-0.639977770573052	-2.116173017653392	-2.937458109104309
Al	-2.715316169714209	-0.013559461461334	-3.138184800786533
Al	1.916852639748829	-1.519072833484232	-3.462418171970583
Al	3.892208014630352	1.262822467799028	-1.632141094473233
Al	-3.109716903546364	-2.561274135082980	-2.179400105529874
Al	1.069353995105372	2.832901726798966	-2.303283168898118
Al	-1.537300684342097	2.229574505464495	-1.898375627883601
Al	-5.129803670049934	-0.821183496819854	-1.943720984488730
Al	1.067612062059260	-2.489768156264651	-0.853080672919907
Al	3.480909304344374	-1.359194882670282	-1.232284377820326
Al	1.305485484118682	0.262256397661233	-1.307109896607296
Al	-0.181222679044643	4.370495307115613	-0.520772210106852
Al	-3.657909255133466	1.075336175450865	-0.726342485508255
Al	-1.331602703596987	-0.471034610582974	-0.823950367652809
Al	2.612123717268494	2.762098922848590	0.163016129360226
Al	2.776269349673115	-2.411131085749831	1.237812916640372
Al	-1.451746659329038	-3.247381313153071	-0.279269081891620
Al	0.046680608657896	1.789195849503178	0.522205074042452
Al	-2.310027471566589	3.137050976041213	0.551287244992292
Al	-3.672791665497447	-1.507927242155453	0.312481725912248
Al	1.073670481719182	4.164663443529951	1.853629931428063
Al	3.155283636770033	0.231067121371717	0.954275225741668
Al	0.301265739404364	-3.616268100292602	1.649936425149383
Al	0.467367170827432	-0.838895505357543	1.322401535279754
Al	-2.284888325035650	0.639772017821270	1.559058449064354
Al	2.249920963298626	-3.551478464254196	3.619933544885225
Al	-1.962745126711837	-1.938526287209921	2.265014083170207
Al	2.213065602484894	-0.748706273450843	3.425001320475536
Al	-1.028929343288308	2.869000203320775	2.945357295084650
Al	1.772290061072392	1.753509234966506	2.736795932585570
Al	-0.539967888725929	0.325424752255644	3.620525514872110
Al	-0.036415399170535	-2.218660570794492	4.010540042325822

2.16 Al_35

35

Al	-0.538233276045817	0.971734771859058	-3.518290807343323
Al	1.910592060712272	0.029393907380268	-3.727666691275817
Al	-2.658556368460377	-0.587062517234557	-2.490405752474440
Al	-1.101408318013016	3.655134346409216	-2.055483021882206
Al	-0.162195938834316	-1.649071433347116	-2.834367260867475
Al	-2.956830651331162	2.003255513014961	-3.059567353531734
Al	4.519450674584887	-0.885747919975602	-3.136785511796102
Al	1.336305911592508	2.627194891784582	-2.221677303442179
Al	2.404565877916733	-2.214499404861276	-2.106104634194828
Al	-2.301189446946436	-3.067116863890454	-1.684150894310275
Al	3.712688037181611	1.501322702791988	-2.247214157835963
Al	-1.255870268407383	1.173332551449560	-0.812284726546087
Al	0.380283145666175	-3.702714030461355	-1.124115415604317
Al	1.283535076147189	0.138597267109402	-1.044943039851786
Al	3.956055867433257	-0.570079756828472	-0.429328510030071
Al	-1.548965947116013	-5.348902899243620	-0.193377584735321
Al	-3.557647607536847	-0.972731987624602	0.151203534504488
Al	-0.847325917772210	-1.427289813950232	-0.010472064008770
Al	2.893771627734658	2.088507222160624	0.176913758017506
Al	0.424806602722976	3.180016264545801	0.284483131645347
Al	-2.313946653579444	3.412872243467142	0.404721216931568
Al	1.800954632518170	-2.086430191316388	0.549007986447611
Al	-4.010000124532089	1.514743467952041	-0.644989469167498
Al	-2.938729584489874	-3.391173152111334	0.978643330486225
Al	0.288779837371607	0.611792507467333	1.520822837959621
Al	-2.530466859013276	1.004657150487432	1.717005925050561
Al	-0.261529731435482	-3.670824458602731	1.615812642969532
Al	2.967596612040520	-0.086955280442996	1.976042822171440
Al	1.919507352956119	2.570351093690748	2.557902707970038
Al	-1.999637079122836	-1.509779298889576	2.550094819561183
Al	-0.883943313010812	2.951058983532166	2.652861278305817
Al	0.775993953316663	-1.697207446485848	3.037650556955755
Al	-0.973656391885891	0.442201606438058	3.960428479211942
Al	1.784311070419434	0.389077499603683	4.269144598750845
Al	0.480935137218552	2.602342464122041	4.938484571958774

2.17 Al_36

36

Al	1.303807163274493	1.450344834560378	-3.646114239940347
Al	1.459504743658870	4.239303428488414	-3.397987634687738
Al	0.787080591996421	-1.099992826376580	-3.319737024825664
Al	-0.921798964782944	3.074796154788009	-3.356593957120663
Al	-1.482877600585736	0.506889240626307	-3.226703572066469
Al	-2.007207450164802	-2.050570066362720	-2.976854258701393
Al	0.259940506441929	-3.638929070686460	-2.871895731806346
Al	-2.055767891868165	-4.747676705496916	-2.209352957983109
Al	2.693935416261315	0.014149990720879	-1.719154908167373
Al	2.592064431252284	2.757627942281479	-1.470709813702607
Al	2.092468103154268	-2.611732950843209	-1.287144984727581
Al	-2.363663231459701	2.380675180513609	-1.267201644577314
Al	0.192036771246094	1.261321146082452	-1.122147852868622
Al	-2.989524335612063	-0.267993299906173	-1.088842005448093
Al	0.093520614214453	4.019318982752749	-0.958661667900763
Al	-0.398336866053093	-1.439501770596832	-0.812962433572313
Al	-2.790206844526590	-2.925665643468113	-0.383633576564549
Al	-0.215989779094635	-4.125460735361177	-0.186418327382096
Al	3.844983810979846	-1.491279975103964	0.310373154747328
Al	3.806189339182444	1.353209823575153	0.418436391270795
Al	1.459234986866681	-0.203033845383413	0.848726301844847
Al	-3.720986076398541	1.594972365842391	0.834610929265176
Al	1.451620832661689	2.647678872301631	1.036219163690395
Al	-1.251023764204939	0.378018516867440	1.085937960201269
Al	-1.222989097855477	3.171013579346775	1.144776010525309
Al	1.493231545684962	-2.939075148008362	1.410247710163736
Al	-3.608346626030078	-1.184082038053667	1.436114511982943
Al	-1.155251190547848	-2.395502135380662	1.771966659111534
Al	5.127913231801390	-0.007049745608876	2.314414021387838
Al	3.151889005835837	-1.641777786500340	2.988455428376264
Al	-4.532082597523872	0.516073061990141	3.292831037004868
Al	2.633743846685162	1.079203360702888	2.997771807734338
Al	-2.491085102382153	2.207006621430088	3.240129910634360
Al	0.612199179353871	-1.064443588943105	3.367488790253537
Al	0.082728689640613	1.660944612370349	3.178932747555665
Al	-1.930955391102045	-0.478780383160490	3.624684056292825

2.18 Al_37

37

Al	1.291467587870505	-1.762430639158910	-4.251668456253457
Al	0.065827186230139	0.468478512221811	-3.638620198300393
Al	3.714931006947596	-2.485513423250991	-3.508581880708847
Al	2.884740321916066	0.134650726564411	-2.967487460769646
Al	-1.201932445006975	2.624056153539014	-2.840933907974335
Al	-0.960401630249494	-2.221563364366165	-2.959662921589810
Al	1.585170166421609	2.260436065104095	-2.094676307487558
Al	-2.170235320498493	0.081461546873109	-2.166390150113759
Al	1.512522855051238	-3.371544567406096	-1.995686401063604
Al	-2.397532252730887	4.798996519021300	-1.708717153086521
Al	0.170951084839961	4.292533804336996	-1.078480601171355
Al	0.848040945138179	-0.767186740272866	-1.321393949799825
Al	-3.150610803370349	-2.394899536617409	-1.489563534466285
Al	3.562418954767988	-1.777134039199479	-0.947942294574494
Al	-3.200661743017180	2.316606403452264	-0.891586219575602
Al	3.115501242428769	0.811771816025487	-0.300886998422563
Al	-0.492832435119674	1.489548671457269	-0.400562793145959
Al	-0.686674859437518	-3.622905977451593	-0.566120397941921
Al	-4.024309986543248	-0.067069405144546	-0.118710856718275
Al	1.760662433661247	2.884854908285508	0.572243145732182
Al	-1.385849118981140	-1.052628927225761	0.251397337268282
Al	-1.655538635406407	3.708860647539209	0.841803457034361
Al	-5.117541597955740	-2.405308281154284	0.537338979517944
Al	1.505313551278560	-2.669175746271323	0.663846301157188
Al	0.970720548633128	-0.004686273359514	1.374984961986986
Al	-2.850871314434176	-3.665371574775271	0.956024253149044
Al	3.586236213266021	-1.171426860038359	1.648239268439527
Al	0.544060183645847	4.921165285267364	1.858171583996960
Al	-2.416260797283754	1.272736038372424	1.652920465844170
Al	-0.717644039844323	-2.863313439621681	2.232027014221568
Al	1.481212738858947	-1.954102713672244	3.351935479993184
Al	-0.993768635720219	-0.288484281863141	3.360157058169435
Al	-0.020012038383467	2.269441140365279	2.608805260646617
Al	1.300846334027581	0.620839843015583	4.282631297975000
Al	3.075852221696016	1.463468203448807	2.435815909498006
Al	3.692764275228754	-0.601726291236176	4.302563573443244
Al	-3.226562197925146	-1.273434202804102	2.316767135090416

2.19 Al_38

38

Al	1.971522221702559	1.261204940437686	-3.541348054873320
Al	-2.670097641729762	0.455430818923874	-3.775636298489649
Al	-0.694168376173190	2.146866741558634	-3.459895497154189
Al	1.214726539651430	3.840622363377786	-3.038877427980128
Al	-0.105583422825454	-0.481245747587389	-3.244403541431219
Al	3.849960174420533	3.395051879480169	-2.870521709711163
Al	-2.350979298597703	-2.094706561081195	-2.937823109513090
Al	2.303832787574386	-1.122736862751662	-2.233675350521561
Al	-4.608896606206741	-3.012430449051241	-1.572915047794443
Al	0.198733675387947	-2.688199434353888	-1.874703371709781
Al	3.634554294277457	1.148545975199896	-1.420788336017967
Al	-3.919244966188391	-0.342291489278971	-1.466956954485677
Al	-2.165773867935512	1.712323156040998	-1.217562401414812
Al	0.579998428607889	1.178583713034907	-1.025682957256473
Al	-0.422371541674540	3.758745302242804	-0.897734401165781
Al	-2.057554114814183	-3.750619090370882	-0.796638803054559
Al	-1.316285724546615	-0.735462592542445	-0.569081996680866
Al	2.259754362616018	3.355273531940917	-0.578063046254380
Al	2.602783696803526	-3.336104557607677	-0.699175948269911
Al	0.334235424187989	-4.715343460329046	-0.016176626326546
Al	3.942271671768715	-0.992631549787198	0.060055668998130
Al	1.157355029536795	-1.156423358015045	0.420641507670998
Al	-3.531879100680072	-1.941301660934175	0.718961923950632
Al	-3.412670445985589	0.799224319336984	0.961874257747210
Al	2.355034470793113	1.165866846850060	1.049535566721326
Al	-1.945414231081504	3.181078400461523	1.223346978549268
Al	-0.910276726504138	-2.599889440905611	1.400164936507029
Al	0.747425922487672	3.270402221147213	1.615321577548713
Al	-0.568839854483425	0.899584022508083	1.728795093511250
Al	4.229667375038487	-3.222793860888467	1.515956928089613
Al	1.585952819401610	-3.319410242953187	2.055536648944482
Al	2.924768442532789	-0.950650604448338	2.657555977472100
Al	-2.312943472331325	-0.805620870126148	2.878648898351432
Al	0.348243568074940	-1.277962053733159	3.355344866869762
Al	-3.028254823738735	1.855130294678517	3.390789730876010
Al	1.432582123015584	1.265219928575659	3.582230566472639
Al	-0.716503831536246	3.198195272670654	3.867251090098227
Al	-0.935664980846335	0.658474158279338	4.755648661726676

2.20 Al_39

39

Al	0.769185795776082	-2.436949627720938	-3.715233198288293
Al	0.562365813929331	0.146926749796366	-3.450914997573470
Al	0.643248010713240	2.692477138664451	-2.885606623633043
Al	-1.628073725303466	-1.500481679520792	-2.889293993410174
Al	-1.761421919849509	1.168847573880502	-2.585864975340890
Al	2.122335186339868	-4.418387037875296	-2.576290476607337
Al	-3.913342616384819	-0.466341011293498	-2.081657760830405
Al	2.938181349555569	-1.794086406386130	-2.074668441041549
Al	2.552162903823822	0.898445052842343	-1.664505835909798
Al	0.560659245976680	5.226402121689068	-1.779205512350982
Al	-0.447806144532604	-3.777826861642934	-1.598367038009821
Al	-1.554874496808978	3.621709036922855	-1.373921050208356
Al	0.424791291355314	-1.225727562634903	-1.004542865326867
Al	2.530480692410402	3.604423632298900	-1.073074598905455
Al	4.992318998751617	-0.316723677173243	-1.048719710459787
Al	-3.774327665599226	2.201019397437260	-1.039503351792050
Al	-2.751980143538001	-2.848716936582888	-0.705986858119765
Al	-5.992256690819710	0.632166929725912	-0.651457046928334
Al	0.118095829841973	1.457366817294233	-0.497046800254711
Al	4.741858270058747	2.352972380194885	-0.473260448221499
Al	-2.012346902642344	-0.200708282316436	-0.074365510281636
Al	1.846786544721137	-3.507690202165733	-0.047727421088618
Al	-4.986839962046621	-1.675301528356135	0.224718587322169
Al	2.780345800460218	-1.010652222836788	0.552678149996543
Al	0.387736588439658	3.927074618835308	0.656407132213266
Al	-0.637427840808844	-2.963590256443212	0.984445648257365
Al	-2.025999591563062	2.440228265586830	1.058188642769142
Al	2.356842193504370	1.849711217369730	1.064345057351730
Al	-4.165371999736382	0.748960889713517	1.401894464655907
Al	4.796081406915514	0.621298467732354	1.651615406297559
Al	0.237271973362985	-0.325039204862932	1.590479673593398
Al	-2.943432157901888	-1.925034013574107	1.955107374014286
Al	1.667279508450672	-2.641885101895272	2.441065430152506
Al	0.121822633362614	2.271037103561680	2.655518879667515
Al	-2.050207464566105	0.534205651986737	2.956837043654431
Al	2.562749380729741	0.005011595862085	3.095044946596079
Al	-0.816937858275296	-1.999388189318214	3.516004516351201
Al	0.175090162058591	0.416207764974587	4.486150470731562
Al	1.574957599838797	-1.781962603770186	5.000713090958191

2.21 Al_40

40

Al	2.779760244010900	1.810312376512039	-3.168246320466817
Al	0.856452628679085	3.647808092758849	-3.792136898090773
Al	0.182768601801994	1.031213852987015	-3.129275414999467
Al	-1.740992738761616	2.870497356747606	-3.771992945851408
Al	2.134977352907550	-0.711736174983121	-2.409678975419629
Al	-0.448845116907357	-1.580037721985109	-2.625829011071579
Al	-2.426134842938548	0.267285249815760	-3.245631772373326
Al	4.782133513269347	0.143051645971447	-2.344149393315284
Al	-4.721930908181282	0.364160404675776	-1.746305031879164
Al	1.564520922037506	-3.295429432726158	-1.783924024278667
Al	4.147662996982632	-2.387179477924892	-1.609601325211175
Al	-3.090258256848147	2.532815319042284	-1.418190766295842
Al	-2.744720693557891	-1.429426517596605	-1.145673934387824
Al	-0.463083817784925	3.354441850922829	-1.302651942334609
Al	2.256638010283908	4.064881628826795	-1.393600563058298
Al	-1.110055555830222	0.721006201273347	-0.743335116355055
Al	-0.793090600783486	-3.175901592332344	-0.432537326691126
Al	1.535793752348145	1.449812753015776	-0.653165280768849
Al	4.206792604358883	2.319851857758865	-0.674350701610534
Al	-5.138617086001998	-1.390578725782760	0.278894132827505
Al	0.985046765045894	-1.154079999658503	0.027712622771583
Al	1.164063323391998	-4.896774136279277	0.406485425266318
Al	3.609079707041031	-0.287403473543240	0.198394409222885
Al	-3.175800408276068	-3.199540522927824	0.862721837398196
Al	-3.451459492047508	0.842414500460107	0.726933087676903
Al	2.986146629892723	-2.899541935510702	0.810232869711390
Al	-1.853902316147620	3.022216503965060	1.008243301117307
Al	-1.415687949540178	-1.033548495245503	1.345028509284012
Al	0.918789363419947	3.656437234434717	1.051732952673307
Al	-1.213844892084301	-4.904923062798523	1.706442359425619
Al	0.293136700653736	1.037876235892941	1.719544184712245
Al	2.945297264007591	1.843707169816497	1.802045600832436
Al	0.621224972546573	-2.804224568666316	2.220061674376410
Al	-3.847257521224689	-1.071735708608673	2.748350831167015
Al	2.471302589824484	-0.848481677779866	2.598295463101714
Al	-2.103130207350411	1.114935083328156	3.106228479958876
Al	-1.900835894720746	-2.823780920682037	3.455850107680314
Al	-0.403870058915967	3.190633258576060	3.350729190566126
Al	-0.081020425130353	-0.703481915488146	3.845177053344639
Al	1.682950840529390	1.312447483737708	4.121172651344658

2.22 Al_41

41

Al	-1.058794427570684	-1.020294426625927	-3.278050712099232
Al	-0.329113028953811	1.707779064209960	-3.895370954607547
Al	-0.542724141473277	4.321538346879098	-2.959395666017612
Al	0.908117579863818	-2.536008625950129	-2.050497259517187
Al	-1.615826124189292	-3.549794721751199	-2.434693644984424
Al	-2.815988811896961	0.780003678233296	-4.298515249502582
Al	0.336491321494302	-5.151320557074119	-1.342865064704416
Al	1.540750664617224	-0.001180977683276	-2.892514479966295
Al	1.320730921098804	2.620301785326880	-1.982441518695735
Al	1.060103709168301	5.290480394263469	-1.024461387118926
Al	-3.288799328472281	-0.165997718093312	-1.749034484486206
Al	2.848251463628957	-4.158428527400914	-0.927492649944513
Al	-0.733062385997469	0.891746089087544	-1.242971954745567
Al	-0.996138932161289	3.510849743851853	-0.331176818081849
Al	-1.742659170182439	-4.440384072239021	0.316899128814010
Al	3.460252649116379	-1.596838339310530	-1.667555251824188
Al	-3.778131373289575	-2.732471848253920	-0.952748467559701
Al	3.141321034774572	1.009625825932510	-0.904021820664440
Al	-1.229526155705624	-1.672098424152386	-0.423921177173538
Al	4.797888402437797	2.048284794337048	1.073653432651977
Al	-3.064015920028441	1.842912707175449	0.238455066281022
Al	3.312155067776571	-2.408060232744046	1.140037211361966
Al	0.927335586661608	1.793980055039427	0.746888064175852
Al	-0.998736065707625	0.088532848516969	1.627699429473704
Al	5.089757327372745	-0.530696744520679	0.257283539987210
Al	2.953028074746543	3.672526178196408	-0.032305022084669
Al	-3.505669602509023	-0.755577529063308	0.925770067081906
Al	1.281109881406254	-0.772952263050302	0.006027791909737
Al	-3.846234170062171	-3.416507150985084	1.702764973001084
Al	2.601456556713062	2.853951595434005	2.686286171607009
Al	0.709276925720511	4.561325093276182	1.620301103386057
Al	-1.227537260759284	2.805108476546261	2.337052619246514
Al	0.792647625673425	-3.376646732556365	0.744181408400292
Al	-3.224035869845046	1.151989406816838	2.823451848166032
Al	2.943157075391843	0.220757107210494	1.943406211126810
Al	-2.605309735694560	2.590239913781335	-2.316016358010636
Al	0.760669287764600	1.098431136392412	3.499229945914575
Al	-3.399437868588243	-1.435411822474325	3.635757871817574
Al	-1.257488938950106	-2.571614540496094	2.252497671271158
Al	-0.828430198898220	-0.863899551591164	4.261736456295989
Al	1.303158355508156	-1.704179434491326	2.866669929818761

2.23 Al_42

42

Al	1.288398893562944	2.592648670819079	-4.198846286137164
Al	1.921561393695340	-0.040359743926663	-3.729622616447640
Al	-1.220129979512958	3.575548706198660	-3.688759688511284
Al	-0.579439678219911	0.874152657325247	-3.159723713706938
Al	4.445711012291271	-0.138153628398884	-2.707528336794345
Al	-0.005582929719898	-1.770615368838017	-2.738859866271747
Al	3.024816527311433	2.128406590135910	-2.097460909440416
Al	-3.082409482521229	1.880091802110142	-2.636972264195935
Al	2.520198725281015	-1.851818505198406	-1.769736133745569
Al	-2.465457049919564	-0.743750263883555	-2.108727295661118
Al	0.514058338385730	3.079337792456862	-1.563940060048909
Al	-1.954721856884078	-3.363091678335216	-1.575474210219395
Al	1.097441749451017	0.433124214804124	-1.051985172655803
Al	5.091973001113722	-1.878953987355663	-0.709927178026026
Al	-5.030798007684562	0.303757325623410	-1.558360329180930
Al	-2.074505318970127	4.094069453585281	-1.110524523814439
Al	0.648787713190135	-3.461710470287516	-0.731844426081318
Al	-4.431978414591816	-2.314346791374370	-1.013017993672388
Al	3.659633414121885	0.400976442137823	-0.044940098254390
Al	-1.432471845258521	1.357885173657127	-0.478601368610677
Al	3.203771347021972	-3.579664903868397	0.236693299917992
Al	-0.907587623044535	-1.292907784071296	0.064464127716933
Al	2.318206141683810	2.677676013518825	0.497768595785763
Al	-4.085348431419762	2.367597534039311	0.014540424338115
Al	-1.258875348606125	-5.029664842255768	0.463165048148229
Al	1.650430014257651	-1.310996963332983	0.938691221696459
Al	-0.313377492949801	3.498603575081624	0.956165949929110
Al	-3.416799048879047	-0.301099764234266	0.630784662938435
Al	1.305478413251910	-5.134302793088906	1.391074440341526
Al	-2.855360489151562	-2.919841596087765	1.178524095694257
Al	4.320524782040005	-1.453291744294749	1.920485698405649
Al	0.176600290025233	0.867231138734331	1.658108848815003
Al	-2.972735582482513	4.422464822431429	1.478040326741281
Al	-0.271683464517050	-2.979257972856122	2.144701370487272
Al	-2.422899195503280	1.685518733085278	2.135864552902781
Al	-1.916168093847169	-0.965633787698920	2.861272914638096
Al	2.855576476692358	0.735811467541419	2.615036401100163
Al	-1.185002875834508	3.687827602871097	3.566384095877780
Al	1.370332210810739	2.913086652119761	2.999625621401467
Al	2.364267456134833	-3.139972118613164	3.004669017223137
Al	-0.777045881847418	1.061735205529837	4.200795412060705
Al	0.882610191042394	-0.968116865805985	3.717996345316200

2.24 Al_43
43

Al	-1.610274542508295	0.048282533709465	-3.447237721096299
Al	-3.496337682687113	1.874079670315009	-2.827385487700468
Al	0.379858867374196	0.415105119036982	-5.300625317200580
Al	2.443833264379908	0.214033487340355	-3.596316254148393
Al	0.401254384796006	-1.878406459132842	-3.907385188624088
Al	0.405431091729627	2.108611555494415	-3.141940894256632
Al	3.077866636194173	-2.480556112583783	-3.516199079633680
Al	-1.558573394912305	3.854585307481337	-2.535927600398002
Al	-1.525585389754539	-2.396163158857656	-2.044106695124850
Al	0.543353475566871	-0.286532185486449	-1.648487597172295
Al	1.171620397955174	-2.982110597143964	-1.576277478786158
Al	-3.329531307446007	-0.470032238318462	-1.367476126561240
Al	3.902299579131876	-3.627432665507710	-1.202978762391286
Al	2.616402566996076	1.843097137384067	-1.412134550124435
Al	3.220816600824975	-0.883000416448988	-1.263064763399512
Al	-1.392952845009196	1.500191517454422	-0.944764138743070
Al	-5.231384514395317	1.411904521011367	-0.734290292424326
Al	0.551476985366115	3.502199758619993	-0.779275958688482
Al	-3.402190680789429	3.373650453625723	-0.331328811538976
Al	-1.465360688798560	5.265360697272451	-0.167118307834446
Al	-3.243678352004157	-2.768362514478348	0.116365563825722
Al	-0.601309795057789	-3.412384912371658	0.367872255799773
Al	-1.343481691809181	-0.772781759744509	0.522730573683853
Al	-5.104870715964935	-0.851621068085597	0.770205054119348
Al	2.116005496489826	-4.172064213373657	0.761947522526990
Al	1.305448294750354	-1.389544966483658	0.765894739178009
Al	0.640236402568542	1.258244025497179	0.823665545703008
Al	4.085337965378365	-2.154051689343354	1.064747218545124
Al	3.297871245628134	0.580056823319248	0.964456378797061
Al	2.606809402834086	3.221459524243874	1.007323490617063
Al	-3.250946158260596	1.134293543802153	1.220809188877871
Al	-1.410744690445231	3.017661360771720	1.499228728022311
Al	0.554094178230518	4.941493275442040	1.628228257175570
Al	-2.338435317661048	-3.821582470661784	2.510396171369369
Al	-3.141930932533098	-1.187003167518858	2.650441142580094
Al	0.285047850835076	-4.545538728513559	2.754041927212606
Al	-0.498882858840526	-1.840307318230899	2.936223953642076
Al	-1.293522851034648	0.799947730872615	3.120349027531798
Al	2.166410382556247	-2.577404370855043	3.094636443742298
Al	1.369227259611019	0.072772098977278	3.220360904974093
Al	0.676053875787440	2.721710782624809	3.230000796476551
Al	4.096110584091898	-0.641732943910558	3.339541592473241
Al	3.327127620835418	1.979873032754897	3.374854548973277

2.25 Al_44

44

Al	0.979638404963167	0.778785655607951	-4.159801839175485
Al	-1.754260860955373	0.148098127596057	-3.972202482991848
Al	3.733372186249419	1.358963324046426	-4.282955124860052
Al	-2.471620217294497	-2.224787538299033	-2.946659646587122
Al	2.786919582135075	-1.013114322151681	-3.311037599651656
Al	0.145153931116425	-1.519850507329439	-2.976227245861579
Al	-0.621697642667852	1.991334714188998	-2.355680185720557
Al	-0.605257537018469	-4.120032471506920	-2.489080562354324
Al	-4.474955428541820	-0.532855009747417	-3.717169094689660
Al	2.099876041885077	2.642074040563786	-2.575020842670470
Al	-3.356235365624672	1.383569084699390	-2.198551476580469
Al	2.011706334703689	-3.516496221009179	-2.668722263820335
Al	-2.431392305684351	3.492776067133626	-0.962192170245284
Al	0.517141603562122	4.172474434443423	-1.165789779716068
Al	4.018794164810121	0.894512077434985	-1.559496297074288
Al	1.292686491553924	0.306690248917892	-1.185371168828008
Al	-1.439156214121768	-0.323644227785813	-0.996359344789047
Al	-4.172779494012408	-0.995331726050313	-0.995043258866808
Al	3.484079099187143	-1.698090162631997	-0.838229223693553
Al	-2.470916644937628	-3.072888957873801	-0.427414329458344
Al	-0.901874573595489	-5.119141947071699	0.002470684087571
Al	0.587835871684810	-2.680800622845537	-0.449560988603475
Al	3.038362217419168	-4.210404644530770	-0.268824158334539
Al	-1.235851377701582	5.450803069666136	0.306835971073163
Al	-0.446789940557279	2.058934655936968	0.408303923806638
Al	2.582412080478145	2.768369311767884	0.137196880814265
Al	-3.487223594565118	1.367988038541450	0.555242131906169
Al	3.076029174606399	0.243770023209148	1.009874706108228
Al	-2.539644511228778	3.524422892347596	1.783867222815408
Al	0.957124992832727	4.330735664201834	1.542392853645577
Al	-2.714300135392881	-1.091759624741155	1.408878833416292
Al	0.217743728712572	-0.561341600360857	1.284261263675422
Al	-0.982742236823697	-3.103703029546143	1.764372360447663
Al	1.218330874725423	-4.790254569011045	1.629041644290606
Al	2.458981361403881	-2.309660354826573	1.527667519663611
Al	-1.771699664099536	1.033569265505649	2.629355362362340
Al	1.468600539454684	1.780376763944034	2.405788640899692
Al	-1.091197324849947	5.609922740448699	2.938515627620530
Al	0.967962315943080	-3.094268995196819	3.691992153448684
Al	2.090829423007706	-0.598307261093170	3.542281018524806
Al	-1.141421261922217	-1.344210120810159	3.764310025853581
Al	-0.482312325289444	3.176237353958197	3.627010885737649
Al	0.122391027282278	0.867136925637174	4.693475262012111

Al 0.737357209167746 -1.460600565377815 5.848254112362975

2.26 Al_45

45

Al	-2.250555778190532	-0.715219243784238	-4.080387017295015
Al	0.183052194619018	0.920730435491574	-4.239303168184971
Al	2.587018132303134	-0.489623102959847	-4.038310943456543
Al	0.235045520479462	-1.815589557535087	-4.302078672386088
Al	-2.363581089418928	1.959121418760869	-3.956204008080005
Al	1.711041090077662	4.208315596362636	-1.354934071948167
Al	2.310689174607930	1.997703095498029	-2.886753598405523
Al	-3.711324830645768	-1.353939937318291	-1.819433795873218
Al	-2.850263573489304	3.032006736627318	-1.507494688353491
Al	0.898631846565362	-3.779864722621939	-2.547308317806882
Al	3.248006094932155	-2.505352748561187	-2.281219257644935
Al	-1.480352810548572	0.581395803009421	-1.810706173775055
Al	3.930536112533515	0.132342820166173	-1.733572431520802
Al	-1.807794918181379	-3.190423729204567	-2.788620440007318
Al	-0.313396274340509	3.258683292382443	-2.800819264070413
Al	1.034120409387905	-0.638880324264456	-1.810051296070815
Al	-3.106392385545186	-3.653214184975233	-0.454727109901576
Al	-1.109207798332744	-1.785506112201188	-0.464781850451921
Al	0.601243795386980	1.784838897833675	-0.576370021920994
Al	-4.316581886918838	0.973724922566758	-0.471280074479075
Al	3.470921365191044	2.430880650617228	-0.399962907986637
Al	4.234101283618145	-2.059063099338476	0.196394118252348
Al	1.599152172501046	-2.842597328199934	-0.068135657907931
Al	-0.848494770265864	4.310623689525675	-0.216464320738769
Al	-0.549933258737374	-4.564291141462033	-0.384077446496905
Al	2.246950483879154	-0.136114732876736	0.616625661132721
Al	-3.848640381213069	-1.500625620075068	1.010498150332882
Al	-1.802788082115672	0.593106050702071	0.843997765263497
Al	4.864461958916161	0.472750412138067	0.813523977637436
Al	-3.079652626881389	3.207690523004111	1.203892340363296
Al	1.696136029388761	3.846524116168109	1.342426783439244
Al	-1.995090962044629	-3.266048100085281	1.987646084660250
Al	0.106233819402130	-1.321907325041771	1.880806667144142
Al	0.429047089690856	1.340630416891901	2.005905230205212
Al	-4.148530683257718	0.859067611360251	2.241928664933194
Al	0.565215748652086	-4.151641167945160	2.083363256998977
Al	2.757293688303090	-2.616030440365062	2.403834773324679
Al	3.261586368267446	1.911172640519936	2.429821973460175
Al	-0.721994971409773	3.925763523843209	2.467712540994967
Al	-2.471511852858684	-0.986312495477783	3.326955437496681
Al	-2.008949595192425	1.836310307205457	3.578442089931864
Al	2.274793194673684	-0.266245521011792	3.695546239084704
Al	-0.370291249257539	-2.604798420168708	4.141624164796623

Al	1.143932002598152	2.586499234898120	4.176894030197543
Al	-0.233879797128854	0.073406859900853	4.545156585112538

2.27 Al_46

46

Al	-0.210768845157771	-4.256117333551958	0.617954167411254
Al	2.313425607740385	-0.127124463825430	-3.772936917639191
Al	-2.356346270195679	-0.221835931040829	-4.445258110331390
Al	0.075205860490657	1.298268183864307	-4.211139966180753
Al	-2.574375905075281	2.290909597784891	-3.673940491892535
Al	2.053251600350890	-2.885914454026133	-3.234194768188364
Al	-0.089309448163688	-1.585519668046018	-4.098561500881339
Al	-0.536715432775196	3.560286107262543	-2.518748204991903
Al	3.800427088454493	-1.600790513505604	-1.656974598322391
Al	-4.022694614106545	0.332594905552524	-2.202947549726371
Al	2.078857411438289	-3.709517051377015	-0.653500003939319
Al	2.080006696202904	2.568441340299801	-2.946230837356803
Al	-2.568143077406280	-2.209515750501053	-2.658223393164537
Al	-3.010349816113492	2.861191027014486	-1.090112130904837
Al	-1.299874894507134	0.455103111006922	-1.875504263697623
Al	2.445467301966124	0.169951944953850	0.163935184548516
Al	3.825446942946877	-2.256776525356632	0.955919479795002
Al	0.571553311417770	1.836739900989931	-0.547416890750078
Al	-0.281620378570356	-3.679874835802828	-2.116646662717552
Al	4.143553348397839	1.010064540373728	-2.146591174523815
Al	0.835026511581152	-1.103234637471141	-1.446845098169755
Al	-4.468926311781731	1.075639040916485	0.462655024109157
Al	1.405181506338934	4.479606887696113	-0.971924558473614
Al	-4.205411883152169	-1.838480086221330	-0.447325211019100
Al	-0.966748646036679	4.134686211647363	0.283173147796999
Al	-1.710185401709086	1.014932125562762	0.861980013950941
Al	-1.471100546920674	-1.589391422938503	0.064502550072556
Al	2.125265459219852	-4.009081486566014	2.065729923419578
Al	1.425366620432506	3.719977208335667	1.627029562494279
Al	-3.205051788436822	3.238785655032048	1.565841027151674
Al	0.640284487719164	0.815481079987142	2.120802244445319
Al	3.225570960835395	-0.593793781767248	2.954574251813163
Al	3.416018556476400	2.834216086132280	-0.326653143263034
Al	5.022491687928758	0.285537766997187	0.505902257267197
Al	0.879308920990225	-1.747110095496176	1.344157605548636
Al	-2.570954571931389	-4.022028789144343	-0.667274083097215
Al	-3.999749329798337	-1.025943332228961	2.150019934798632
Al	1.567129630451708	2.426320037513669	4.047373150452627
Al	-2.591343363120085	-3.324527977529081	1.970184225128163
Al	-0.853771157593561	3.096633793583452	2.878252259172941
Al	-3.008832241217779	1.187631920040223	3.347814836994914
Al	3.470557282134827	1.949362046303667	2.212462231295913
Al	-0.201603683014531	-3.451133746096237	3.295148453792857

Al	-1.551927951695307	-1.141342938854784	3.273231341165229
Al	-0.610110375573141	0.956462273297721	4.638718215426254
Al	0.966519140537677	-1.219767970801353	4.301588471179610

2.28 Al_47

47

Al	3.620623126506262	3.553611262250820	-1.941561348898237
Al	1.046189484953246	2.682832457514971	-2.514604698508089
Al	-1.591578720461746	-0.793661899877870	-4.145354153233464
Al	0.818769383675976	-2.328991987942253	-3.814702748361261
Al	-1.611688581411601	-3.466862315194031	-3.950985405854373
Al	3.126024480061442	-1.098054741393824	-3.538022424087788
Al	5.263521346432732	0.493706624699836	-3.011411580664004
Al	0.775393363084049	0.449804078382028	-4.169624288768762
Al	-1.285409531622332	1.452922131747121	-2.590809594337205
Al	-3.770501172399071	0.282318694314096	-2.698028405497102
Al	3.100628814110076	1.748379314473432	-3.971506371527921
Al	-0.054312803727118	-0.810218570682261	-1.689439745715369
Al	2.554461317735623	0.605132772752702	-1.446230682724391
Al	-2.656434633143631	-2.178768648198742	-1.774644196095529
Al	-0.306591717633149	-3.581192692156244	-1.543268055233378
Al	2.160090405562054	-2.336206732670323	-1.339181579179435
Al	-1.000471135741781	3.815674914053682	-0.936186927433230
Al	-5.914942420287647	1.482955564561781	-1.424344770527856
Al	-3.421676089769724	2.604304724988395	-1.169552508725777
Al	4.588794649450506	-1.201363295753383	-0.998890388884485
Al	1.549118803148970	4.691355730188750	-0.701846460152920
Al	5.049926397098121	1.611762027774825	-0.586528439987896
Al	0.313592018562757	1.408882949679537	-0.122393696442664
Al	-2.233736095399829	0.205984447552527	-0.291454693235208
Al	-4.850074202855096	-0.888439136965751	-0.444594671171245
Al	2.792078445909894	2.560551495744797	0.516917761521869
Al	1.401928756113715	-0.915006191611676	0.842800231716275
Al	-1.272499953479546	-2.213476389703755	0.642084179094653
Al	1.052043013377610	-3.679270898371462	0.815990930263739
Al	-3.865371240212734	-3.220557833115215	0.558941482861364
Al	3.623711895964714	-2.527227097789766	1.056975630391012
Al	-4.501838681791082	1.430822919491639	1.038477535582917
Al	-2.037896641098964	2.545807495557868	1.279636762467003
Al	4.006256560221424	0.221604746404417	1.441237312316840
Al	0.441116544717175	3.714877901915910	1.566974224054171
Al	-0.863386592123973	0.107708765384883	2.089043344538254
Al	-3.457202544413455	-0.924047454762198	1.953515593473215
Al	1.643190992637590	1.245117196557135	2.494149623091133
Al	0.120062337411131	-2.379434487122207	3.048196217564010
Al	2.481154400018399	-3.756855205764256	3.155261607401071
Al	-2.540586421800000	-3.317782074915248	2.859168966562477
Al	2.754291872381256	-1.101392417986293	3.399007353216231
Al	-3.106963787272701	1.329736522123758	3.460375685674832

Al	-0.615365832470395	2.403527946893654	3.702087274119979
Al	-2.083978566819741	-1.088608773427511	4.357469216407797
Al	0.446389151068480	-0.020454592618856	4.622437504091748
Al	-1.686850194267889	1.178490753014568	5.914419398837010

2.29 Al_48

48

Al	0.301899832630578	-0.694184775728370	-5.360218486047732
Al	-2.094437008155129	-1.829088175388051	-4.588863826173792
Al	-0.578651490473435	1.863611833032760	-4.956402485978772
Al	-3.863445483974847	-0.345717386334329	-3.218208415916992
Al	2.491633976449856	-1.379824357375840	-3.754173558960298
Al	-2.793877927716262	2.279973626571991	-3.480492268388654
Al	-0.209412358092742	3.306541080867484	-2.690865602889600
Al	1.307754661438928	1.081818524075352	-3.270708134928171
Al	-0.058514519092414	-2.294213478183410	-2.969105961469340
Al	-1.249715104313260	0.173960879043564	-2.819161576546527
Al	4.731568536093752	-2.129742776658348	-2.225111204823458
Al	3.193107352378883	0.192290758473327	-1.604775778282923
Al	-2.678956964526054	-2.740341469893638	-2.125593985396371
Al	2.049572158693778	-2.751967442391063	-1.408302222027313
Al	1.684463525324643	2.399983768561237	-0.951845241095977
Al	-2.529996900672481	3.801616575824474	-1.268461103119257
Al	0.562048759480209	-0.402244328119609	-0.897452368873646
Al	-3.486776561325799	1.253884561316120	-1.024200993796777
Al	5.221846460310607	-0.456995965630879	-0.073152704427452
Al	0.042626626076498	4.549808200715621	-0.356988982165928
Al	-0.523159214542098	-3.129060404219906	-0.490703075769344
Al	-4.573248068197347	-1.262194871944065	-0.758117500462946
Al	-0.946455623504871	1.852820832879008	-0.238544984430760
Al	4.046372687018346	-3.423361456755083	0.160615273687521
Al	-2.021043783987814	-0.793821542314726	0.022414908429804
Al	3.854791809470623	1.788988795099138	0.582056160159288
Al	2.626132722580813	-1.113571505364106	0.738037243724600
Al	-3.152016962793120	-3.397487695882241	0.429274297325854
Al	1.566539512873112	-4.115946648913416	0.986588533209769
Al	2.203676401580720	3.808023671014853	1.333863158221279
Al	-2.198604064565086	5.279523447081830	1.005733535885360
Al	1.034208192610960	1.191359299905240	1.461860731249324
Al	-3.247092358620990	2.811191150837731	1.258869967677303
Al	-0.024872370322786	-1.479007375481856	1.695572799301985
Al	-4.224386914382967	0.359296695621262	1.514279576221352
Al	-0.966779366295901	-4.094223854084825	1.991607416429266
Al	4.485030876094704	-0.268498804273571	2.504939413349883
Al	-0.611063682833608	3.390853616303119	2.209122679042956
Al	-5.172435292173324	-2.147386263777646	1.768447113465744
Al	3.348638452618717	-2.829905494267975	2.711341647021396
Al	-1.612357975841414	0.809924163494934	2.398059213454331
Al	2.969992661698914	1.870479778093440	3.226638602006483
Al	-2.637476771964597	-1.716679980874742	2.705715112075650

Al	1.876477262380041	-0.601652960277930	3.424360930175862
Al	1.402773291642795	3.980094490172380	3.915230958905374
Al	0.823679492305212	-3.138597980018146	3.747911070820013
Al	0.325284374553394	1.506506543017700	4.235149608304999
Al	-0.695342857937764	-1.016835297848745	4.503760511826590

2.30 Al_49

49

Al	1.292534131588038	-4.569740489149821	0.858005198332940
Al	-2.166279724438157	-1.543489843898820	-4.288139326829584
Al	0.353998472683346	-0.669409049146827	-4.829739136312480
Al	1.370263010346392	1.540294845437771	-3.875861688184359
Al	-1.399603722304636	1.035644975544361	-3.667316847197740
Al	-3.986971450442901	0.053047784669436	-3.101291708208019
Al	-0.462863868995134	3.280650305142974	-2.781415953413322
Al	-3.216982647474322	2.495144996888477	-2.255838675107464
Al	0.018051981884323	-2.747718620606441	-3.097381558807429
Al	-2.665463794261791	-3.466865308804201	-2.450644540408364
Al	2.471966207477228	-1.398875422706848	-3.417428258123216
Al	3.161384461383356	0.781834352486413	-1.932869430733758
Al	-4.601172679379957	-1.891164707506983	-1.269457314552088
Al	0.548013330673527	-0.202497934125130	-1.817265687953929
Al	-1.948740497098017	-0.935680991201076	-1.448090471083948
Al	2.353969217435742	3.580980005495029	-2.451830716031960
Al	0.623154251073515	4.928846148882592	-0.846441708092842
Al	4.287055995572041	-1.736641090853965	-1.440173010988117
Al	-4.006543237938067	0.682656998803376	-0.361700275531998
Al	-1.324915441708729	1.582295422360719	-0.479257845875814
Al	-2.084876668533745	4.441735060988133	-0.885259839995879
Al	1.885166489449650	-3.045573051921080	-1.315008775674649
Al	-0.598745046795051	-4.272035169504821	-0.924311066544401
Al	-0.048727604778408	-1.861811485352460	0.458042831004223
Al	-2.590183356662320	-2.962655379477723	0.420434533514969
Al	3.653672128605587	-3.278497935433442	0.771943542734421
Al	2.325994649704779	-0.720421377104129	0.328519679825394
Al	3.971599398227005	2.936598211595665	-0.332875487246868
Al	2.152881589500108	4.199895274922744	1.273574602520812
Al	1.253733990539743	2.105652236392995	-0.385373339611368
Al	4.855097982667038	0.440498793433767	0.181696351875615
Al	-4.738296528245702	-1.403359155295274	1.375475917451775
Al	-2.143281684263579	-0.288418764850933	1.457714284769944
Al	6.095196555065225	-2.020466437672194	0.694529205065809
Al	-3.299397258078974	2.958614220748254	0.894920521991448
Al	-0.647090470655732	3.839283584977412	1.361922296560275
Al	-0.753530715800236	-3.799876727663764	2.333483726800951
Al	1.782564913104677	-2.540740166348531	2.620737786185355
Al	0.270525625239840	0.698538480808415	1.768926678251383
Al	4.125469673551649	-1.059730513785333	2.418047397930312
Al	2.952398397913873	1.517755089572473	1.835352053274525
Al	1.010966402895674	2.870058437283490	3.321413382506293
Al	-2.931113776140881	-2.429386886197893	3.188530847531911

Al	-2.625938990236324	-0.010706313150841	4.330543096068372
Al	-1.820124502559329	2.326760903260793	3.096175052501172
Al	-0.349043478199157	-1.433800214350192	3.606088336976267
Al	2.047580863349786	-0.076102866695168	3.793920457067172
Al	-4.316138302600486	1.065773622296375	2.489356909759753
Al	-0.137214272340529	1.003106150812231	4.775617972008520

2.31 Al_50

50

Al	-0.082844433460918	-0.155634593848422	-6.429235475905539
Al	-0.026507432458194	1.876017854006001	-4.522909667643668
Al	1.869834107182733	-0.180601760263160	-4.425082839921967
Al	-2.055853622834928	-0.044972343971271	-4.509123610318191
Al	-0.174009695008172	-2.055787210895982	-4.343415350002210
Al	0.111138096936301	3.499686778520575	-2.407331104858631
Al	-2.259372540405078	2.146369864734554	-2.861155935517250
Al	2.114663021712163	1.701339447974345	-2.456459471322296
Al	3.970818150271093	-0.273697175395302	-2.695227539999180
Al	-4.087197874723653	0.075879457553063	-2.721590470637221
Al	-0.081295355220712	0.045148311929676	-2.428964402977744
Al	1.879297555740775	-2.013677662635965	-2.413774159519313
Al	-2.261491221367962	-1.962225271530802	-2.550597937577418
Al	-0.224733469704656	-3.788465808982154	-2.267975366234273
Al	6.317002397396328	-0.329222621622254	-1.168380922823021
Al	4.410401244329744	1.725216624936202	-0.823772908659905
Al	-4.219057907808481	1.840556642147142	-0.763135030922324
Al	2.499961494503935	3.611965047233388	-0.508216319620789
Al	0.453799371751359	1.768540216386315	-0.210168920682394
Al	2.389327874543662	-0.226203499323971	-0.384202635834299
Al	4.314080620640731	-2.209043944007666	-0.703033122429449
Al	-1.954491946376764	3.323306179579049	-0.565157740388040
Al	-1.965249662521327	0.218059930307248	-0.591576487300516
Al	0.205805954499132	4.875210255054606	-0.174922300654581
Al	-4.234540446612972	-1.451339739262597	-0.612927070026002
Al	0.004918099060465	-1.802938396892698	-0.349408389826275
Al	2.117447176799850	-3.669567807224671	-0.303742855195338
Al	-2.399762163369214	-3.452648745068608	-0.443741629197913
Al	-0.168071399309087	-4.878336374290167	0.135639634289568
Al	4.818297036686884	-0.168473725930774	1.140201356379350
Al	3.059982797671466	1.897039883844302	1.569038035353822
Al	-3.730796687705934	3.041166370867035	1.608167802458341
Al	3.113092879708471	-2.213899128596584	1.826108289898807
Al	0.952153227144354	-0.139972807633670	1.825624396053680
Al	-3.819990311047840	0.245018113070490	1.487136873446230
Al	1.124013460483939	3.552415554900815	2.001565940116627
Al	-4.036547171263448	-2.632129256421955	1.783267852081911
Al	-1.868244046104213	-4.226113847410716	2.161562878142616
Al	-1.549713793674961	-1.357571144695052	1.719080539729820
Al	3.461328780517144	-0.028142944207245	3.479913356979997
Al	-1.484954984812852	4.485169419139368	1.926235583095274
Al	1.458732888318799	-1.624069772569163	4.123954109882439
Al	-3.134807628279924	1.602983335924737	3.865107074478580

Al	-0.782491494430040	3.005126749550653	4.094061017669031
Al	-1.288600719706166	1.578605020033597	1.743978055512841
Al	1.526301987359375	1.661772069677468	3.915991168774630
Al	-3.264201404045243	-1.099620583511919	3.932561641214265
Al	0.732145574027708	-3.227592781773637	2.059398525922477
Al	-1.032555545113265	-2.673573985836143	4.193056446730171
Al	-0.717160839920327	0.108929806431721	4.043579087785263

2.32 Al_51

51

Al	-0.142616012793992	0.574094847716967	-5.059622238432010
Al	0.567400145539004	-1.842765983232809	-4.115068606654530
Al	1.050585693991319	2.858355506529918	-4.165763535445381
Al	2.226787158020080	0.422898198423891	-3.630860097106033
Al	-2.136253590019738	-0.560974883399636	-3.736044699492635
Al	-1.330981336772554	1.984921671240009	-3.043634481473505
Al	-1.370208412131422	-2.733547932754288	-2.372978221586701
Al	1.096466612306532	-4.006978602790666	-2.557025366225426
Al	3.326389001675565	2.876434346571797	-2.642579855662493
Al	-0.173811168353467	4.444847319795910	-2.360007722371531
Al	-4.118727056686962	-1.610840964729542	-2.288061319547653
Al	2.600720947281772	-1.736717912057628	-2.256313389255649
Al	-0.002043570805501	-0.292135716157929	-1.922456318071289
Al	-3.561733512464423	1.122272504284471	-2.045894857908905
Al	4.101177980199044	0.517490947494336	-1.638881479395758
Al	1.026490763583858	2.054443517552164	-1.305202631941285
Al	-2.532167798669901	3.667995618439372	-1.257789358476996
Al	2.129132016855952	4.625339516680237	-0.885242646379488
Al	1.621922117081112	-6.215626375631315	-0.832084541238711
Al	-0.777291812056447	-4.789862412521345	-0.650516100150613
Al	3.052887495653767	-3.885347320816062	-0.614749268442058
Al	-3.235189227644581	-3.628329991583255	-0.538931232750690
Al	0.581186915482121	-2.388246500507395	-0.274505240830106
Al	-5.868385993338515	-2.705596880211009	-0.384711390879882
Al	4.664409705886039	-1.743190025659496	-0.422564148005318
Al	-2.219010649178038	-1.039632638855004	-0.377432932128000
Al	1.981245631204173	-0.191337507760879	0.087852433805637
Al	-4.973563313014687	-0.133866117017014	-0.067024406027210
Al	-1.387150167865132	1.443573996687300	-0.119068444398410
Al	3.287849125633715	2.270452353661412	0.261081316008822
Al	-4.349180909403045	2.457117516090308	0.291602304161284
Al	-0.315176255526460	3.975460071820814	0.401332402462955
Al	1.168582283546597	-4.570368561007476	1.361914473322178
Al	-1.423083274908080	-3.122143936530410	1.445989000144646
Al	4.308131888583599	0.029867591120551	1.545527444769897
Al	2.949575852421070	-2.435672279738565	1.712615008937991
Al	-0.414562914654468	-0.549658461375284	1.625733837177155
Al	-4.011356985079884	-2.088966680988502	1.648209091749324
Al	2.069995961448821	4.207913161285397	1.795315582710911
Al	0.781529365625149	1.762214249634207	1.635120681886267
Al	-3.209889761157984	0.516703262786407	1.927792540543887
Al	-2.397656836931478	3.136343127123443	1.905697929798698
Al	3.288384107518617	2.031364419379390	3.021850723964256

Al	-0.239330019619912	3.734351978589604	3.311187963123885
Al	2.028241074681356	-0.407931850147028	3.049801715439978
Al	0.594262635163217	-2.710596772949779	3.181861795971324
Al	-2.172303756564954	-1.469218097522228	3.540305372877221
Al	-1.445290967579915	1.216160751237007	3.673636809061264
Al	2.203860704878890	4.115814009146233	4.599400840338486
Al	1.071340373215357	1.623413920111268	4.614444523044114
Al	0.028409745744874	-0.810289997457886	4.926740738978033

2.33 Al_52
52

Al	0.069398330593453	0.272818317057853	-6.518979328472231
Al	-1.868934680015398	-0.289152270899992	-4.670400059040214
Al	1.960967448860835	0.702375224685785	-4.509528661778723
Al	0.561732901722699	-1.740324345792839	-4.649857550115422
Al	-0.458355522856357	2.077978317874550	-4.385358653005807
Al	-3.991739043822356	-0.841373706512696	-3.137768832750380
Al	3.953859956155179	1.229842287070337	-2.744524090963880
Al	-2.339759918586731	1.355130746981562	-2.543048927987261
Al	-1.602424810196066	-2.433223410538321	-3.015938541595722
Al	1.528521550574258	2.574827890727144	-2.523968052829421
Al	2.657796282030533	-1.207242142526542	-2.610652819614398
Al	0.185119916317047	-0.029674817882865	-2.508085962143586
Al	1.014016450577854	-3.327437234370407	-2.566636935164400
Al	-0.970403243787500	3.762329986032391	-2.323747620418764
Al	6.176259695646836	1.766710857660390	-1.140634492075339
Al	-3.575664816289660	-2.562039940855414	-1.063882991580519
Al	-4.221773262963421	0.432501456976251	-0.820087290102636
Al	3.802119003434589	3.166107394140420	-0.701256109049940
Al	4.746627064156847	-0.677170014343140	-0.874508290318229
Al	1.341835352720805	4.097023155175437	-0.322337128211549
Al	-1.615259071521141	-0.693196932099948	-0.719107006180607
Al	2.305607054707654	0.843504807349614	-0.546651890203021
Al	-0.983185141596959	-3.503600130505667	-0.738435709659418
Al	-2.955995274997784	2.919956998773772	-0.571252996693175
Al	3.350712132726295	-2.984432787554295	-0.597018817570094
Al	1.039498560868953	-1.552910469711692	-0.348356212357929
Al	-0.304434836760176	1.793221085888378	-0.552707978649879
Al	1.433182146830822	-4.918417111507217	-0.483473103475793
Al	-1.111328176632703	5.022621493831432	0.089101601841330
Al	4.751644793581097	1.230820582630157	1.134019748217973
Al	-3.536997339957281	-1.085909033172314	1.283380686251682
Al	-2.834662557354036	-3.763192705253909	1.251646779701950
Al	2.599774718446488	2.760211091117615	1.793696244822746
Al	-4.443904478800501	1.738616143206283	1.484013232371693
Al	3.275604461327717	-1.049711860313547	1.395050853938749
Al	-0.715453579223338	-1.819600034185905	1.583632305093662
Al	-1.775694787296302	1.005771715997501	1.471970834862836
Al	1.959762857584598	-3.246492642652202	1.794334584403009
Al	0.880452002870877	0.453459608689695	1.620857376398174
Al	-0.277315437332133	-4.779425049585509	1.569540261000794
Al	-2.605783318096574	3.837864405218143	1.966388177029883
Al	0.046994543338759	3.197441789011279	1.886590198620597
Al	3.670656429570505	0.736433072258810	3.531287921253842

Al	-2.578197355398043	-2.268578783170662	3.588757790496194
Al	-3.336530804440145	0.336690938522151	3.665274692652812
Al	-4.234438735669542	2.961708801301642	3.983598097903920
Al	1.865984273716942	-1.202354550967820	3.708408602434583
Al	-0.650074686001908	-0.281371203864863	3.851040444038231
Al	0.080316466422648	-3.164090648950358	3.866679005598407
Al	-2.010909926631186	-5.001819234564740	3.675911668328705
Al	1.195044512128543	1.784356185207891	3.984087503419785
Al	-1.454268100685551	2.362416708396418	4.008937441326751

2.34 Al_53

53

Al	-0.993331550774563	0.816206676753513	-4.311541231305792
Al	1.262403569022364	2.145994378500854	-4.355559785184588
Al	-3.012884619750364	-0.841945740558888	-3.999722437974528
Al	3.658488913371389	3.532384060582640	-4.226521627361563
Al	-0.961918711568323	-2.558692882290209	-3.799101555437234
Al	1.195458525058037	-0.738097713155046	-3.764789999425780
Al	3.519299997334505	0.810800201332668	-3.462571267540489
Al	1.476972490958955	-3.465561480567882	-3.237520218611013
Al	3.659815351181125	-1.808533165886656	-2.955309034456249
Al	-2.755559116088355	1.417076370884340	-2.329265535747679
Al	-0.731324655726473	2.987767720672192	-2.613583695369335
Al	3.983872679211911	-4.620540019401575	-2.766122318696048
Al	1.651239487177955	4.215888727543661	-2.468127933932282
Al	-4.636667797078345	-0.557177295993798	-1.897981344081337
Al	-0.800736176358701	-0.627620517426609	-1.846096801396394
Al	-2.853349982520220	-2.669565281154631	-1.780851138850670
Al	1.369615886824230	1.115766698538549	-1.748339945251161
Al	-0.382718728280652	-3.428408293914368	-1.213843690977994
Al	3.769227414842875	2.724246215964337	-1.524675852932948
Al	1.699056572876058	-1.580763198186304	-0.998047863924146
Al	-0.259487954035652	5.155383597522619	-0.840740398232050
Al	3.940897332834666	0.013158480532061	-0.826052271044704
Al	-2.505790133879720	3.570288043674219	-0.604014356941967
Al	1.956946068316752	-4.785609001619214	-0.872046517222470
Al	-4.510804243694994	1.749384104123576	-0.275183002536362
Al	4.078145224375678	-2.990258080670345	-0.505283081227493
Al	-6.450731191771673	-0.265462962413865	0.105633280182371
Al	-2.576044144857885	-0.308955901104497	0.101369464435287
Al	-0.677860846362845	1.543309364672654	-0.167745344517018
Al	-4.486395201900579	-2.220763821995915	0.454703509642506
Al	1.569532122891244	3.204343635302958	0.058565477531026
Al	-0.178159412706703	-1.503712122713790	0.845169450226431
Al	-2.184875523311915	-3.586421630448618	0.769685971131601
Al	1.785861672281019	0.430051533408703	0.935841624058495
Al	3.955317989362866	2.142682067944168	1.048981066728793
Al	-0.026124662435084	-5.213796455406342	0.915697481392092
Al	1.994806365215320	-3.268651719348917	1.324655088905041
Al	-0.592934062577887	3.867601718947805	1.499964731701052
Al	-2.625521018637788	2.135992620502948	1.757204929892611
Al	3.970041093440313	-1.343911288468354	1.529169903917479
Al	1.785929976377600	2.772673735627546	2.653788326925573
Al	-2.716563560368378	2.800339331826880	5.769606496052202
Al	-0.425283153953654	0.611614438529278	2.438379092884007

Al	3.717052823438131	0.632053073674893	3.243323255866045
Al	1.769401542615549	-1.436571361057490	3.123252279311380
Al	-2.410711881994962	-1.587056579239910	2.545738185784696
Al	-0.273216064214880	-3.331202853589402	2.889972910918873
Al	-4.516859221757181	0.152862507087297	2.047070334855469
Al	-0.661569601665757	2.866256112336689	3.990804698495655
Al	1.442975174025030	0.863379097359607	4.595156893549476
Al	-2.725091688771545	0.664083405790363	4.101524366624318
Al	-0.538922380300606	-1.227339095315251	4.563172274078182
Al	-0.740920985687914	1.025030542290933	6.082207155088685

2.35 Al_54

54

Al	3.846903071859114	-1.951078618296101	-4.378042347509639
Al	0.267990697836572	-2.041540843353296	-4.253141873920666
Al	2.105296323987137	0.122315889996429	-4.182430735454237
Al	-2.276158920584832	-1.598089104787558	-3.396995095066855
Al	2.251903057323627	-4.072193509923145	-4.036293932355752
Al	-0.556414787618241	0.519578034393612	-3.338582543741318
Al	-3.183761736865180	1.116004001618348	-2.711392012817772
Al	1.325080855170299	2.519656363237095	-3.371763372604466
Al	-1.455540221713832	3.064158075206056	-2.709771500140242
Al	0.427854585428804	4.951365455770260	-2.757611110311263
Al	0.213284688275184	-4.083780450364181	-2.233284880089290
Al	4.319056231066941	-3.667924077602309	-2.314540887160350
Al	4.149075182579766	-0.147637975606543	-2.200683570016963
Al	2.122431874589621	-1.998857546383134	-2.169183191935337
Al	-2.975946778218441	-0.886764326022591	-0.588857316606342
Al	3.395363674270195	2.385188322850222	-1.498688531682545
Al	-0.408396478084299	-1.452165206946878	-1.344710451500788
Al	-2.252354915929850	-3.537263511675163	-1.382234472325541
Al	1.418460958079585	0.500056756890809	-1.362191823943245
Al	2.583829544675766	4.849975380241668	-0.805467955550446
Al	-1.244143235771880	1.122679402013929	-0.548623714096410
Al	0.607686664632972	6.754319837613528	-0.770723246687778
Al	-6.683426549044088	-1.147093073687916	-0.746031085257894
Al	-4.994059586941233	1.000391788839709	-0.556185681844863
Al	2.274907111714644	-4.068253981318415	-0.290467464380734
Al	0.601795388819795	3.012288949957398	-0.645997071813021
Al	-3.270310970403359	3.002700247790987	-0.461154473115355
Al	-1.428894730122513	4.907637056089857	-0.555687526255220
Al	-4.827954044221902	-1.001461782873195	-2.716733568764012
Al	1.531020631723127	-1.416602731655425	0.562978692866231
Al	-0.340627241191111	-3.515025079844722	0.549640209912916
Al	3.484130055083604	0.590556898715935	0.521857766542643
Al	4.190871337161992	-2.041564012973167	-0.111274049499833
Al	-4.717044151817463	-2.998167208650282	-0.569892672292919
Al	2.797317920973994	3.125495983224162	1.279323232177266
Al	-1.078293979669153	-0.842235199813265	1.427191152148989
Al	0.775253162353586	1.160987638925041	1.396461980786512
Al	-4.879922943433137	-0.999787149029649	1.416597816364142
Al	-2.896263789427342	-3.012250674355288	1.408326912490715
Al	0.661069124686424	4.932609762100267	1.331568151623086
Al	-3.241661130452658	1.184276635947000	1.596050828014512
Al	-1.417071883602491	3.148434422545209	1.583794501610894
Al	3.687404278155736	-1.336517684052303	2.435086699667952

Al	-0.923549045494946	-3.019681543381736	3.227154184375822
Al	0.735823151270944	3.138630781260868	3.313517672269978
Al	-3.030095231423577	-0.927684431389457	3.364583517520158
Al	0.957147295426328	-0.822725988747338	3.301504349641242
Al	1.706140873519693	-3.546986505372843	2.350556458590940
Al	-1.264216336492762	1.210070745762733	3.510699222943860
Al	-1.090097987250434	-1.084364159178444	5.166510561147019
Al	2.977789421778112	1.252620339807279	3.186873086827909
Al	1.259749037422131	-1.081030005614764	6.331651896411017
Al	2.702443820039777	-2.525094163344062	4.598166327703350
Al	1.059126655869198	1.251821775444782	5.148542937103935

2.36 Al_55

55

Al	3.934905779360893	0.597980439290851	-1.175848085658066
Al	0.485549701030763	3.544033104524324	-2.598609360316672
Al	2.984282696397269	-1.398671094942120	-3.013772034409740
Al	-2.229205196184175	3.264799122894329	-2.003944321153009
Al	-3.262080084231968	1.258612096024649	-0.569943366741201
Al	0.699666563993356	6.663705133418102	0.956115216168966
Al	-0.716159126440626	-2.277914513027532	4.103318526696153
Al	1.859585941248795	1.105305856342310	-2.808562127471793
Al	4.642490424293483	-2.082048779733134	-1.044598187937712
Al	1.109824660180628	-0.721328372982747	-4.827774363209912
Al	-2.444675497954455	3.370565211456231	0.960575659600122
Al	-4.005064448095078	-1.099084630908543	-2.029680743288345
Al	2.524857101846438	4.592805271378740	1.342251322275853
Al	-3.391725967034937	-1.564371315722864	-4.643734708725373
Al	-1.535382258888053	-0.042189556265836	-5.951970548272983
Al	0.375391028666360	3.210947478862392	0.166879694291138
Al	3.666244945325611	-3.915599535695276	1.088003590427054
Al	6.190094920721796	-2.712132646566671	1.107961263917302
Al	1.655246422405781	0.962125157861353	0.459449402626355
Al	2.189588947021418	-3.503587363894724	-1.125096105933608
Al	5.262445756501714	-0.043721150548812	1.097204031146976
Al	1.429073069745620	2.542605961031333	2.777146424827453
Al	-4.597863800607556	-0.808083227571180	0.610124966581102
Al	4.388948973862103	-1.901678485447004	2.967905209393914
Al	-0.383119123537044	1.731692658525375	-4.282130284162642
Al	-2.294343328367706	0.117779543536166	4.521592407359179
Al	-3.624869974866860	1.320448332406512	2.256234007491615
Al	-1.126140927241863	5.281000001501834	-0.599805513205439
Al	0.077728236492888	-1.464880470878926	1.398066077525682
Al	-1.763004969262280	-1.030898926549813	-0.487463818405441
Al	1.718637072457675	5.482396589079972	-1.252546665324566
Al	-2.460445440802975	-1.257820384780938	2.189505941965443
Al	-4.786915995004590	-0.776563102261122	3.579380778743186
Al	-2.945735366491119	1.080051193158475	-3.476812843614598
Al	-1.327009332723417	2.448700672435852	3.557603726029349
Al	2.880692944515355	3.046466484035696	-1.131104480102863
Al	0.349968758029297	0.223969311513212	3.629630646668321
Al	-1.733056535270441	-3.832124928533348	2.030936819300935
Al	0.999038600739809	-4.028078699853318	1.571464886112764
Al	-2.197372828008907	-3.201691184041815	-2.700190393891157
Al	-1.060621700309801	-0.805652115306437	-3.200141273265366
Al	-0.950510101996727	-2.605464446103412	-5.376359854925058
Al	-0.513652853374305	-3.476003564380932	-0.579353779790752

Al	-0.570757330153484	1.199193984519894	-1.459091247734047
Al	4.036394012900624	2.349968791424930	1.286738501725916
Al	-4.606788555316356	-3.187583239024848	2.169049373975543
Al	3.032267982380112	0.415532974881657	2.967397995156974
Al	-3.306688939956581	-2.868495918060900	4.467187084470224
Al	0.906580582973914	-1.038414381003273	-1.264296779251540
Al	-3.376357723384070	-3.243234630528031	-0.247904626729898
Al	1.823125476584949	-2.099304590837788	3.403255036724147
Al	0.617918687560332	-3.073368605422088	-3.212091288926269
Al	2.734396430501761	-1.383069037946578	0.770995886482332
Al	-0.974834932559357	1.011985516102369	1.283506277437917
Al	-0.390563379673910	4.620388012613418	2.343346047326131